

Isotopes in Stardust: presolar silicon carbide grains



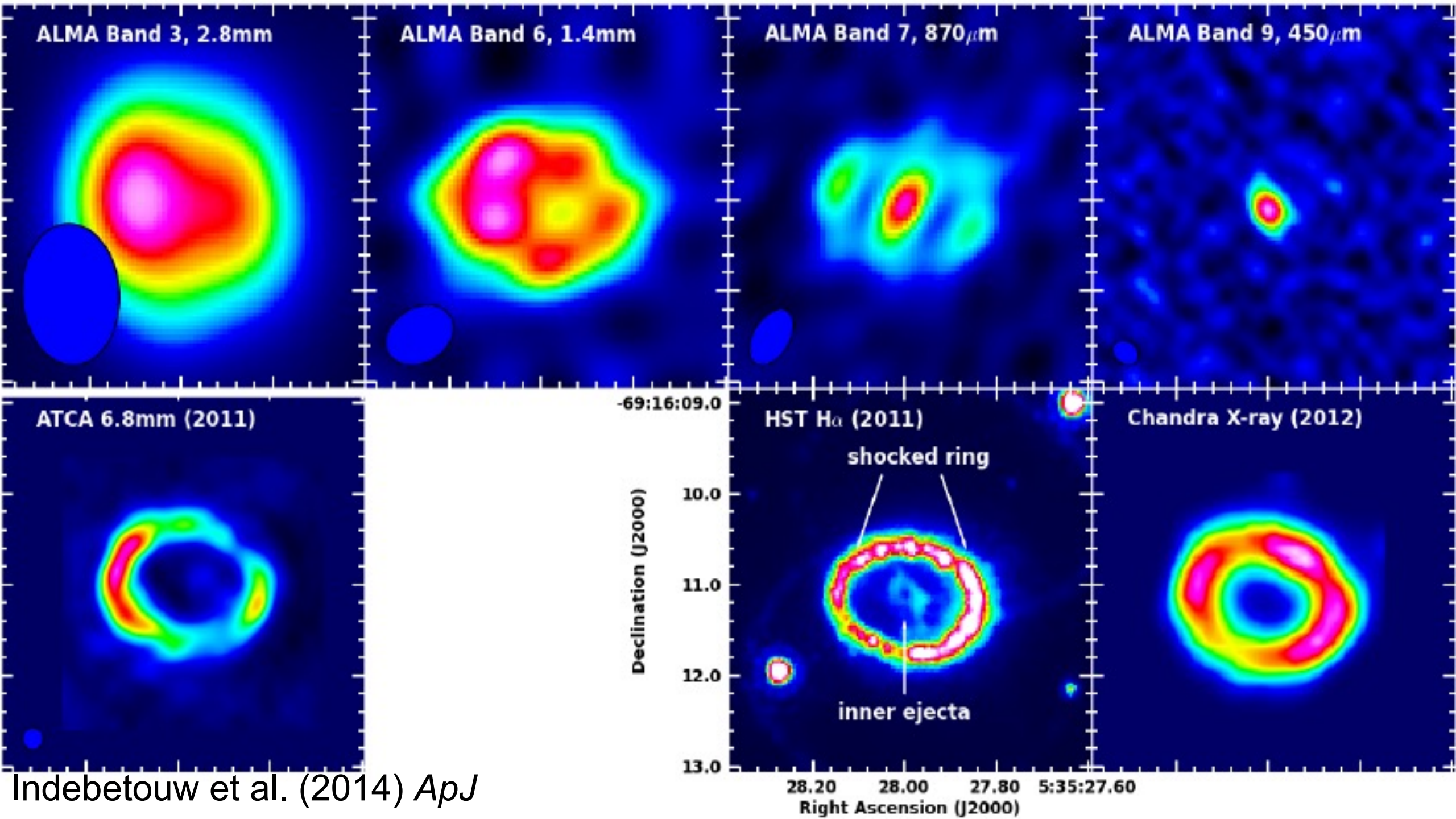
Nan Liu

Department of Physics
Washington University in St.
Louis

09/14/2021

“The nitrogen in our DNA, the calcium in our teeth, the iron in our blood, the carbon in our apple pies were made in the interiors of collapsing stars. We are made of star stuff.”

— Carl Sagan, *Cosmos*



Indebetouw et al. (2014) *ApJ*

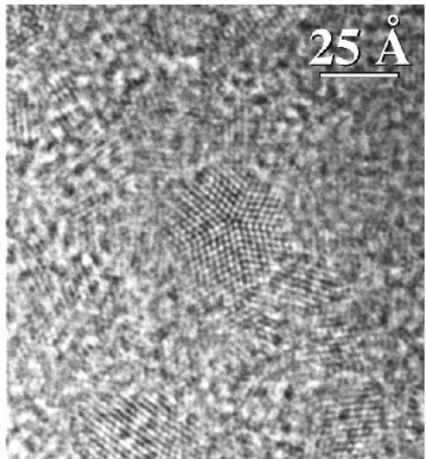
The image is a composite. The top half shows a vast field of galaxies in various colors (blue, orange, red, white) against a dark background. The bottom half shows a dark, textured surface, possibly a planet's surface or a microscopic view, with a grid pattern visible in the lower right corner. The text is overlaid in the center.

**Where the telescope ends,
the microscope begins.**

Types of Presolar Grains

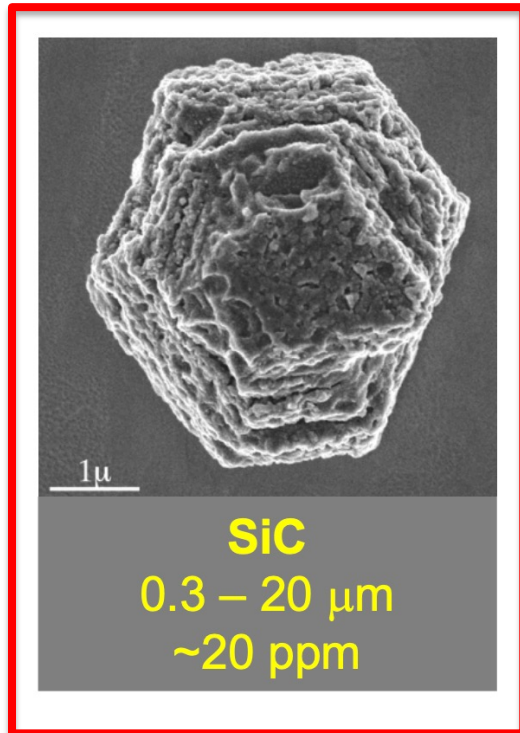
See Ann Nguyen's lecture that introduces presolar grains, solar system, and meteorites

- First presolar grains (diamond, SiC, graphite) discovered by exotic noble gas signatures in 1987 (Lewis et al. 1987, Bernatowicz et al. 1987, Amari et al. 1990)
- More detailed isotopic studies and identification of additional presolar phases and subtypes made possible by Secondary Ion Mass Spectrometry (SIMS)



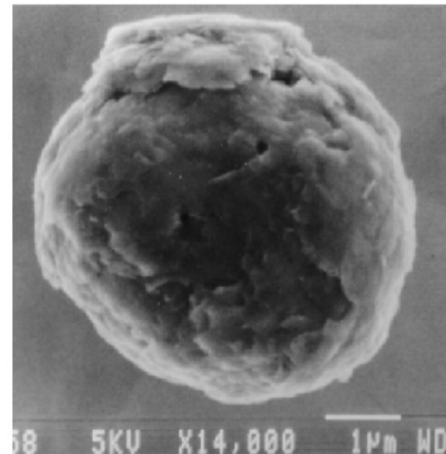
Nanodiamond

2 nm
~1400 ppm



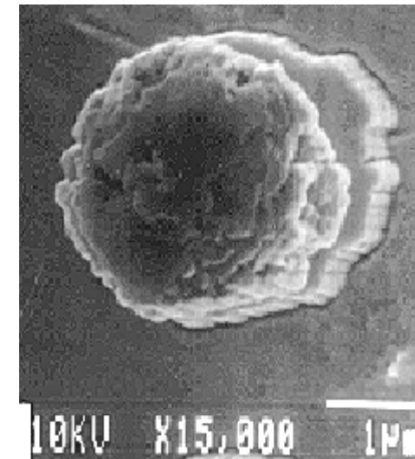
SiC

0.3 – 20 μm
~20 ppm



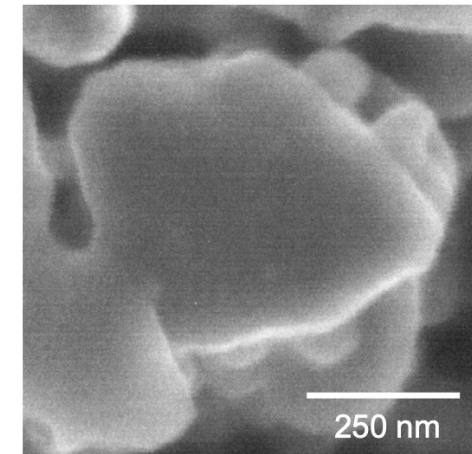
Graphite

1 – 20 μm
~5 ppm



Oxides

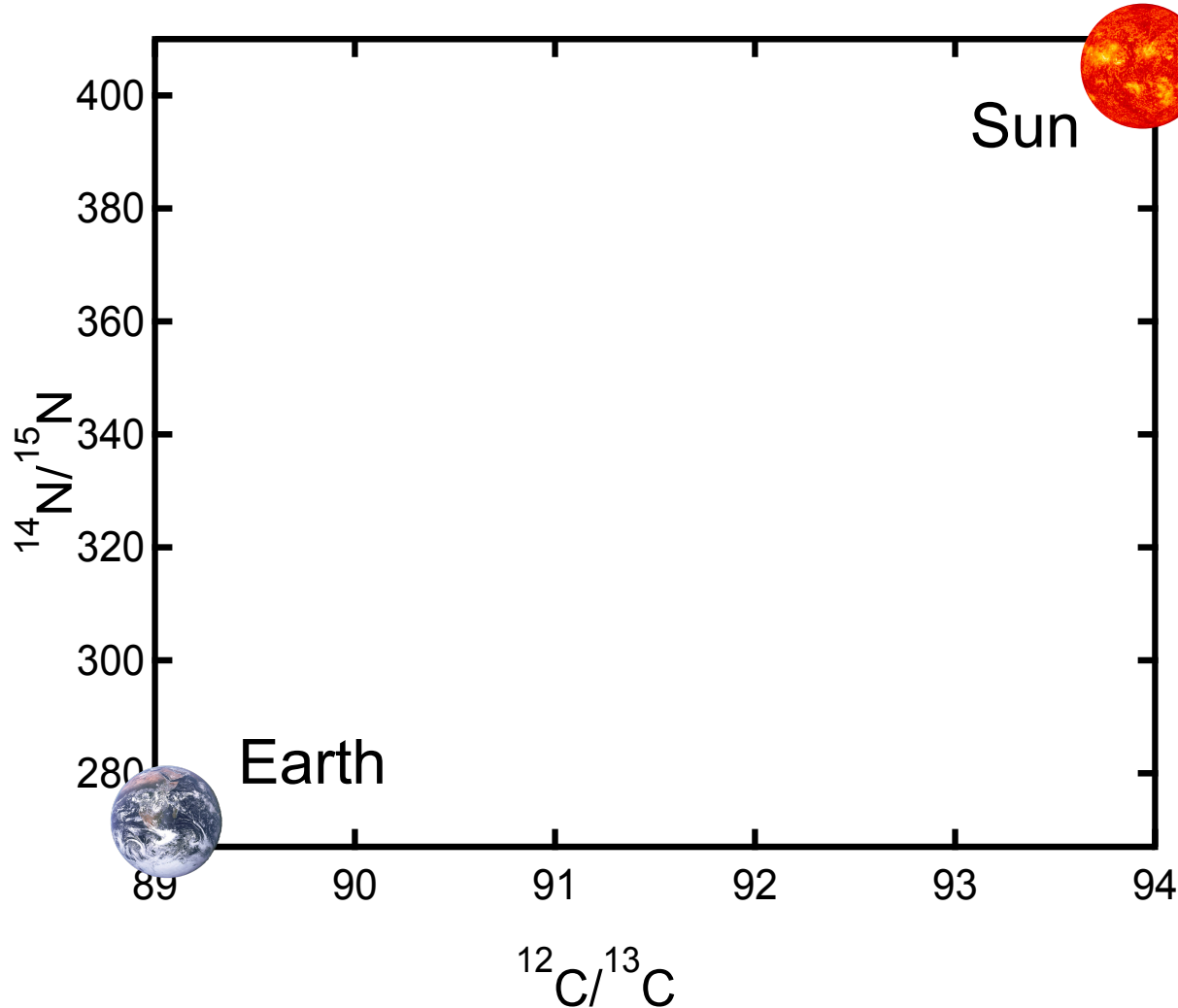
0.05 – 5 μm
< 100 ppm



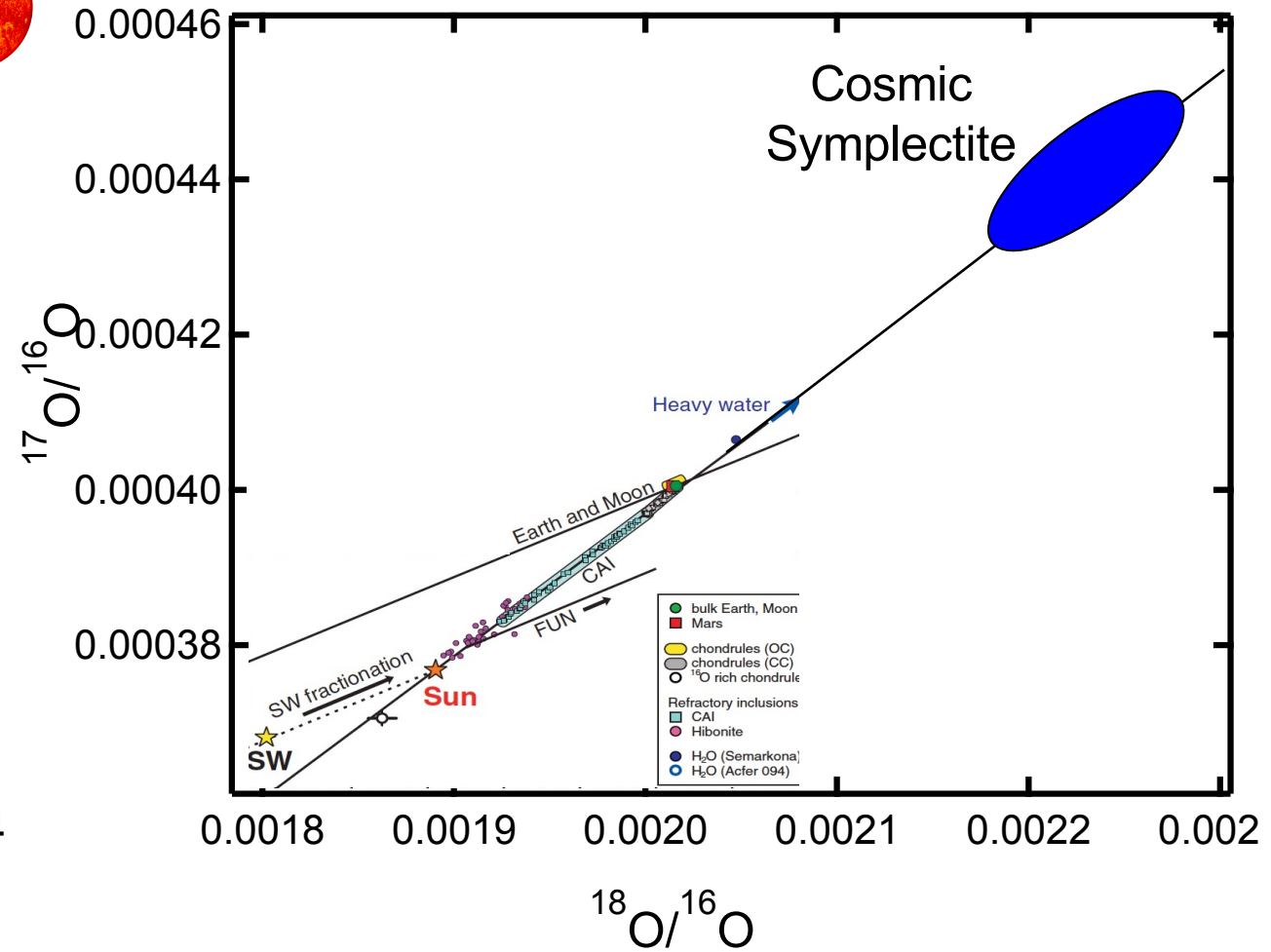
Silicates

0.05 – 2 μm
< 15,000 ppm

Solar System Composition

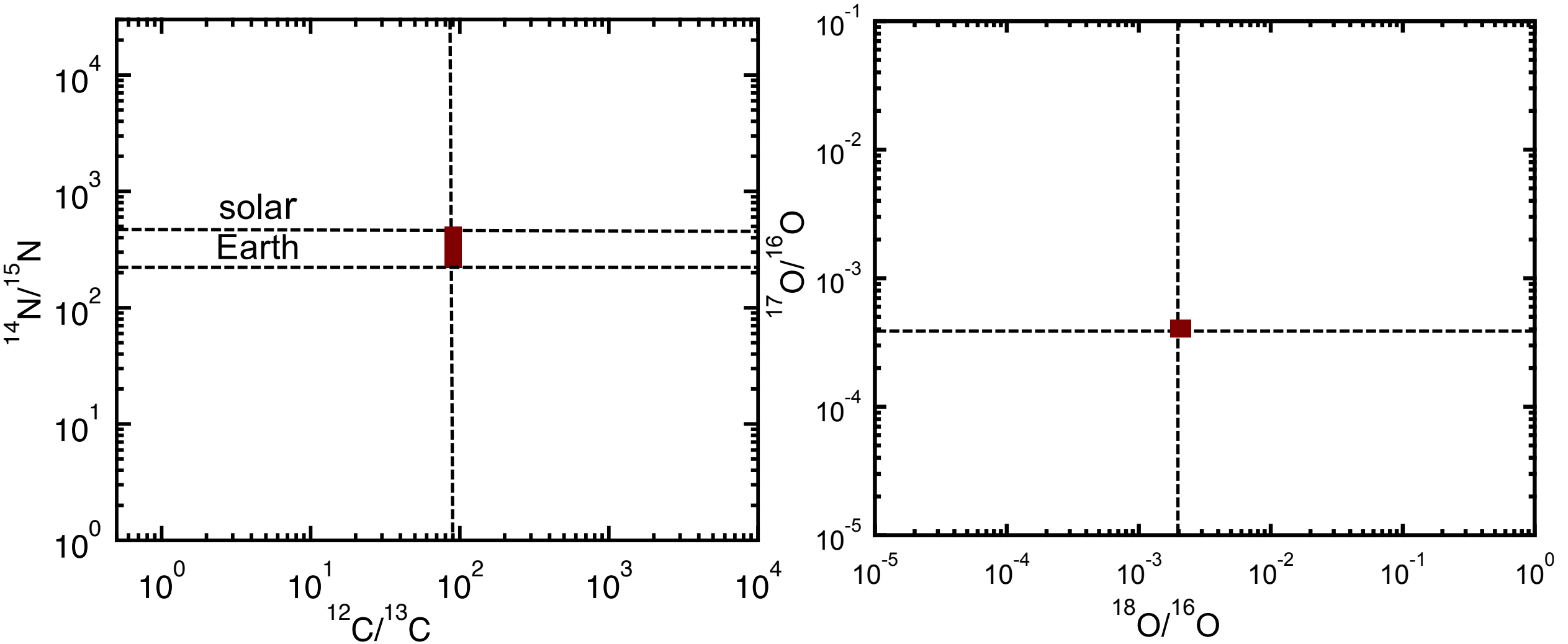


Marty et al. (2011), Lyons et al. (2016)

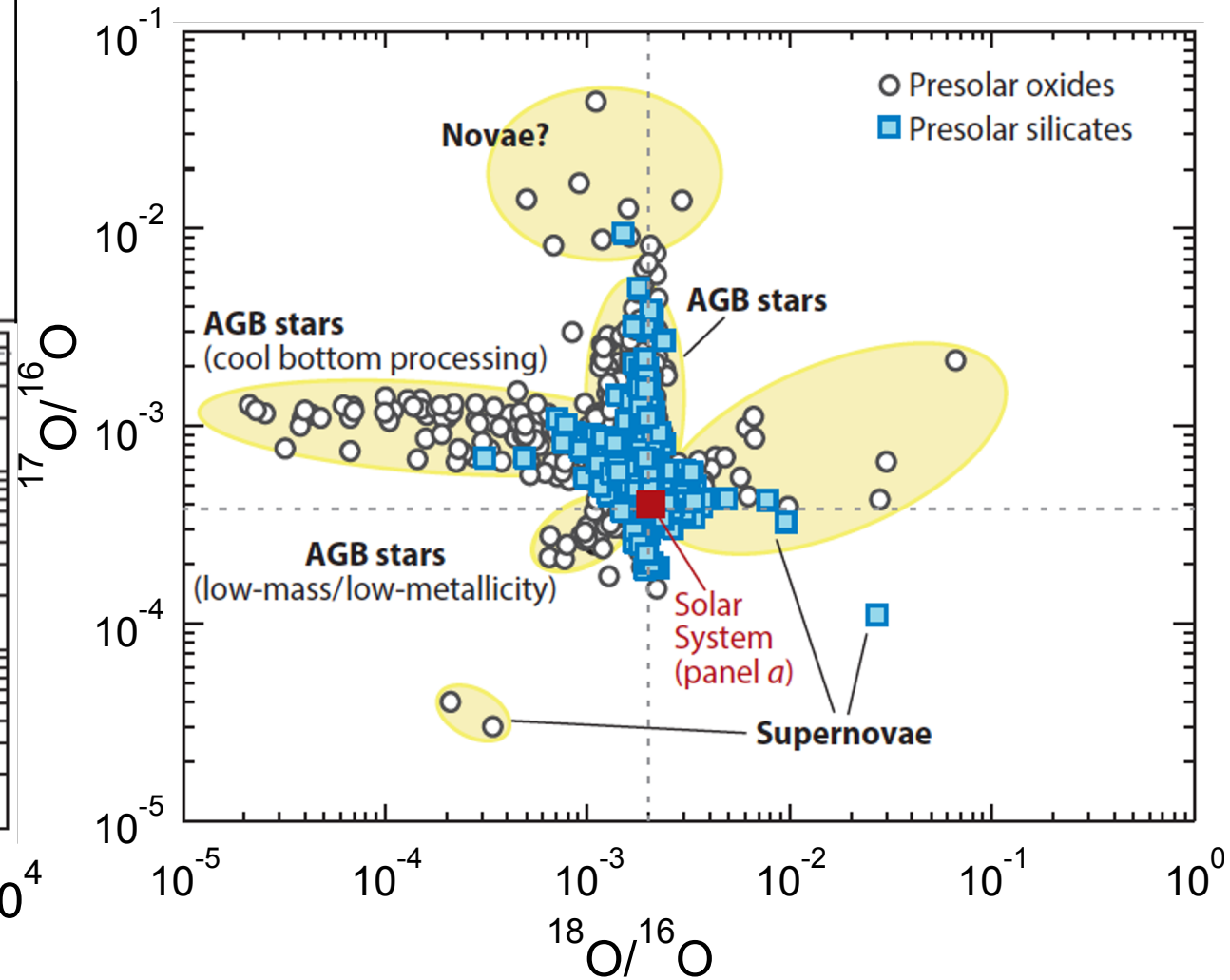
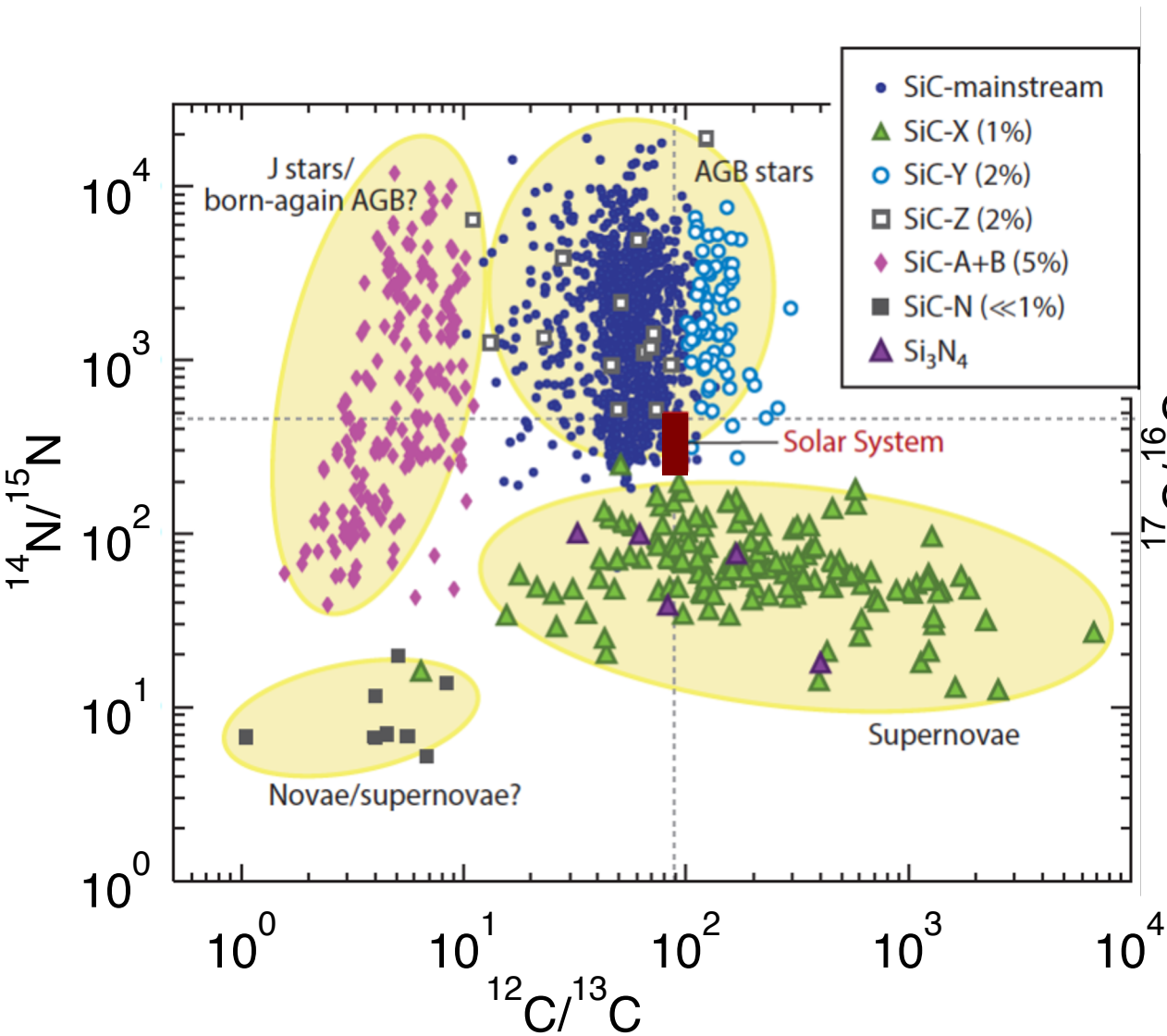


Mckeegan et al. (2011)

Why are They Presolar Grains?



Huge Isotopic Anomalies!





How can we find presolar grains in pristine meteorites?

Cooking
meteorites
in acids

SiC
graphite
Si₃N₄
nanodiamond
oxides



Burn down the
haystack to find the
needle!

Outline

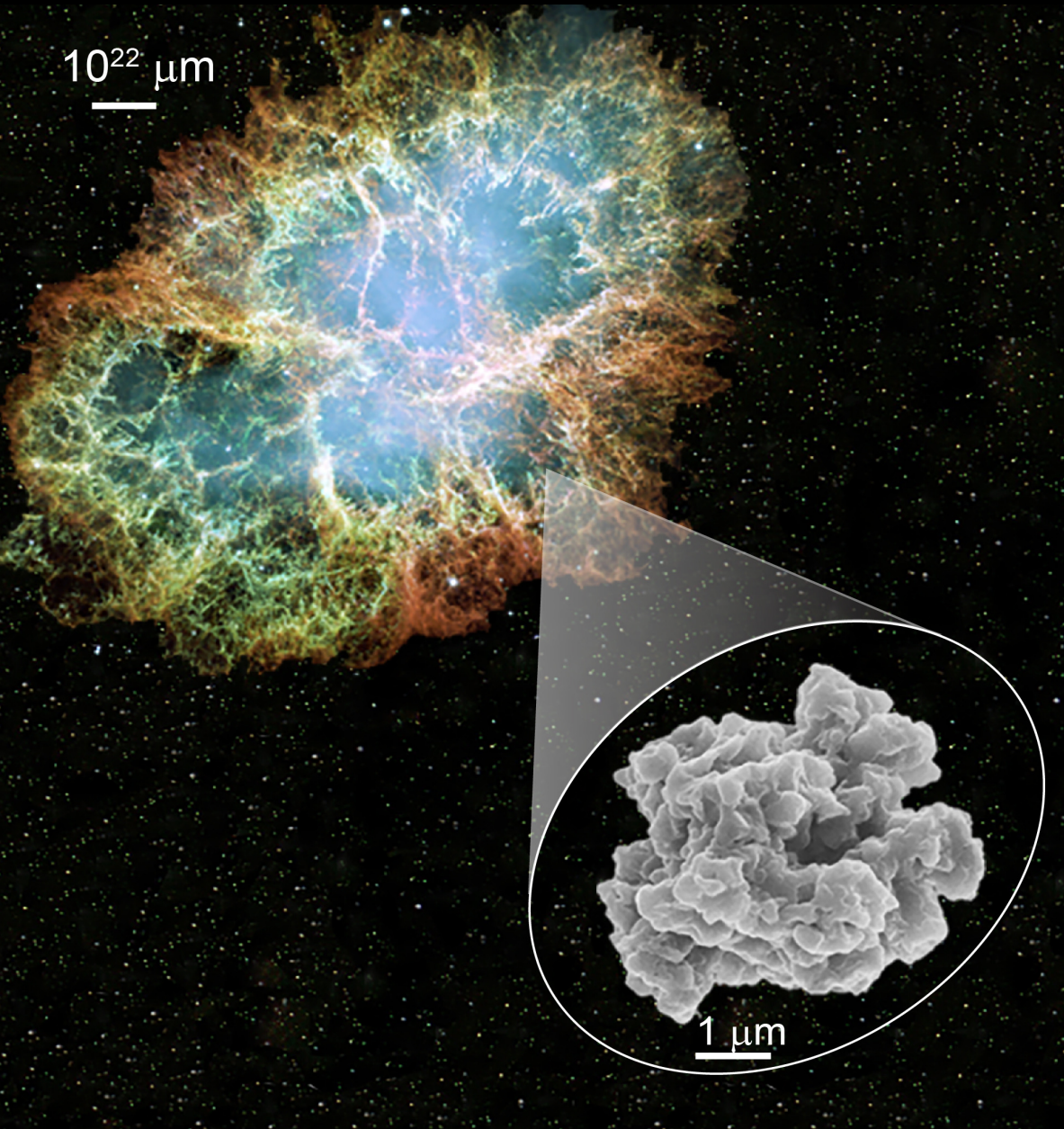
1. Analytical Techniques

2. Different Types of Grains and Their Stellar Origins

2.1 AGB Dust

2.2 Type II Supernova Dust

2.3 Mysterious ^{13}C -rich SiC Dust



SIMS versus RIMS: Sputtering

Cs-Gun for negative ions (~100 nm)
O-Gun for positive ions (~100 nm)

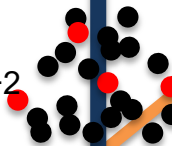
NanoSIMS

electrostatic
sector

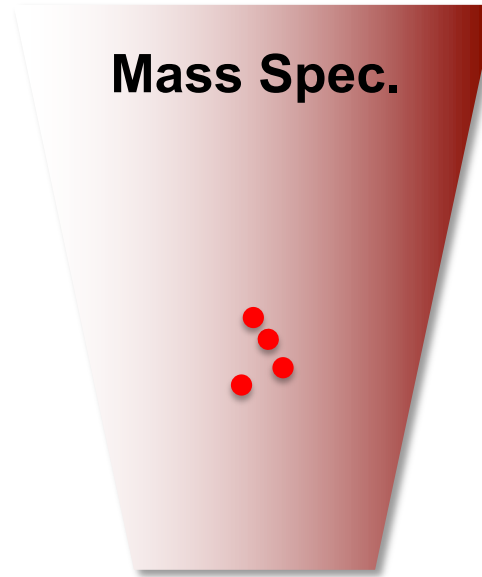
SIMS: secondary ion mass spectrometry
RIMS: resonance ionization mass spectrometry

Ga-Gun
(focused ion
beam, ~ 2nm)
RIMS
laser beam
(~ 1 μm)

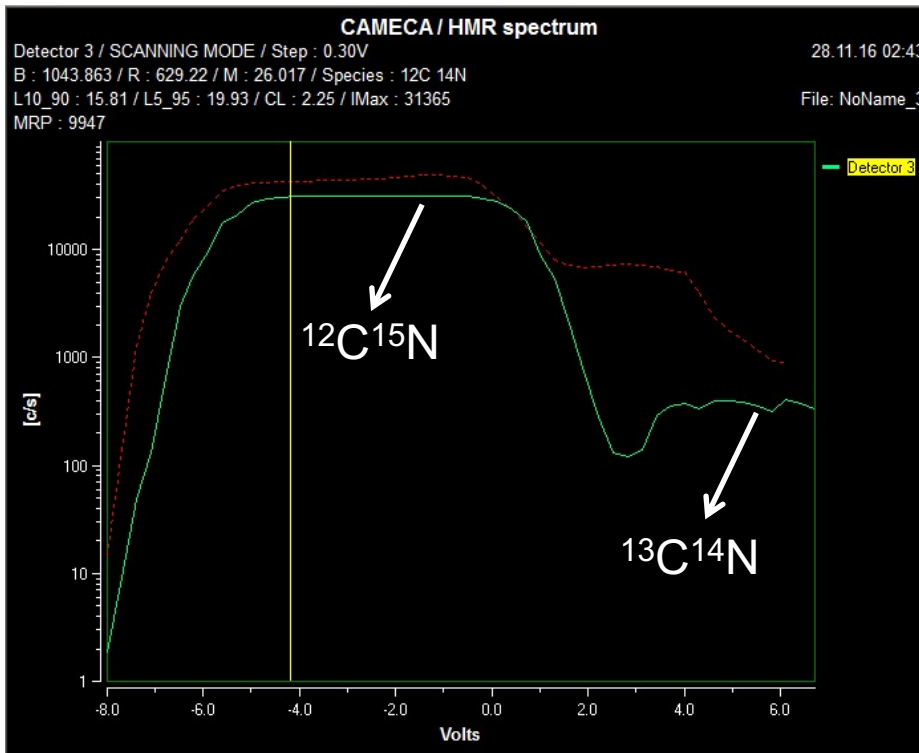
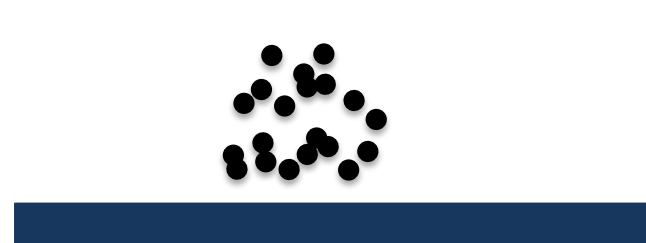
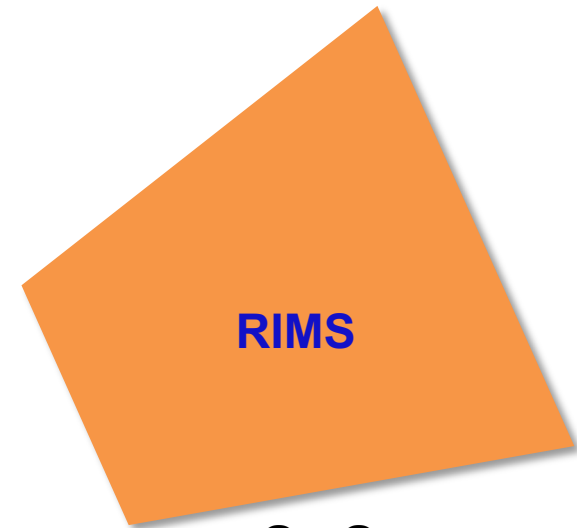
secondary
ions/neutrals: 10^{-5} – 10^{-2}



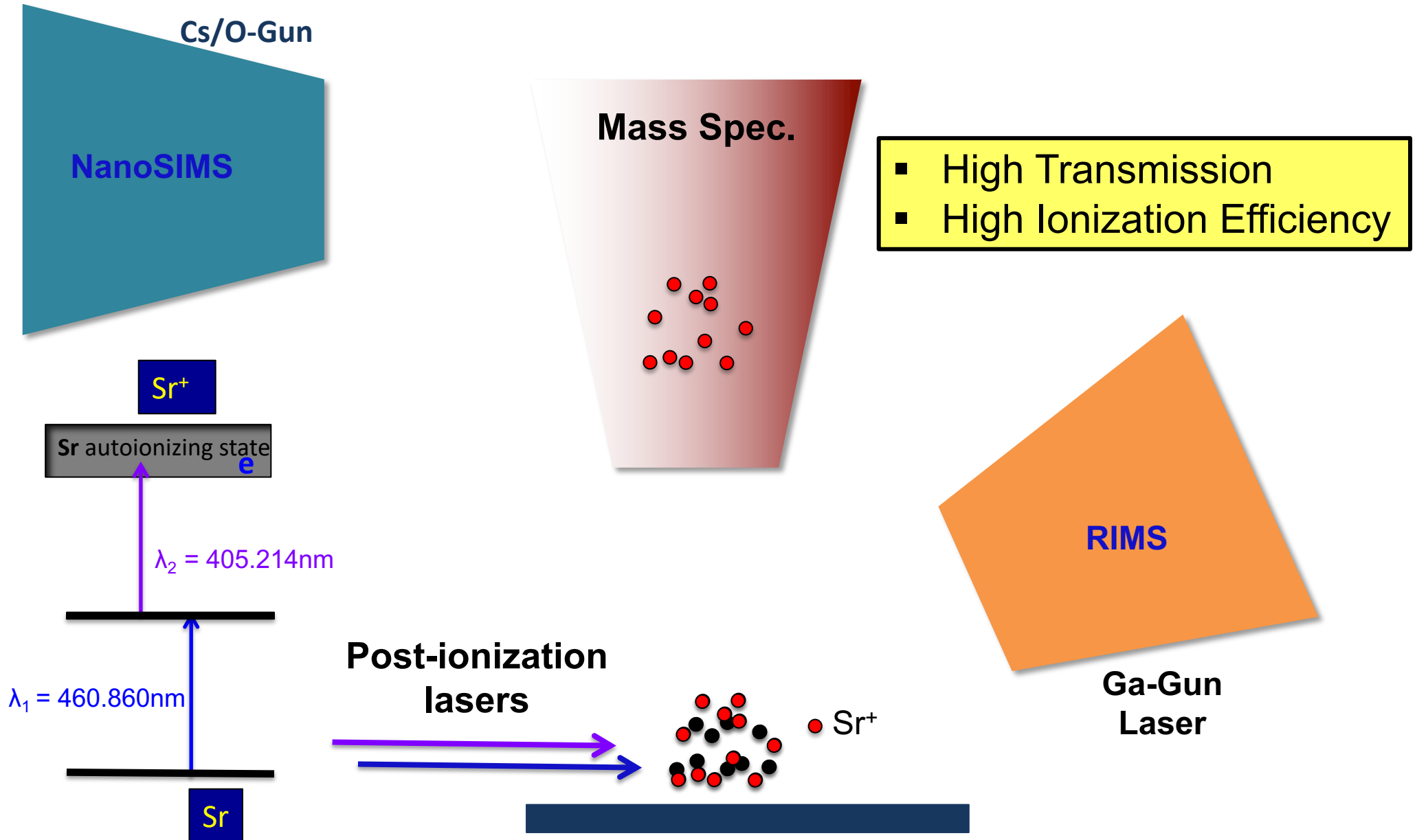
SIMS Ionization



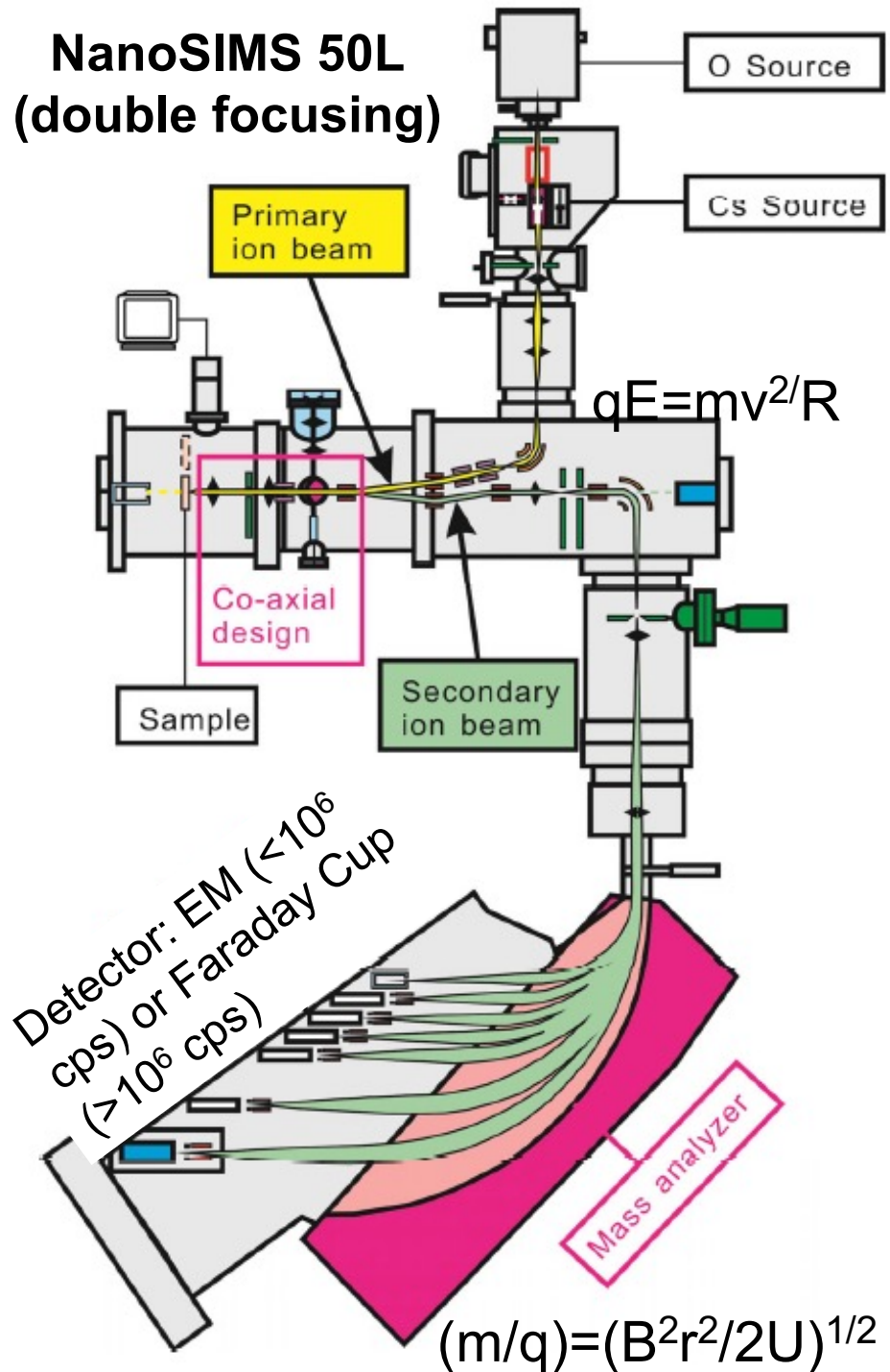
- High Transmission
- High Mass Resolution



RIMS Ionization

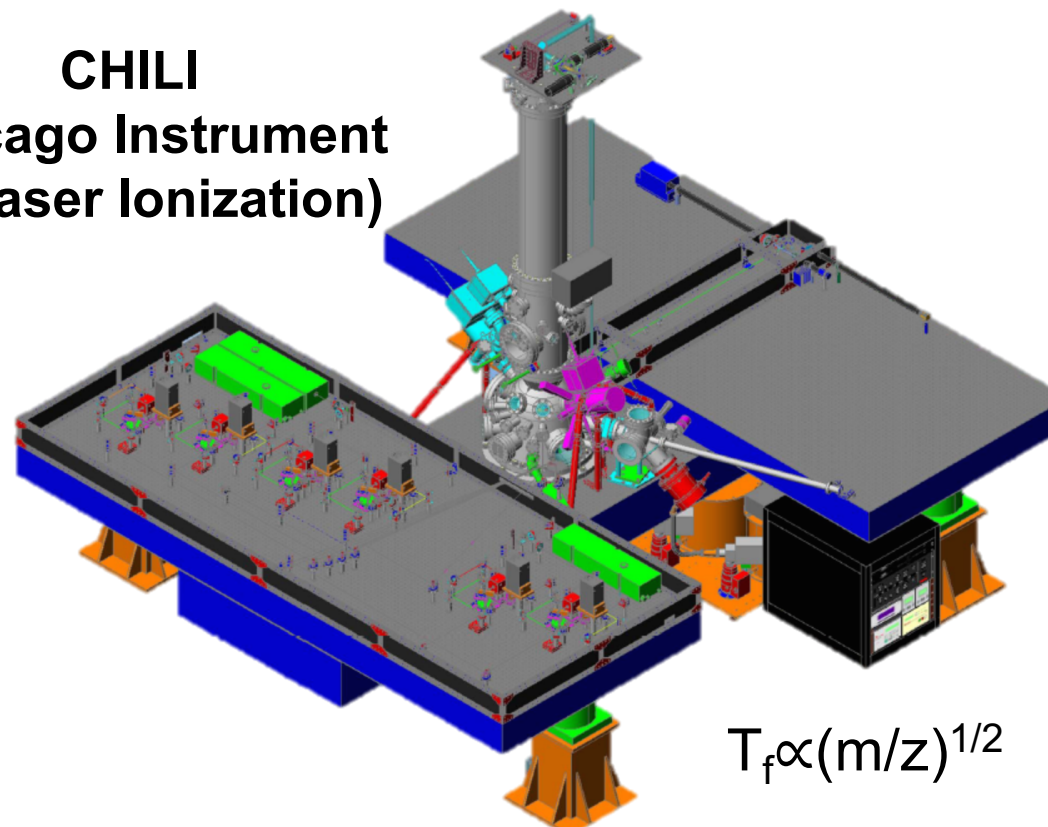


NanoSIMS 50L (double focusing)

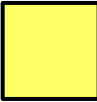


	NanoSIMS 50L	CHILI
Ionization	secondary ions	neutrals+post-ionization
Selectivity	Low	High
Mass Res.	High	Low
Mass Spec.	magnetic sector	time of flight

CHILI (Chicago Instrument for Laser Ionization)

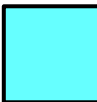


Elements Accessible to SIMS and RIMS

 Secondary Ion Mass Spectrometry
(without significant isobaric interferences)

H																	He
Li	Be											B	C	N	O	F	Ne
Na	Mg											Al	Si	P	S	Cl	Ar
K	Ca	Sc	Ti	V	Cr	Mn	Fe	Co	Ni	Cu	Zn	Ga	Ge	As	Se	Br	Kr
Rb	Sr	Y	Zr	Nb	Mo	Tc	Ru	Rh	Pd	Ag	Cd	In	Sn	Sb	Te	I	Xe
Cs	Ba	La	Hf	Ta	W	Re	Os	Ir	Pt	Au	Hg	Tl	Pb	Bi	Po	At	Rn
Fr	Ra	Ac															

Ce	Pr	Nd	Pm	Sm	Eu	Gd	Tb	Dy	Ho	Er	Tm	Yb	Lu
Th	Pa	U	Np	Pu	Am								

 Resonance Ionization Mass Spectrometry
(concentration down to ppm-ppb level)

Elements Accessible to SIMS and RIMS

Secondary Ion Mass Spectrometry
 (without significant isobaric interferences)

H																	He
Li	Be											B	C	N	O	F	Ne
Na	Mg											Al	Si	P	S	Cl	Ar
K	Ca	Sc	Ti	V	Cr	Mn	Fe	Co	Ni	Cu	Zn	Ga	Ge	As	Se	Br	Kr
Rb	Sr	Y	Zr	Nb	Mo	Tc	Ru	Rh	Pd	Ag	Cd	In	Sn	Sb	Te	I	Xe
Cs	Ba	La	Hf	Ta	W	Re	Os	Ir	Pt	Au	Hg	Tl	Pb	Bi	Po	At	Rn
Fr	Ra	Ac															

Ce	Pr	Nd	Pm	Sm	Eu	Gd	Tb	Dy	Ho	Er	Tm	Yb	Lu
Th	Pa	U	Np	Pu	Am								

Resonance Ionization Mass Spectrometry
 (concentration down to ppm-ppb level)

Outline

1. Analytical Techniques

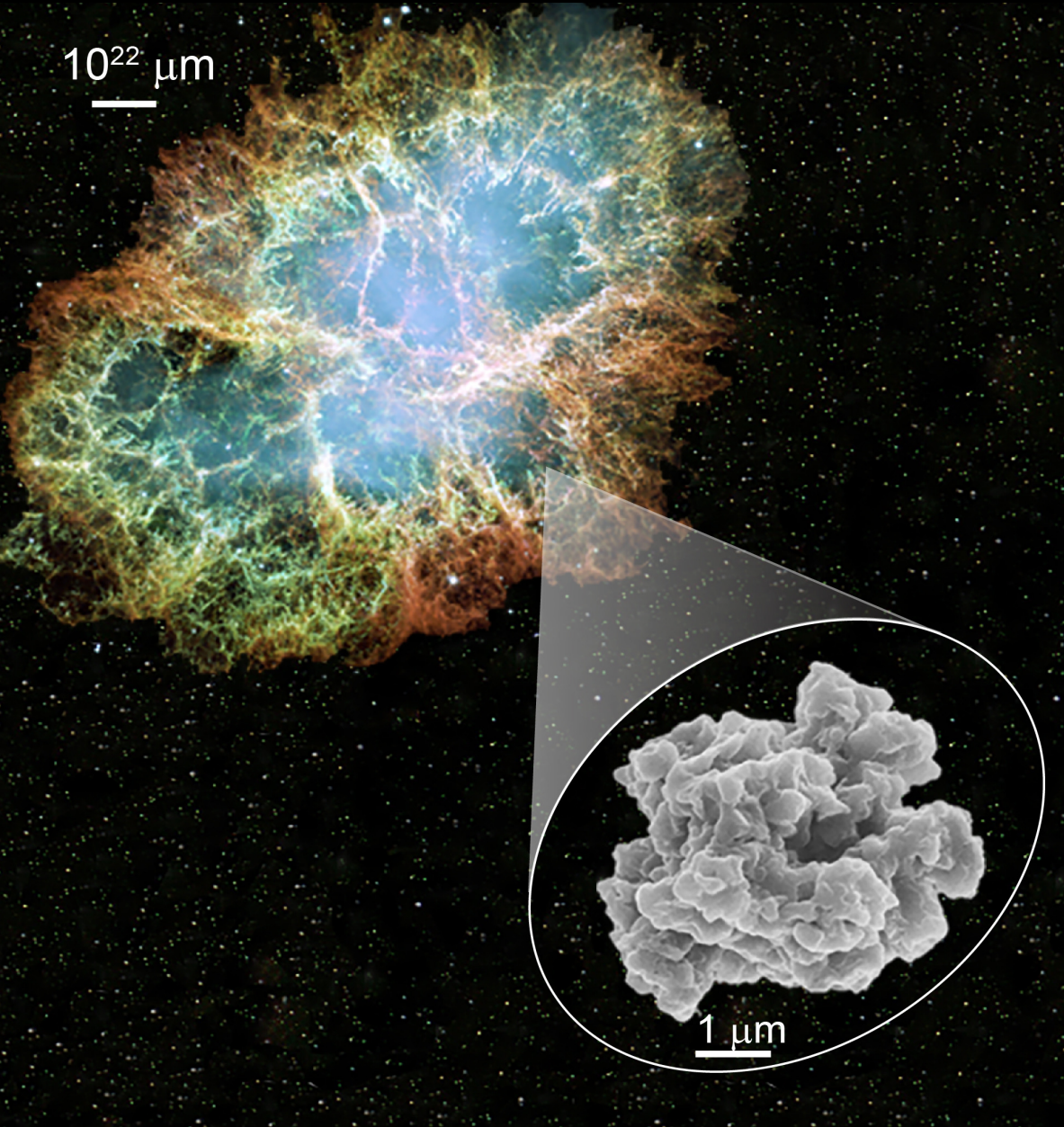
2. Different Types of Grains and Their Stellar Origins

2.1 AGB Dust

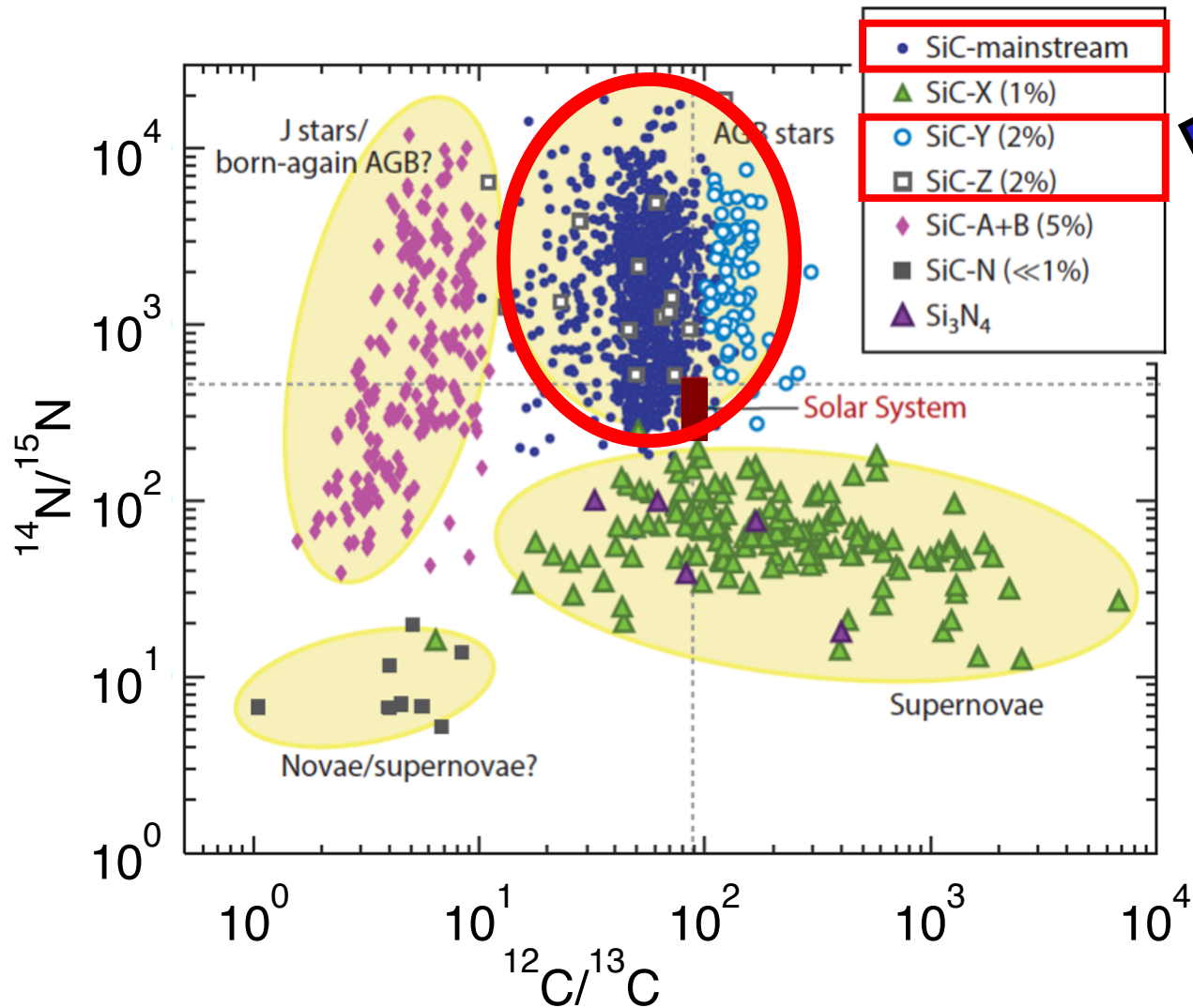
2.2 Type II Supernova Dust

2.3 Mysterious ^{13}C -rich SiC Dust

See Amanda Karakas's lecture on s-process and AGB stars

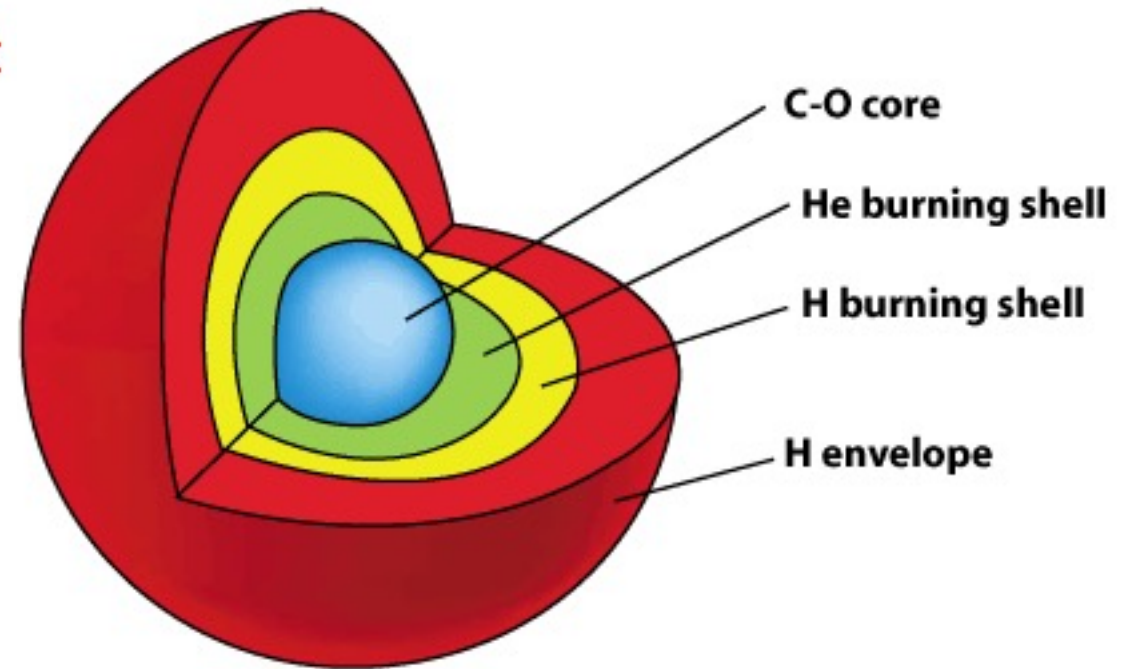
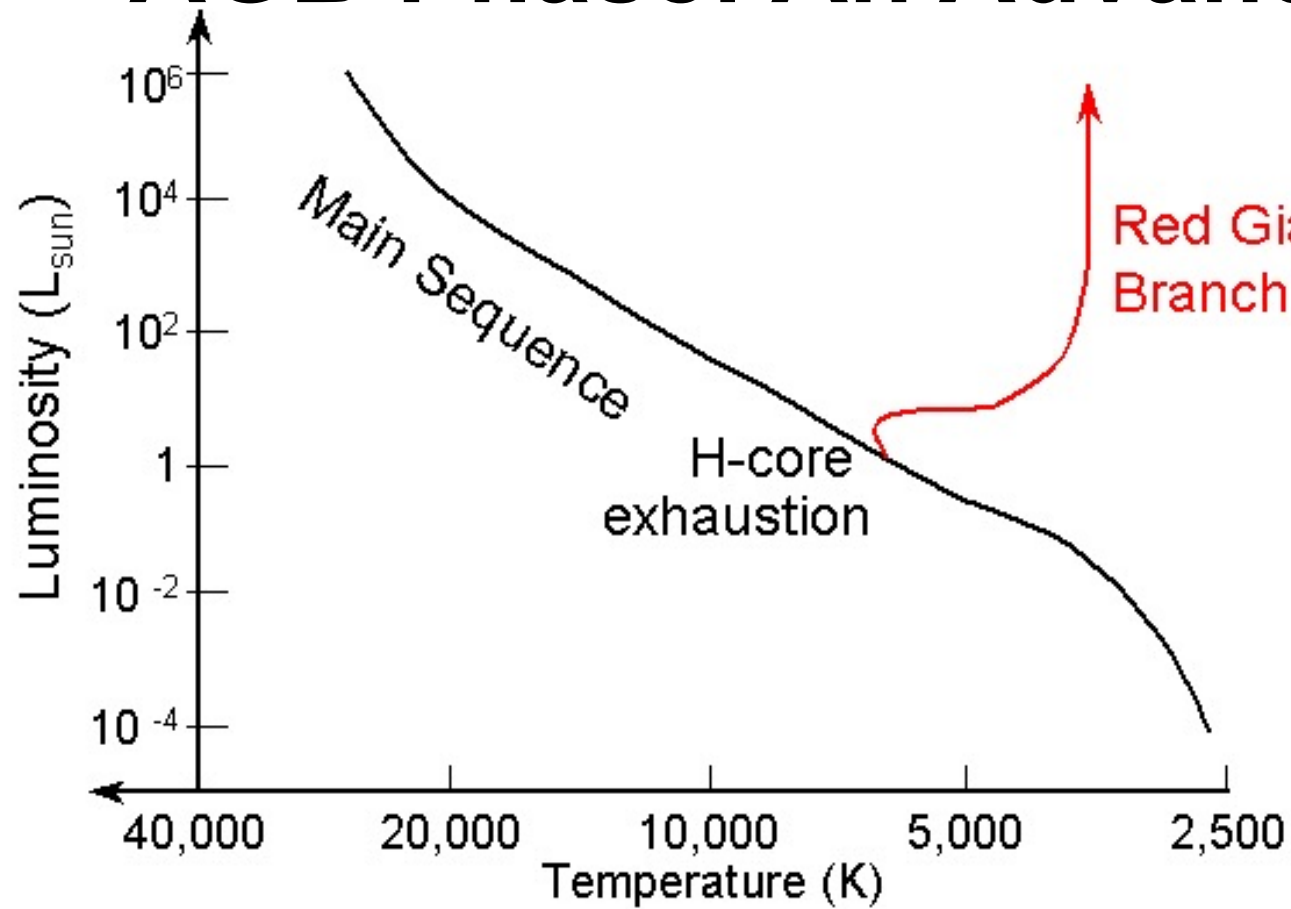


Stellar Origins of Presolar SiC



formed in C-rich envelope of low-mass asymptotic giant branch stars

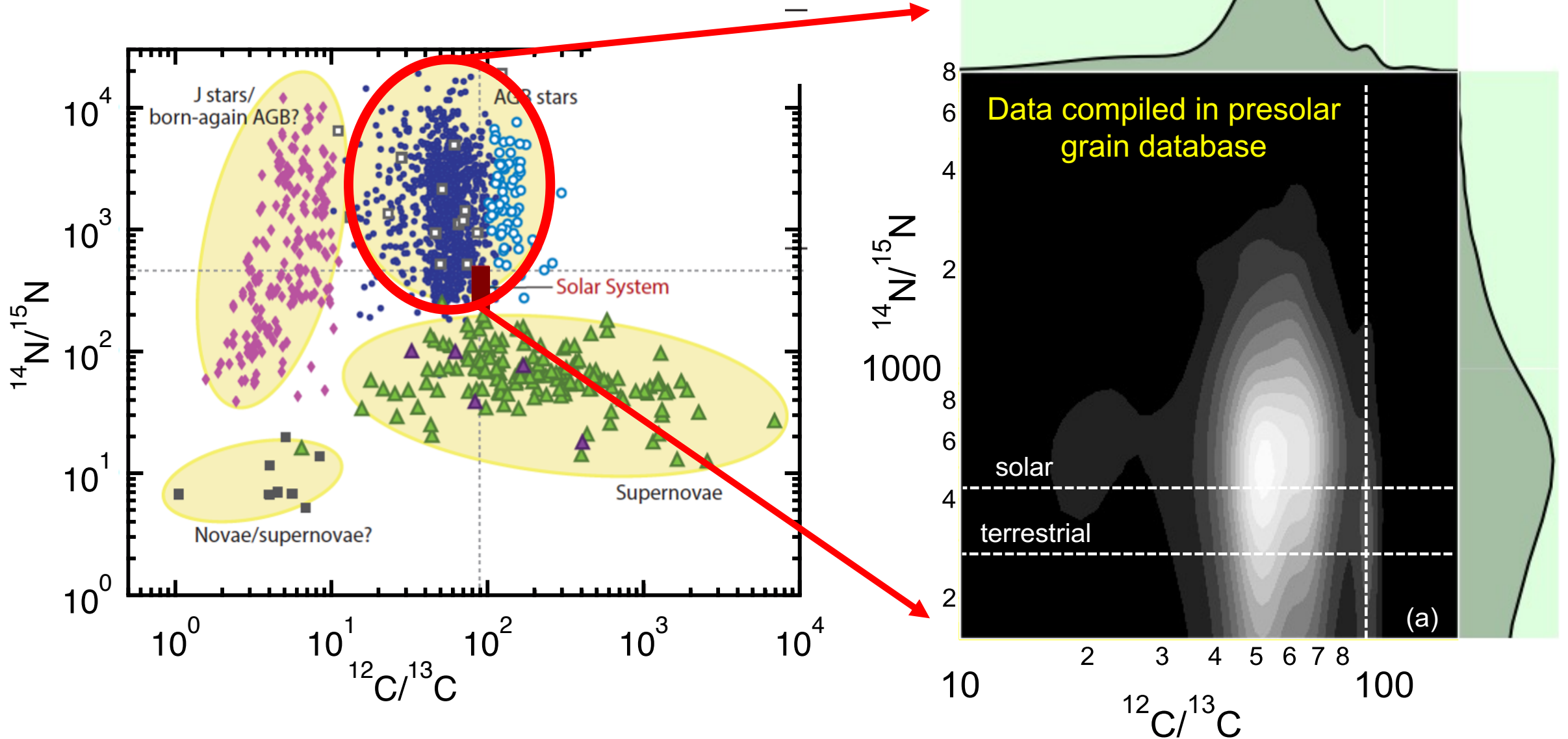
AGB Phase: An Advanced Evolutionary Stage



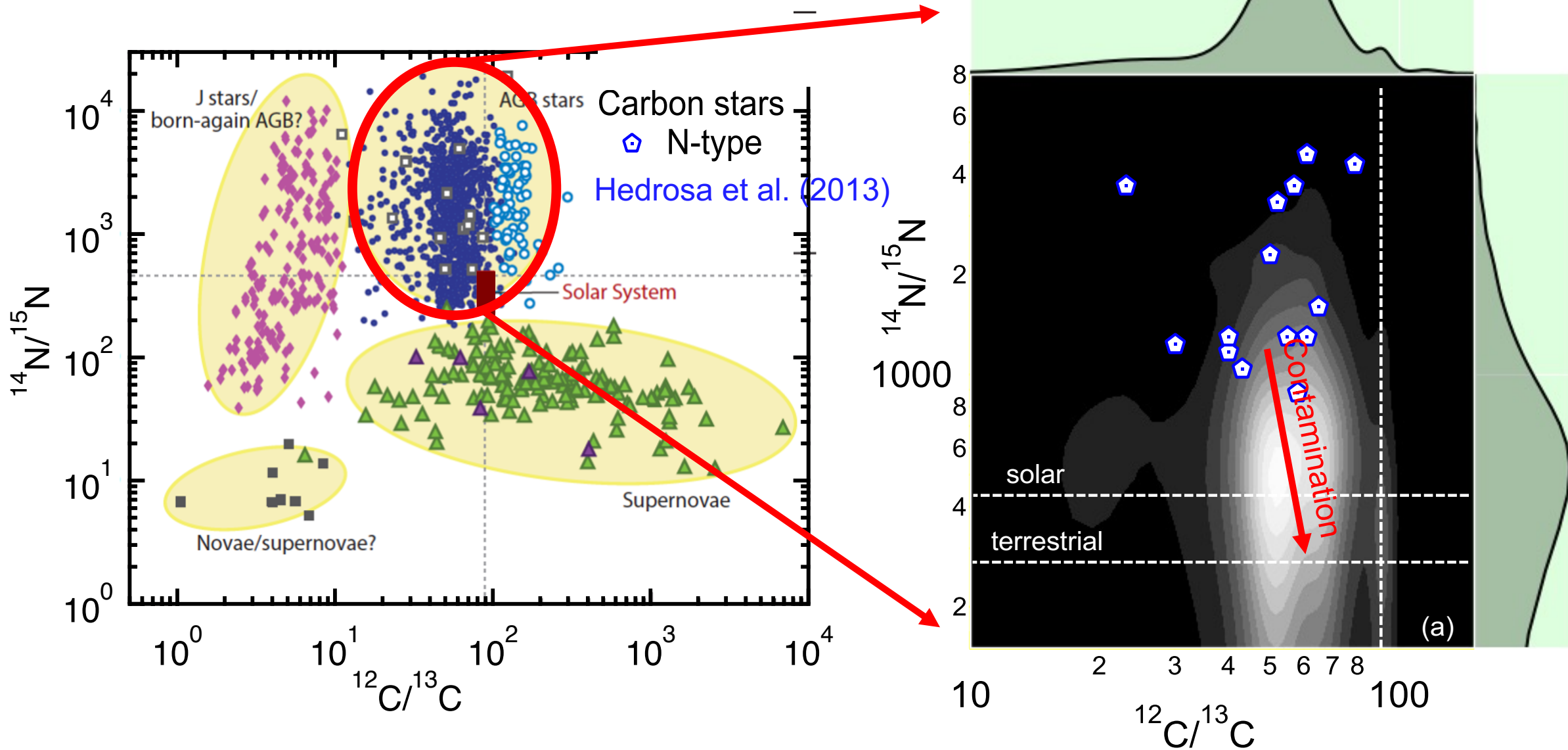
AGB: Asymptotic Giant Branch, an advanced evolutionary stage of stars with masses below $\sim 8 M_{\odot}$.

C-rich AGB: Parent stars of C-rich presolar grains, $\sim 1.5\text{--}3 M_{\odot}$.

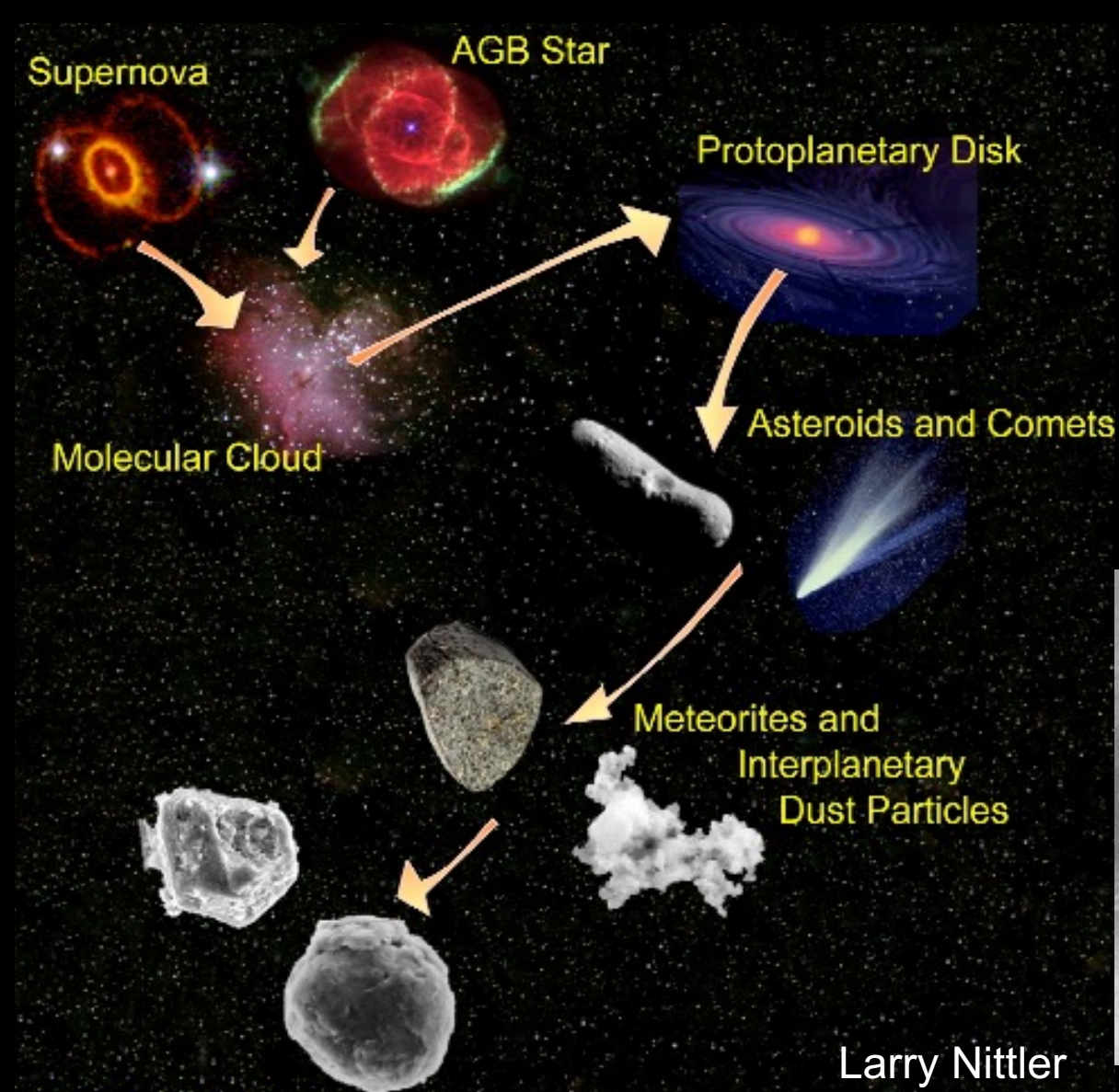
Stellar Origins of SiC from AGB Stars



Grain-Observation Discrepancy



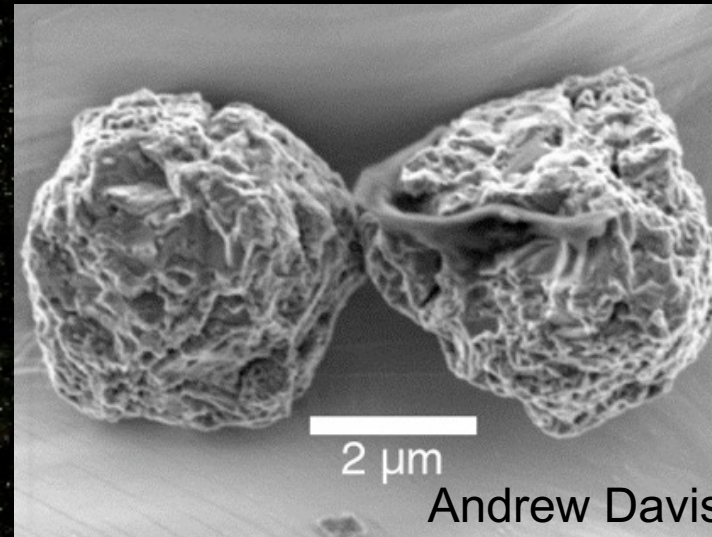
Asteroidal and Terrestrial Contamination



Larry Nittler



Additional terrestrial contamination caused by e.g., acid dissolution and laboratory analysis.

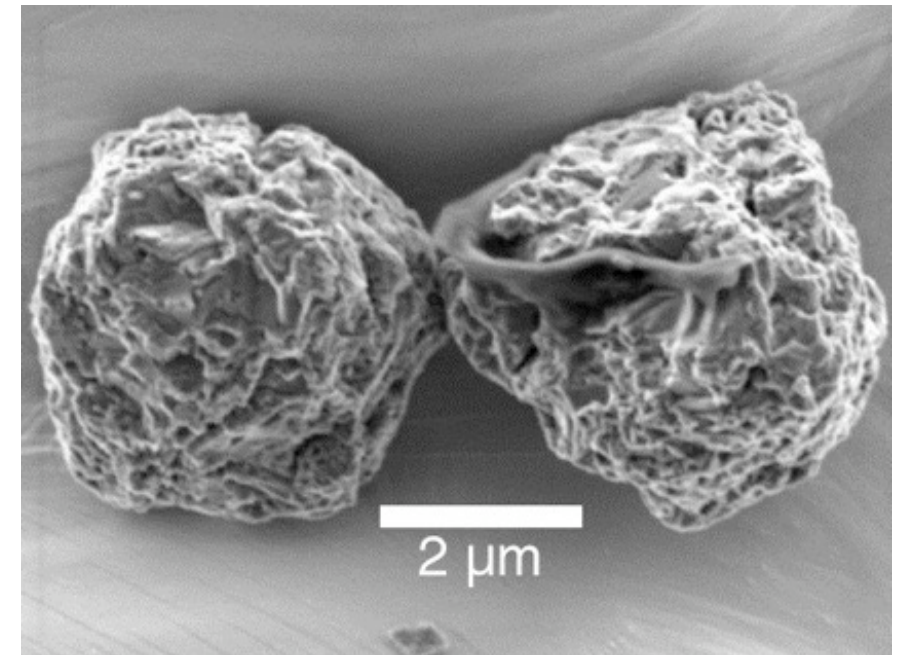
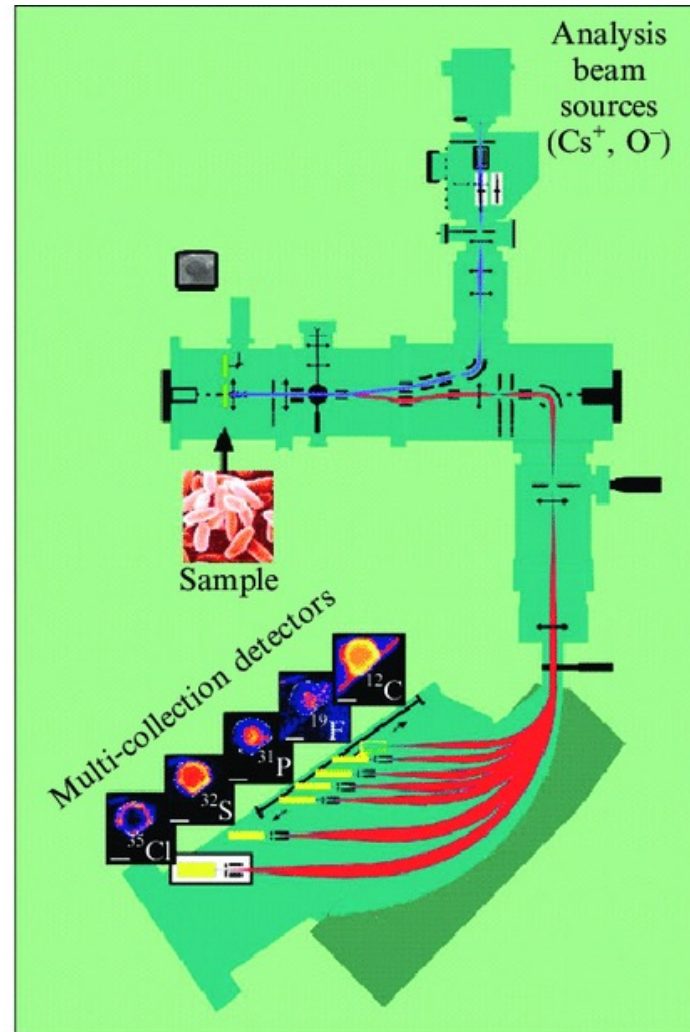
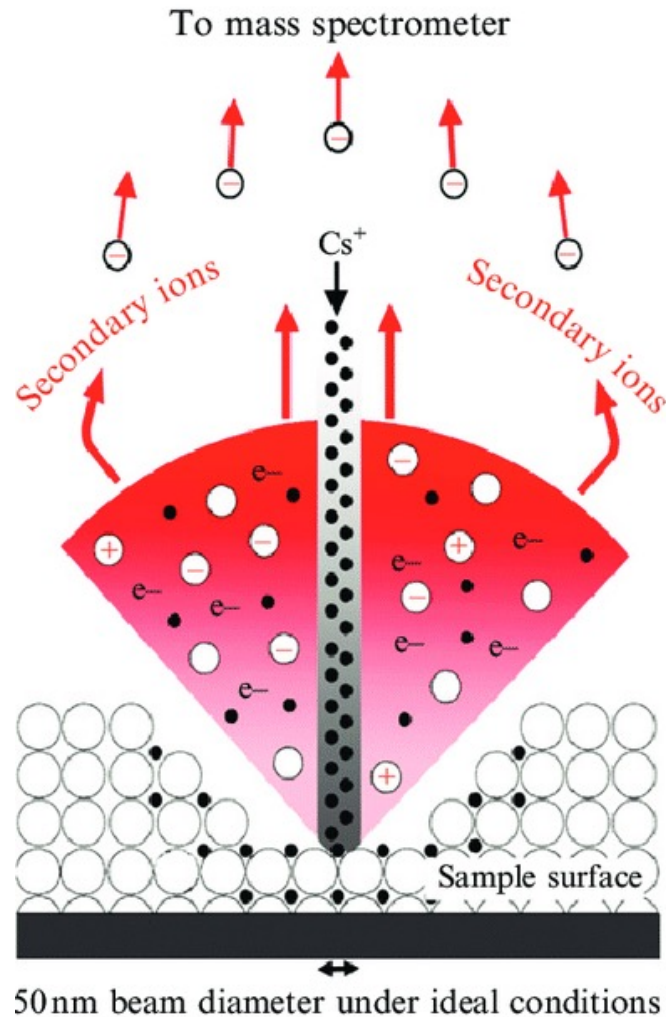


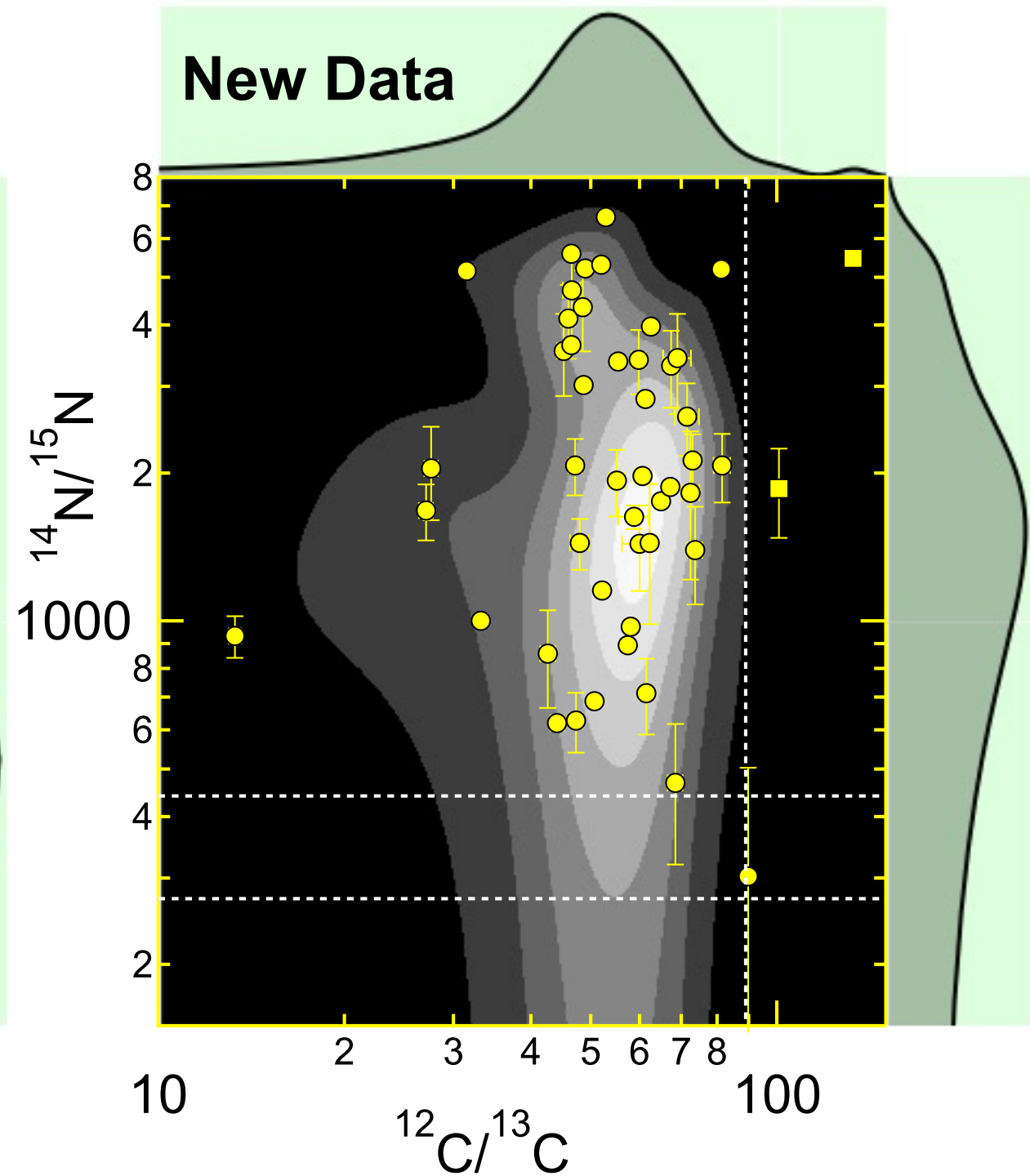
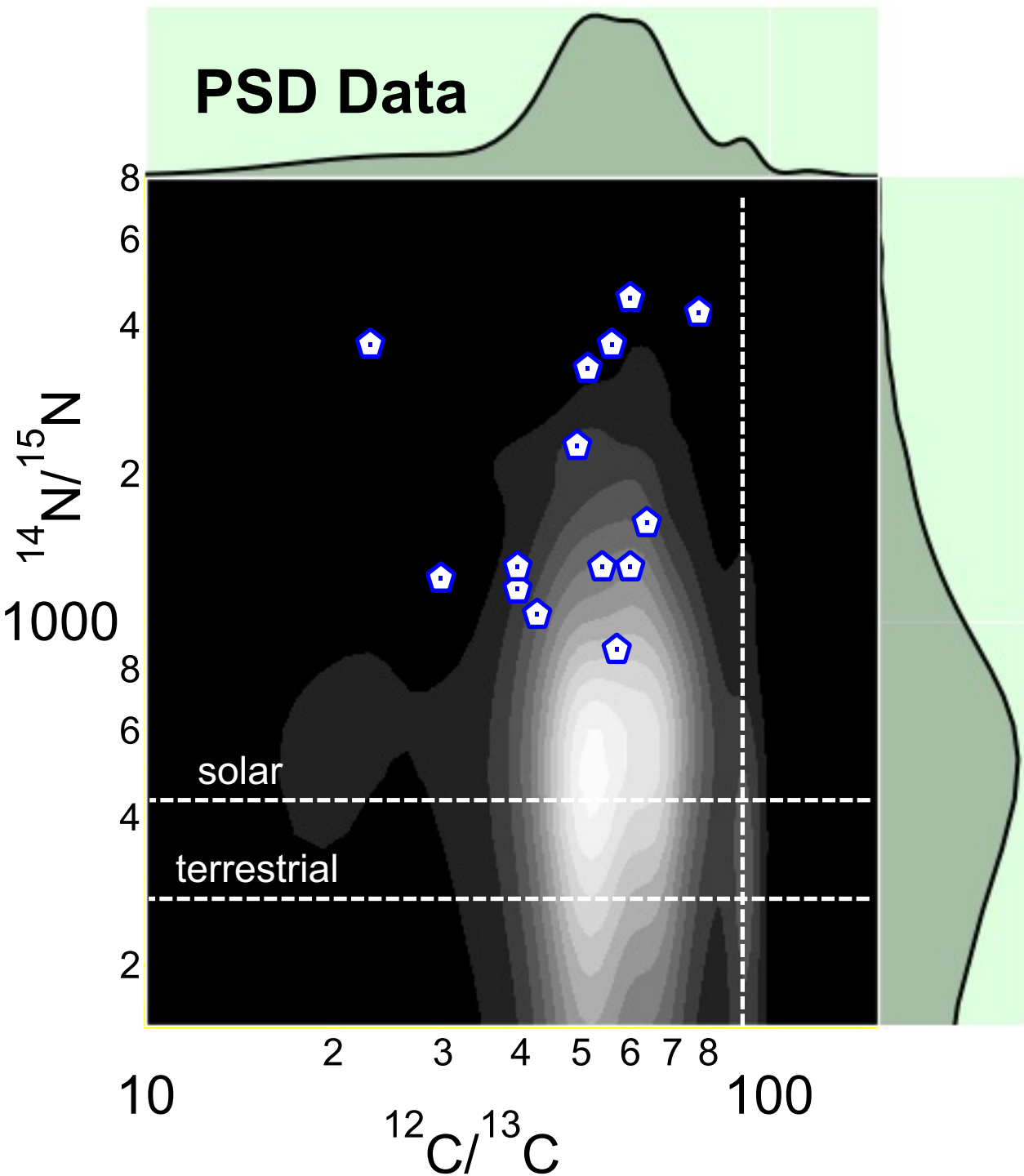
Andrew Davis

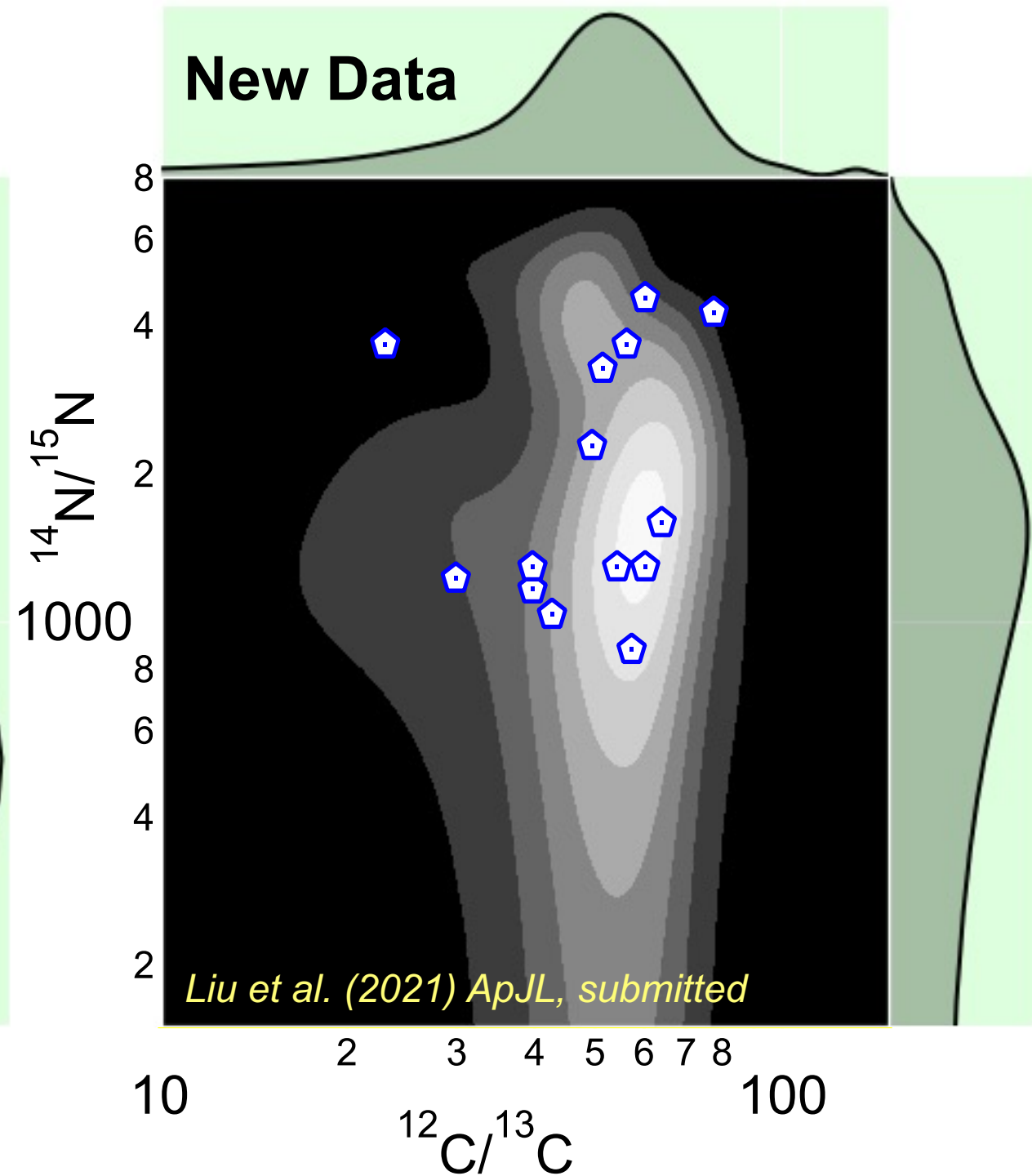
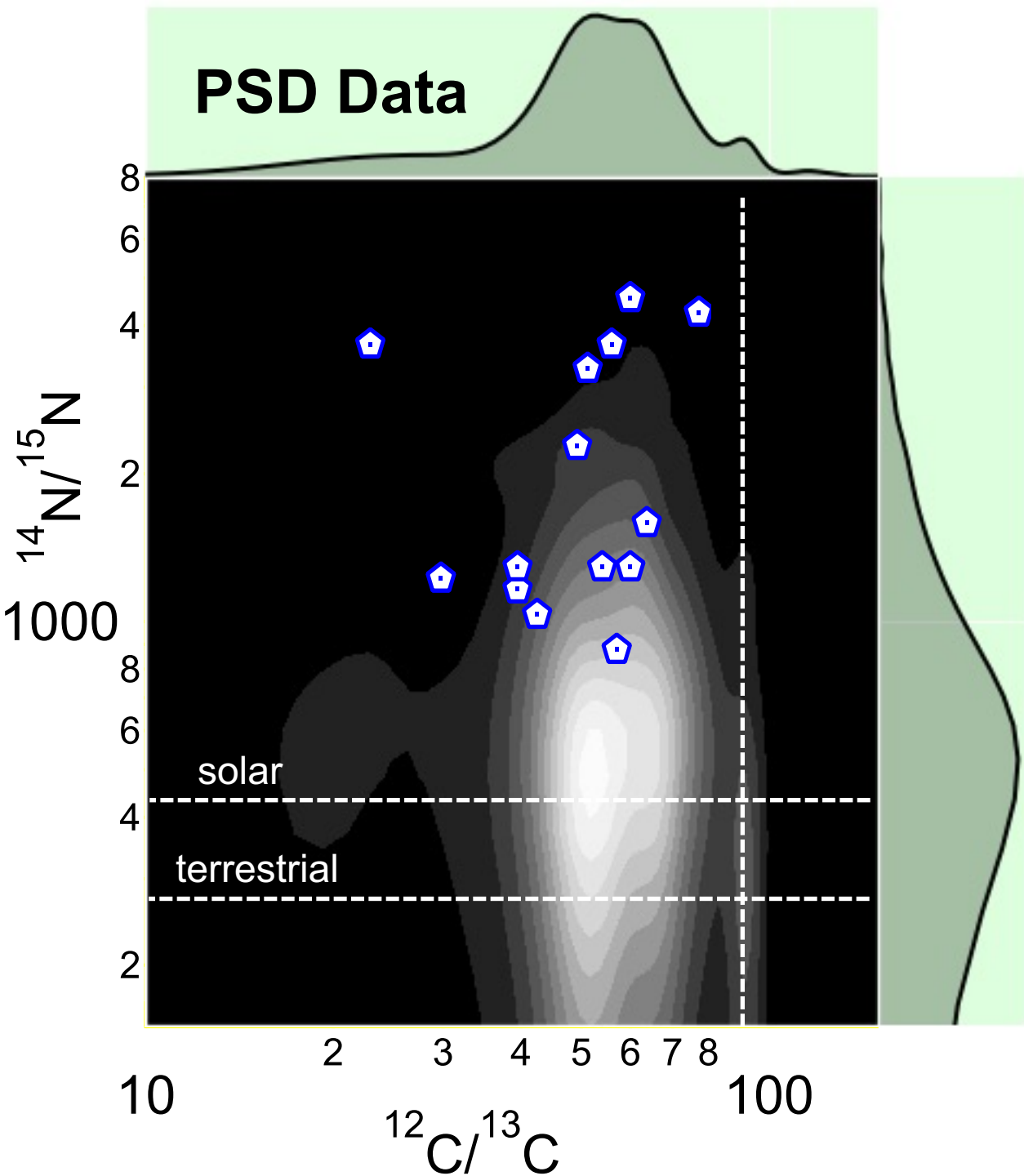
A mainstream SiC coated by organic gunk.

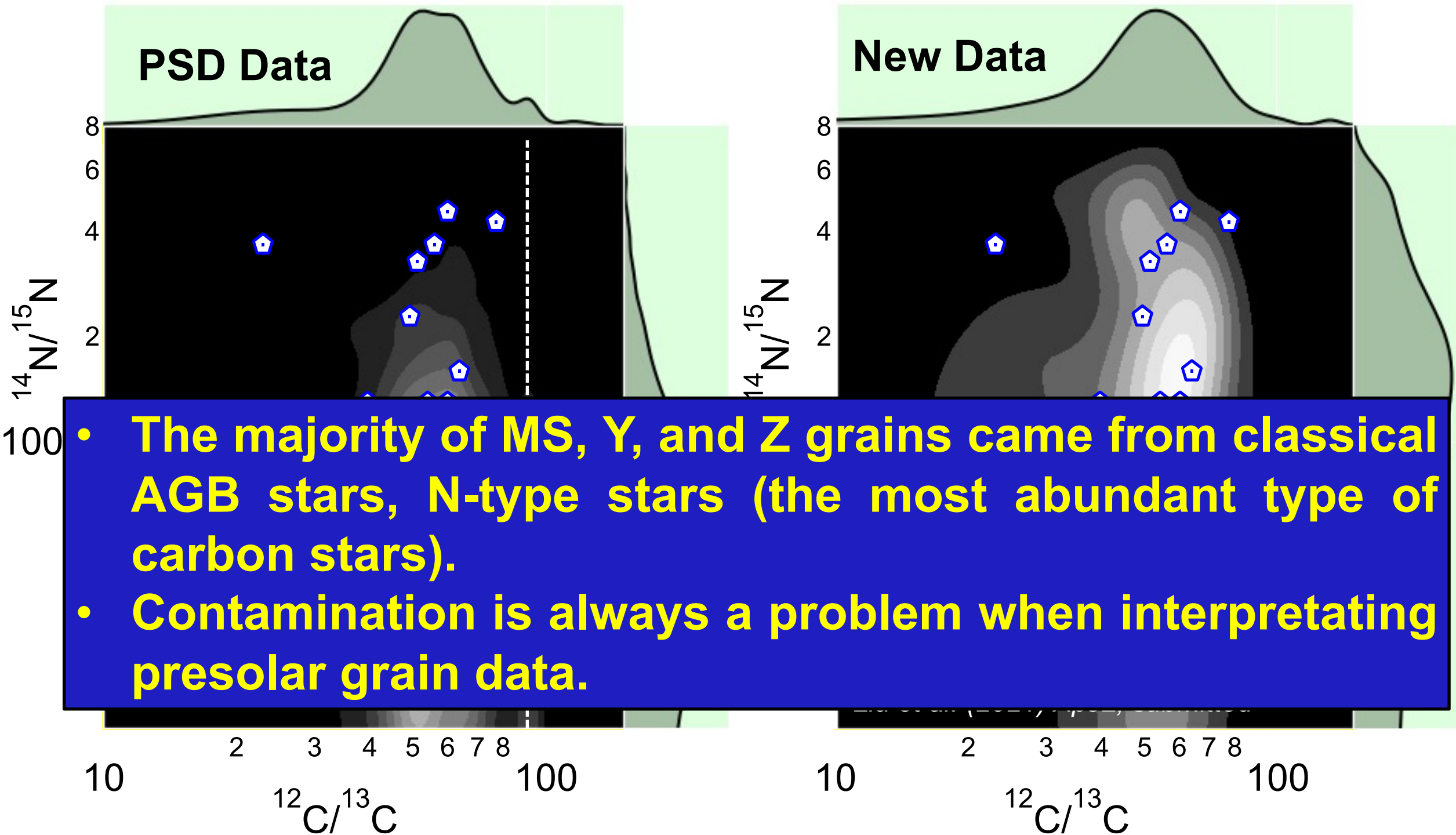
Approach to Suppress Contamination

Extensive Sputtering









AGB Stars: main stellar site for s-process

SPECTROSCOPIC OBSERVATIONS OF STARS OF CLASS S

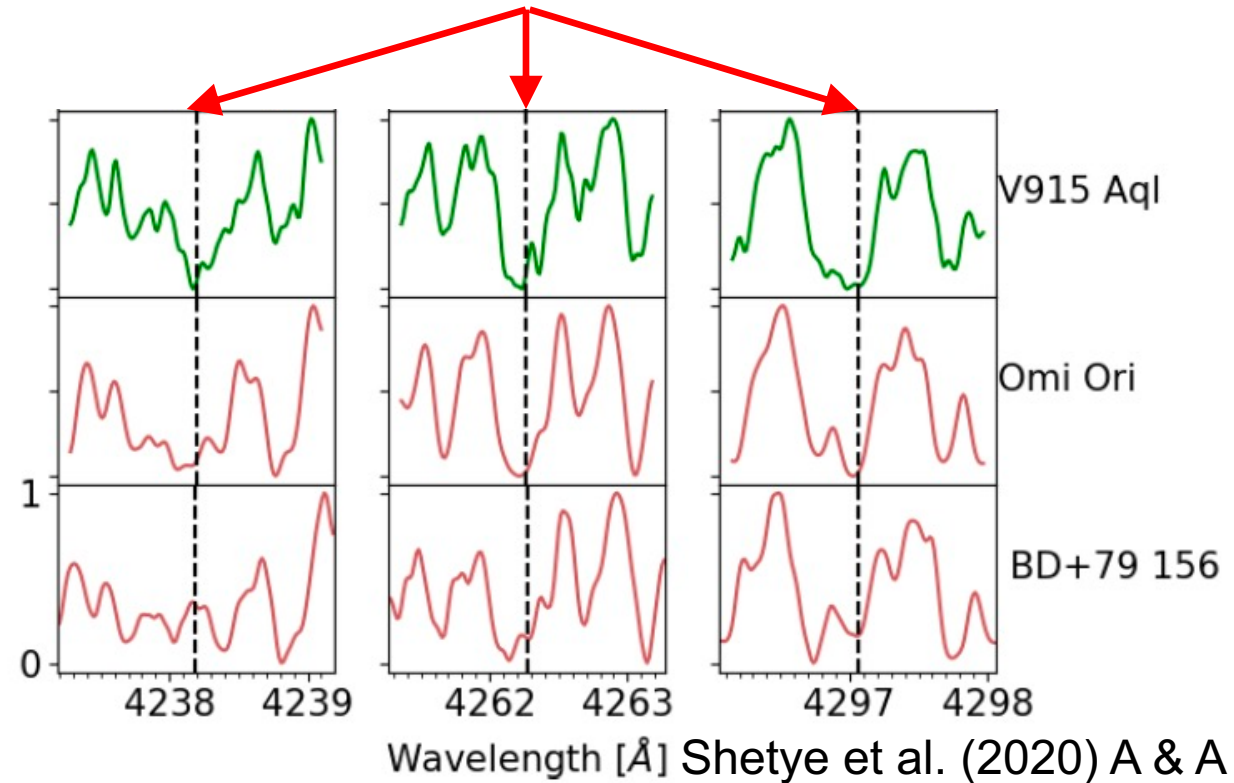
PAUL W. MERRILL
 MOUNT WILSON AND PALOMAR OBSERVATORIES
 CARNEGIE INSTITUTION OF WASHINGTON
 CALIFORNIA INSTITUTE OF TECHNOLOGY
 Received February 27, 1952

ABSTRACT

This paper presents a brief survey of S-type spectra based largely on spectrograms with dispersion 9 Å/mm of eight stars obtained by I. S. Bowen with the 200-inch telescope. The intensities of several groups of absorption lines and bands and of the more important emission lines are compared in various stars. Radial velocities from both bright and dark lines and a supplementary list of absorption lines identified in the green region are included. The remarkable behavior of certain bright lines of V I and of Cr in the spectrum of R Cygni is described.

Ru98	Ru99	Ru100	Ru101	Ru102
0+	5/2+	0+	5/2+	0+
1.88	12.7	12.6	17.0	31.6
Tc97 2.6E6 y 9/2+ *	Tc98 4.2E+6 y (6)+	Tc99 2.111E+5 y 9/2+ *	Tc100 15.8 s 1+	Tc101 14.22 m (9/2)+
EC	β-	β-	β-	β-
Mo96	Mo97	Mo98	Mo99	Mo100
0+	5/2+	0+	1/2+	0+
16.68	9.55	24.13	65.94 h β-	1.2E19 y ββ-
			9.63	

Tc absorption lines

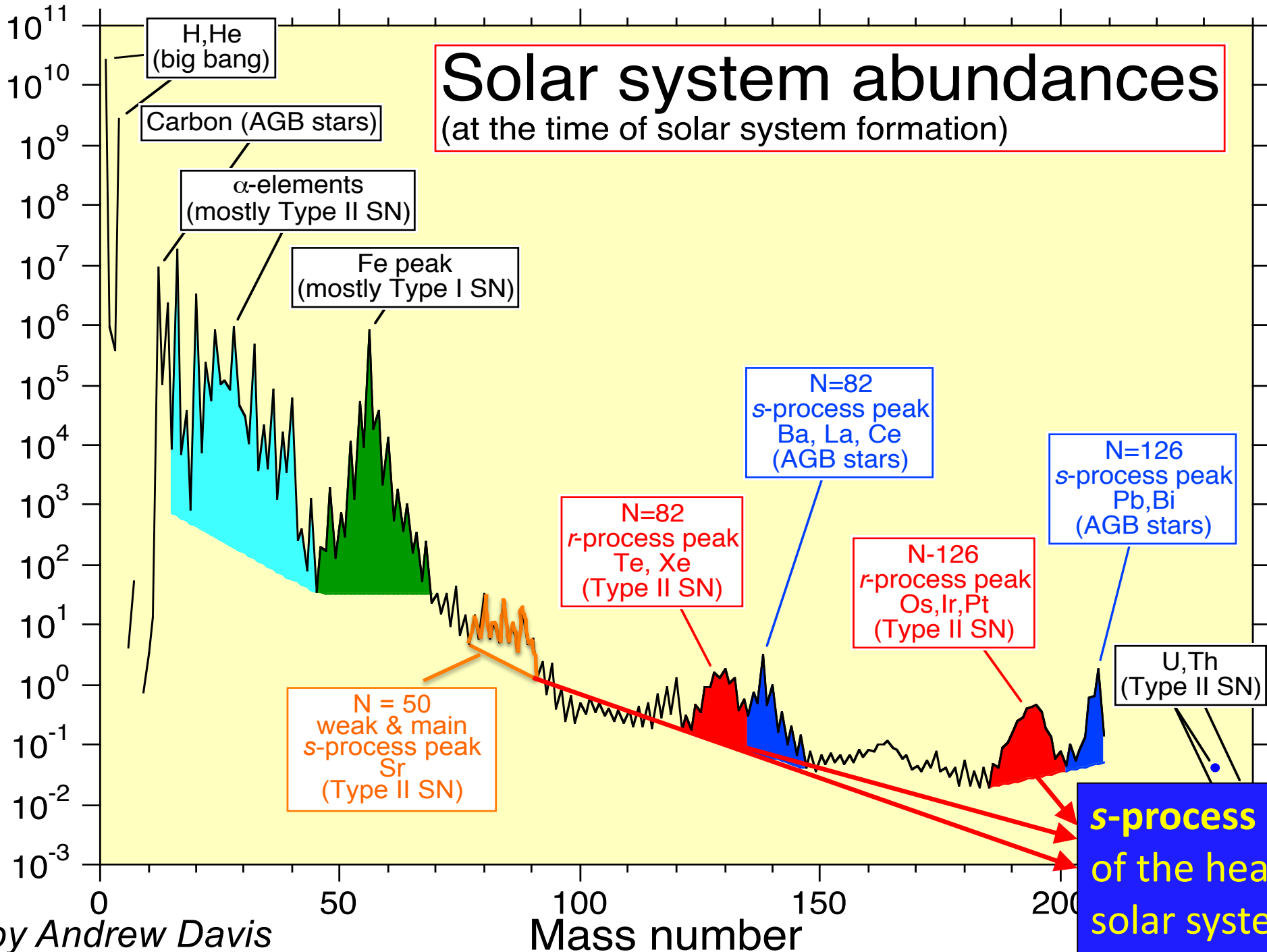


In situ production of Tc inside AGB stars!

Abundance relative to 10^6 silicon

Solar system abundances

(at the time of solar system formation)



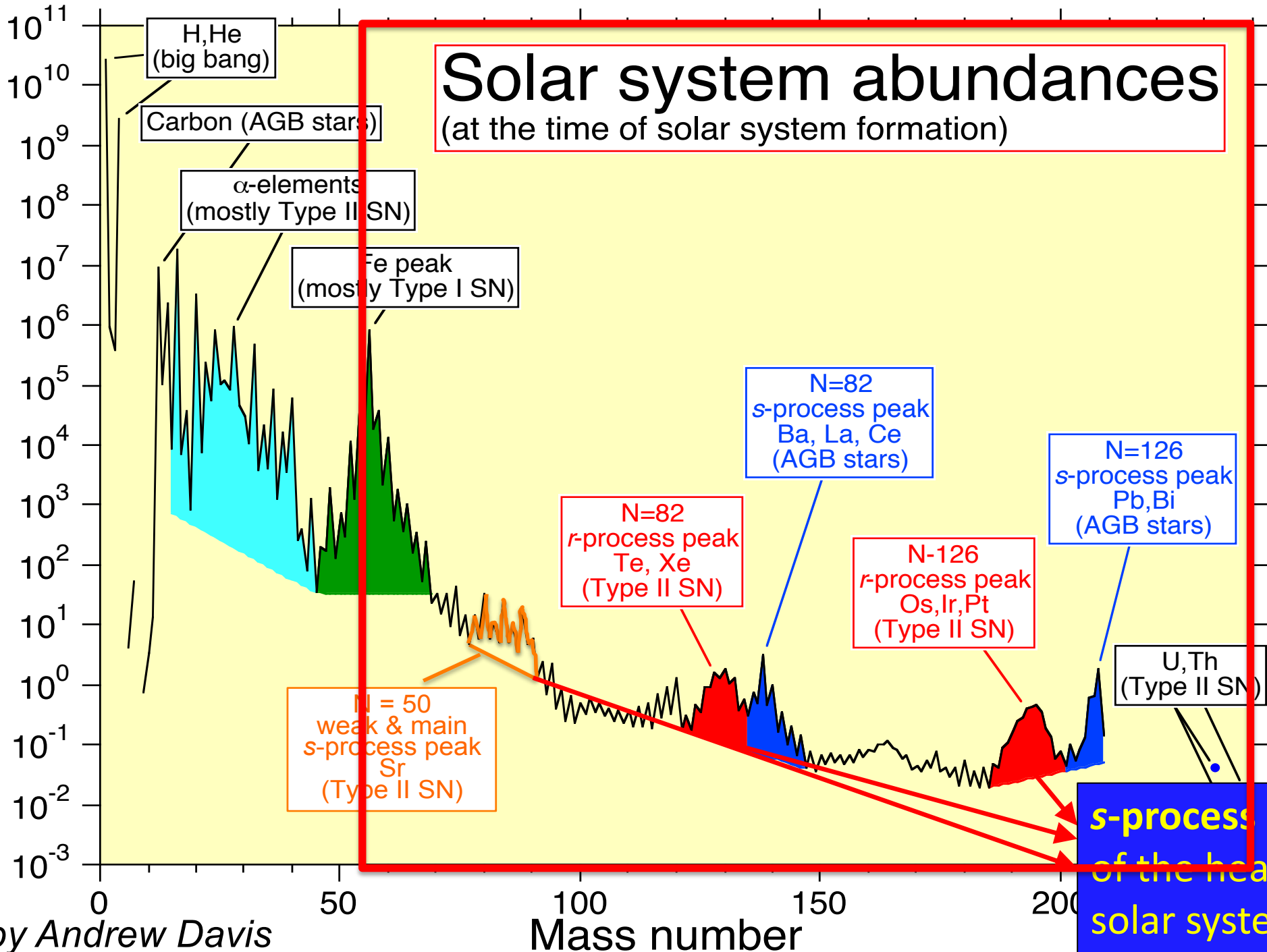
by Andrew Davis

Mass number

s-process contribution: half of the heavy elements in the solar system.

Abundance relative to 10^6 silicon

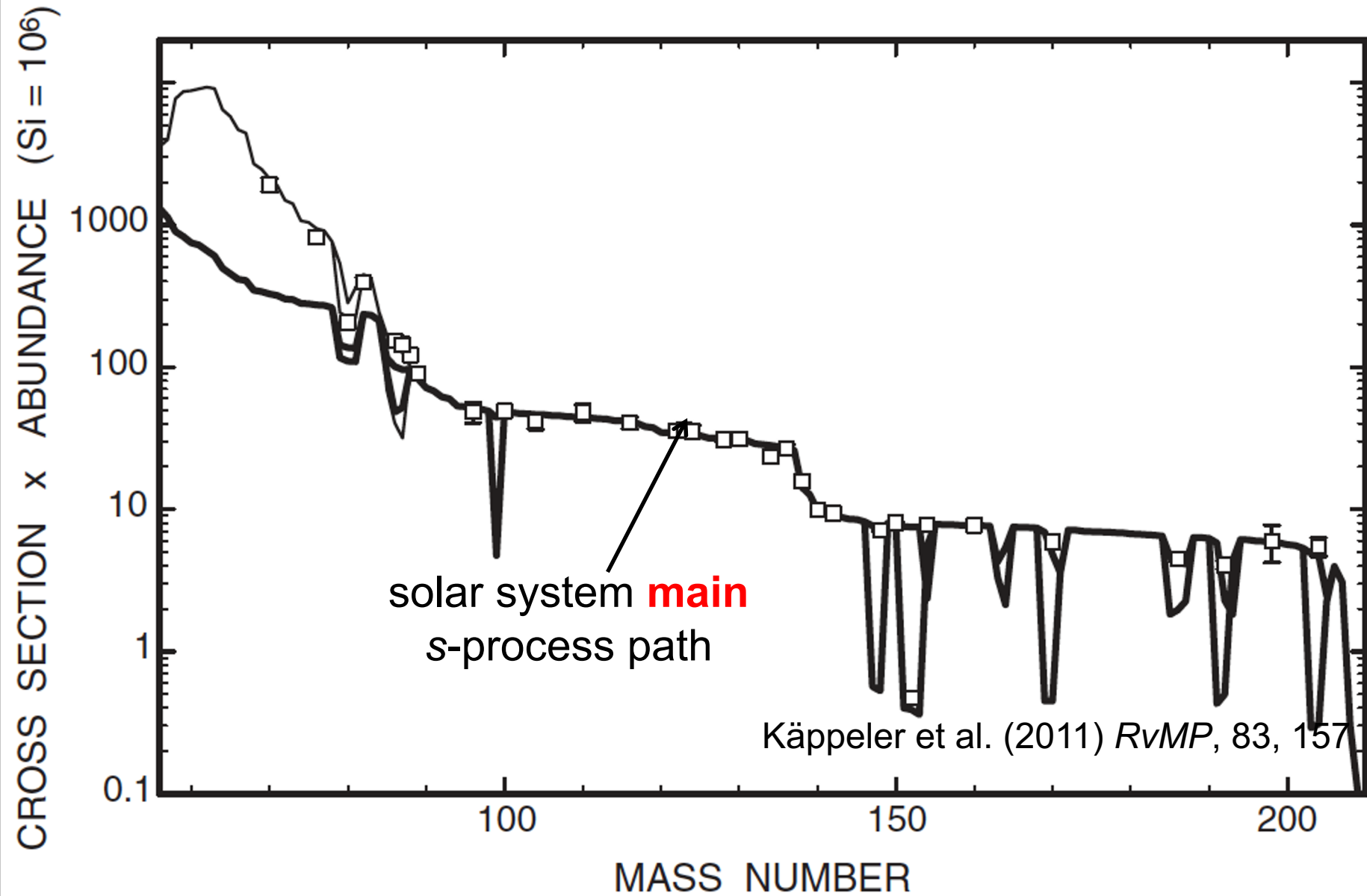
Solar system abundances (at the time of solar system formation)



s-process contribution: half of the heavy elements in the solar system.

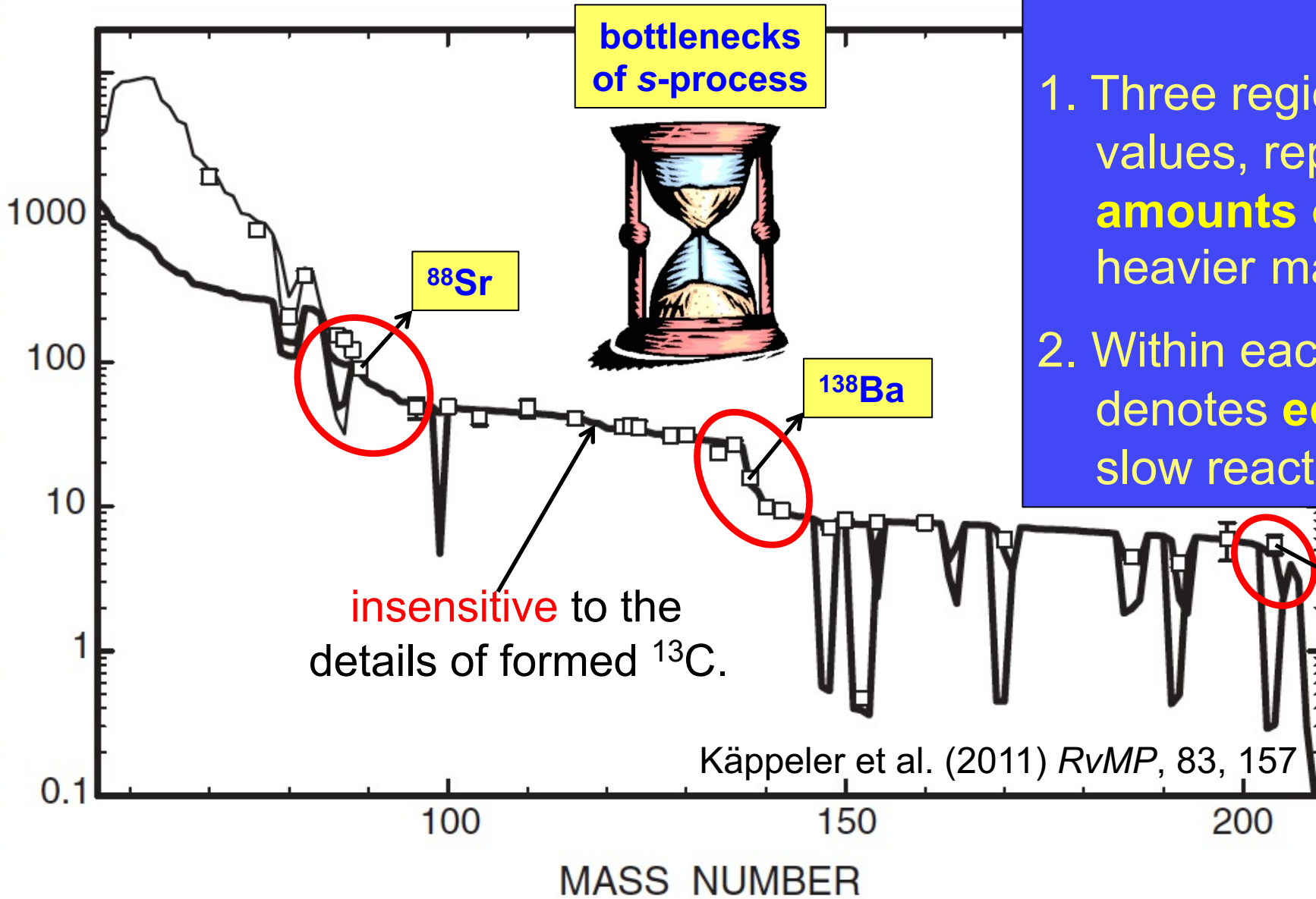
by Andrew Davis

s-Process: slow neutron-capture process



s-Process: slow neutron-capture process

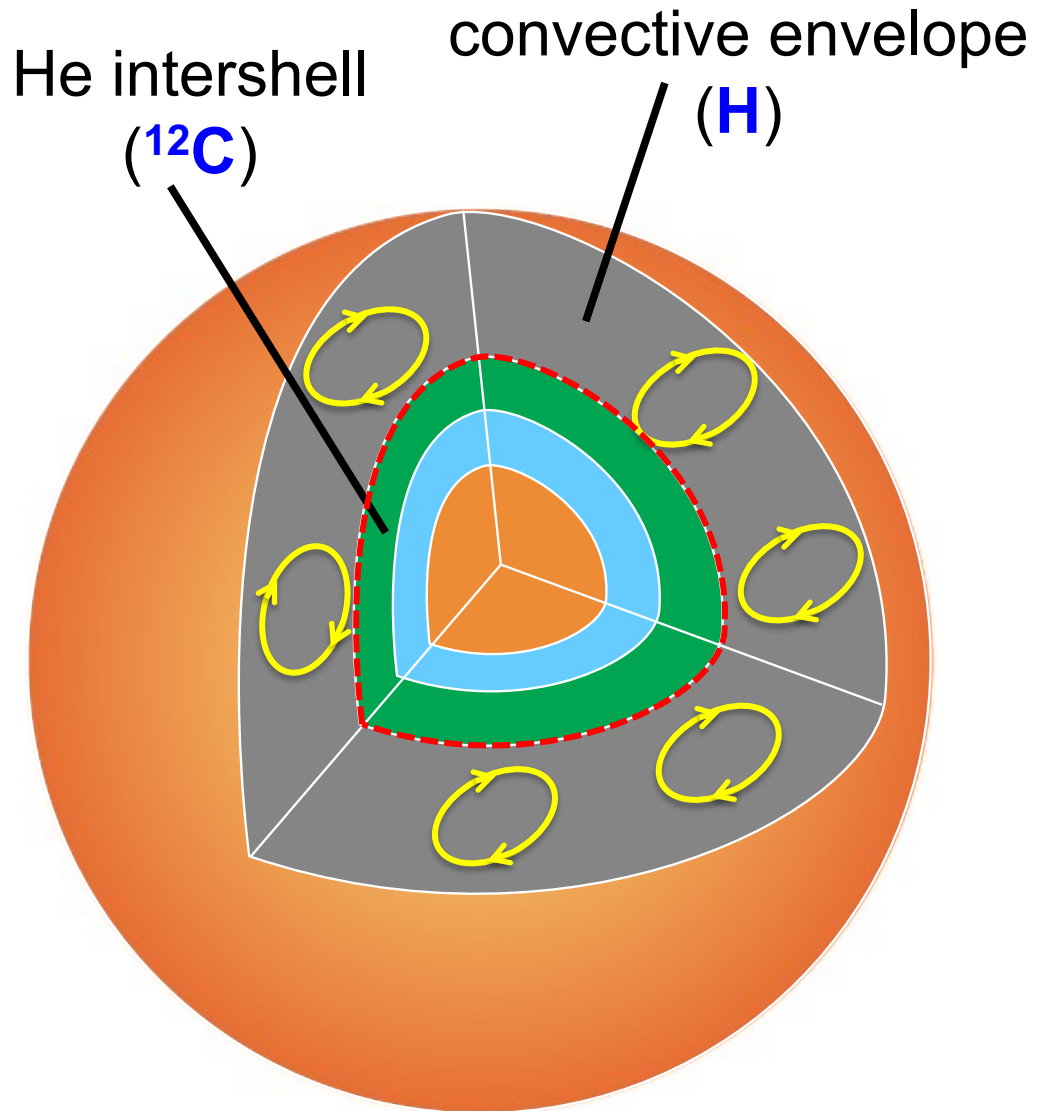
CROSS SECTION x ABUNDANCE ($\Sigma_i = 10^6$)



Features

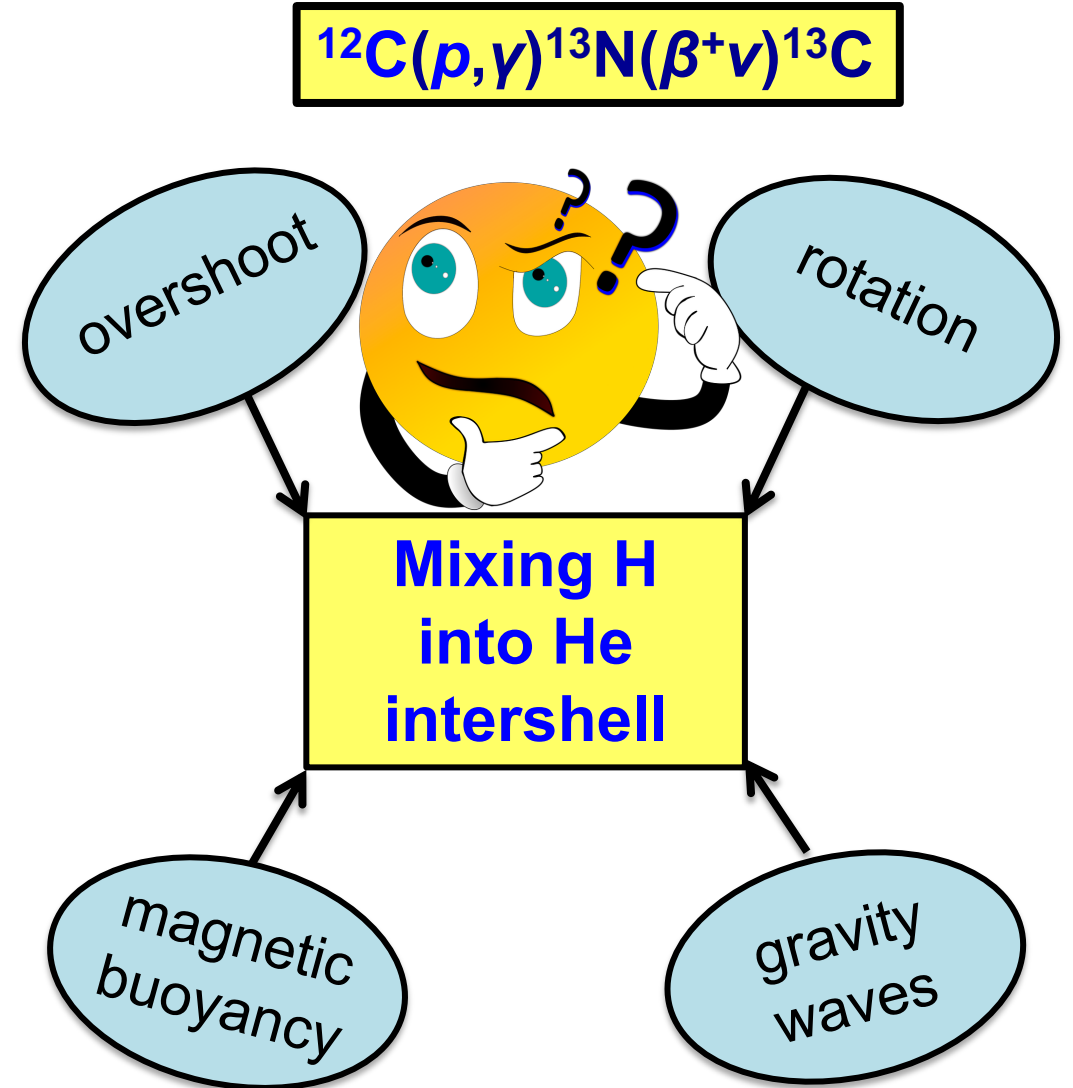
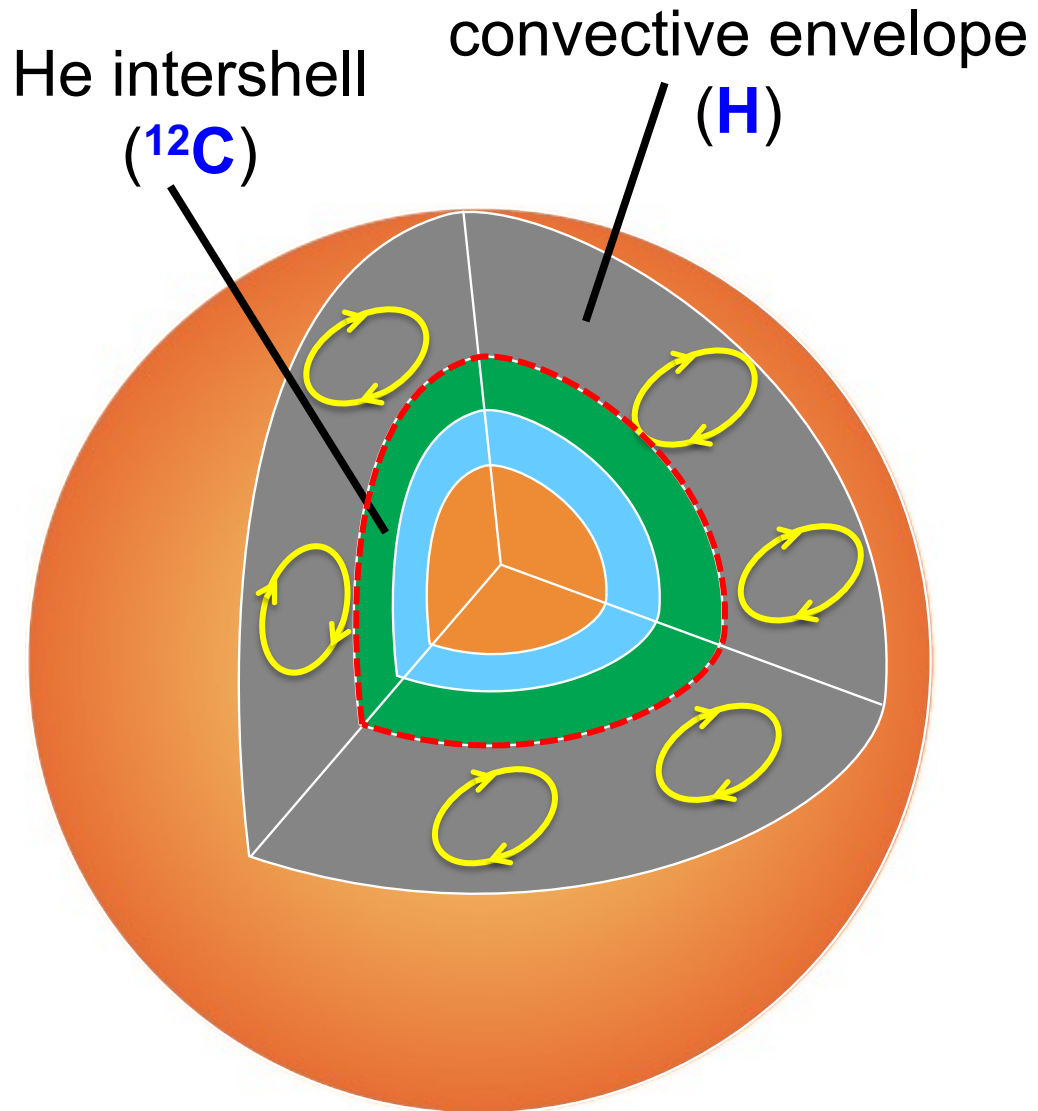
1. Three regions with decreasing γ values, representing **decreasing amounts of neutrons** reaching heavier mass regions.
2. Within each region, constant γ denotes **equilibrium** due to the slow reaction rates.

Major Neutron Source for s-Process: $^{13}\text{C}(\alpha, n)^{16}\text{O}$

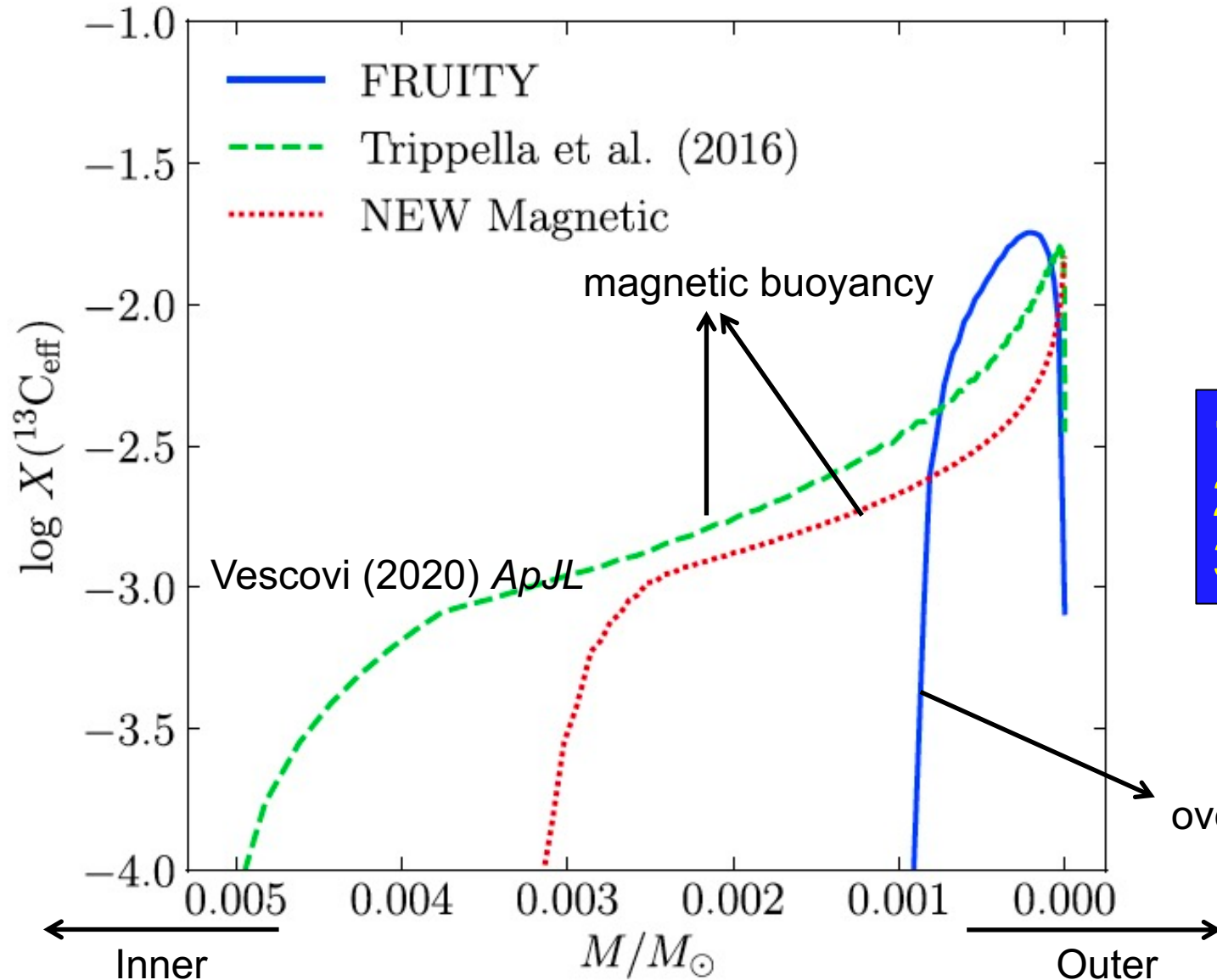


$^{13}\text{C}(\alpha, n)^{16}\text{O}$: providing neutrons with a density of 10^7 to 10^8 cm^{-3} , in agreement with solar system s-process distribution and astronomical observations of s-process elements.

Problem for AGB Stellar Modelers: local mixing of H into He-intershell



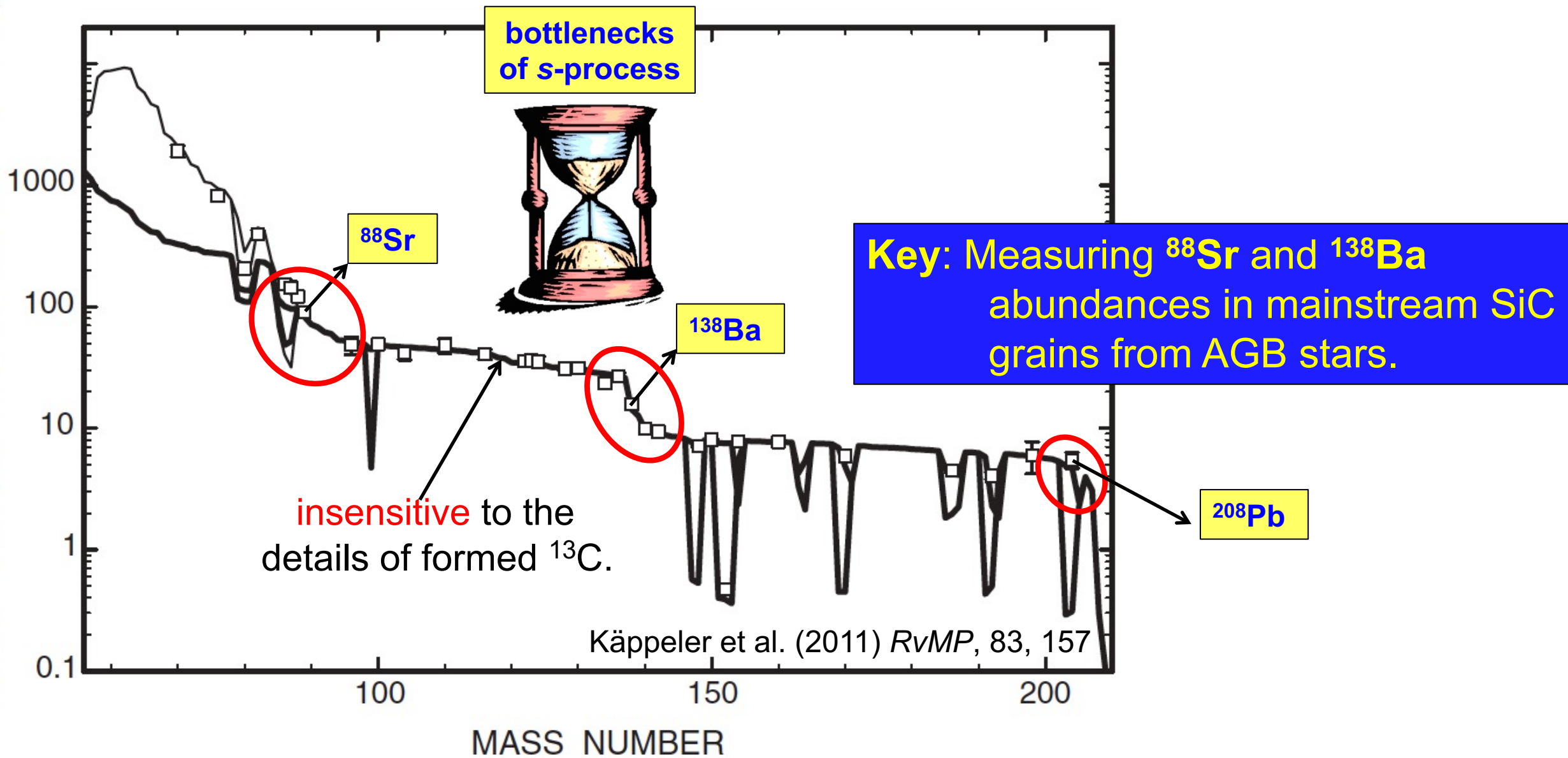
Discrepant Modeling Results for Mixing



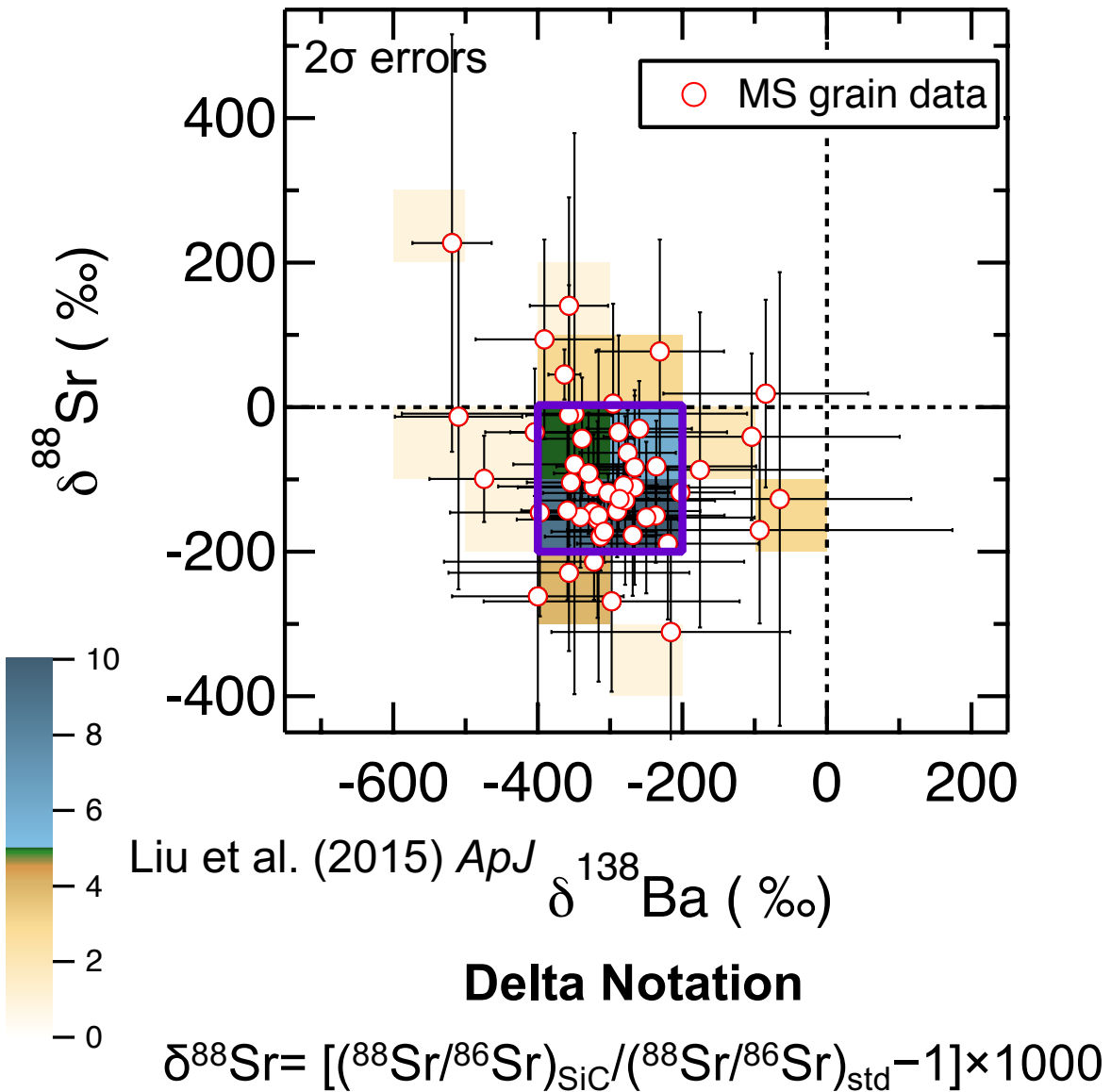
1. Varying mixing depths.
2. Varying ^{13}C mixing profiles.
3. Varying ^{13}C concentrations.

Smoking Guns for Constraining ^{13}C Formation

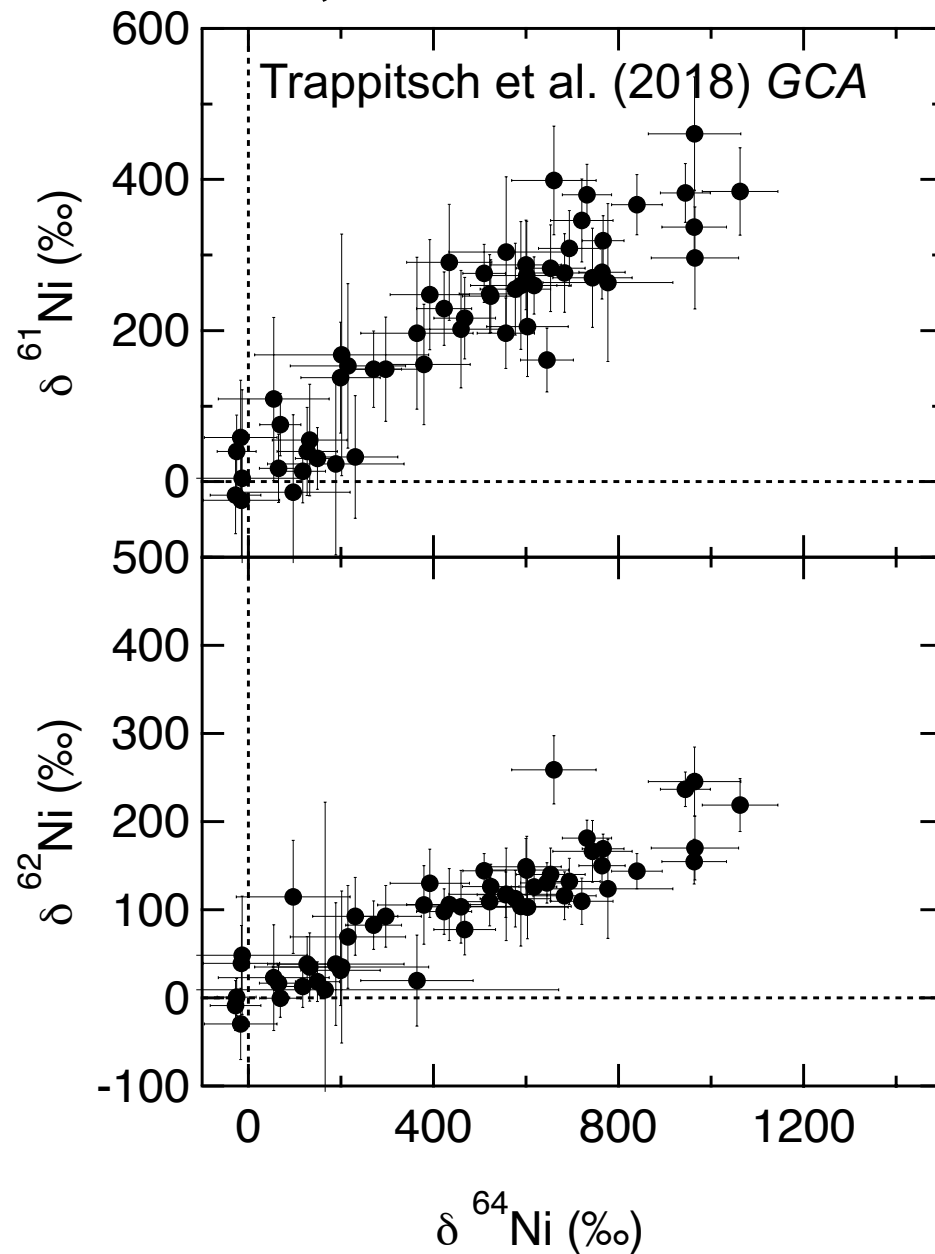
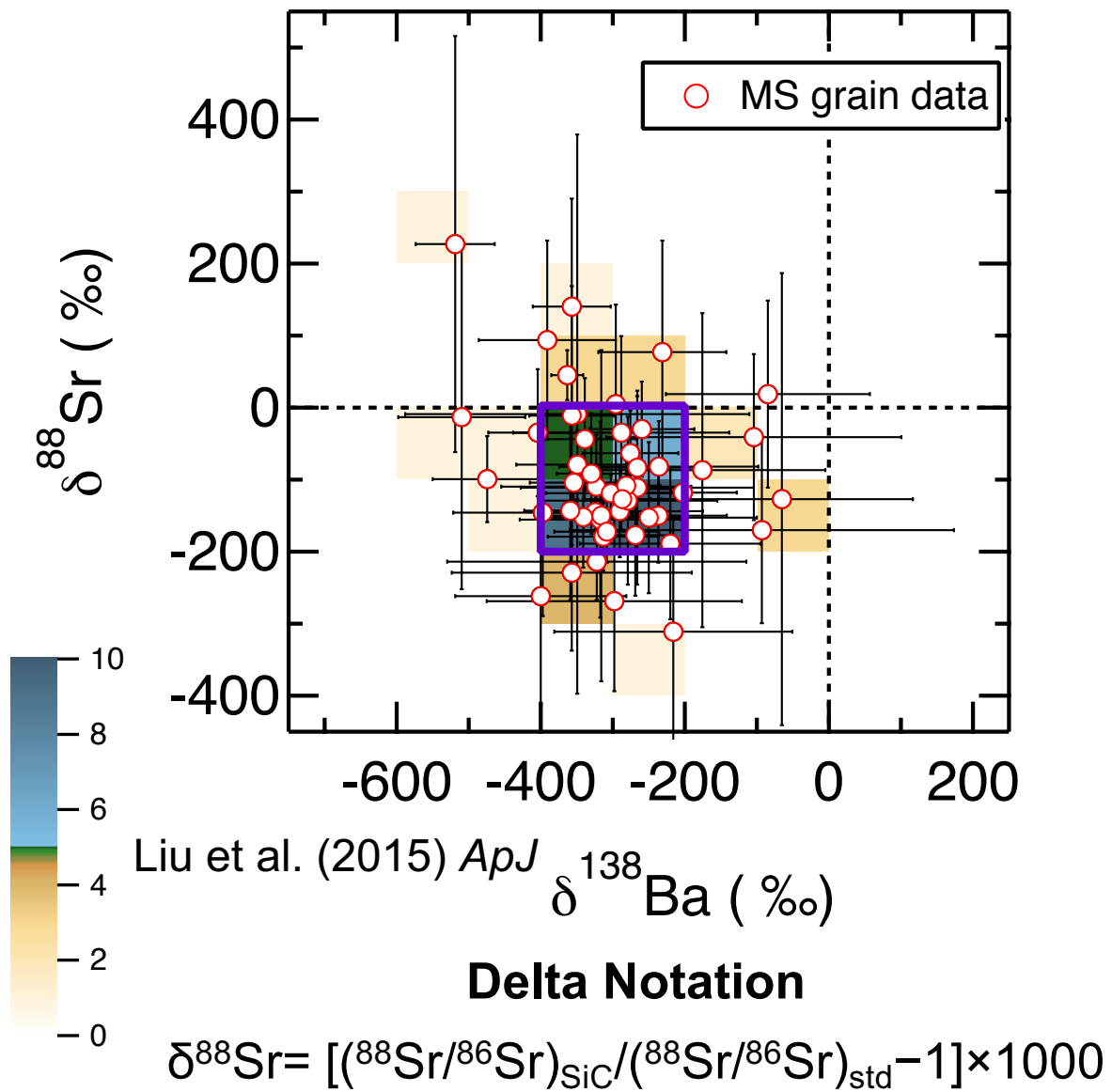
CROSS SECTION x ABUNDANCE ($\text{Si} = 10^6$)



MS SiC Isotopic Data of Sr, Ba

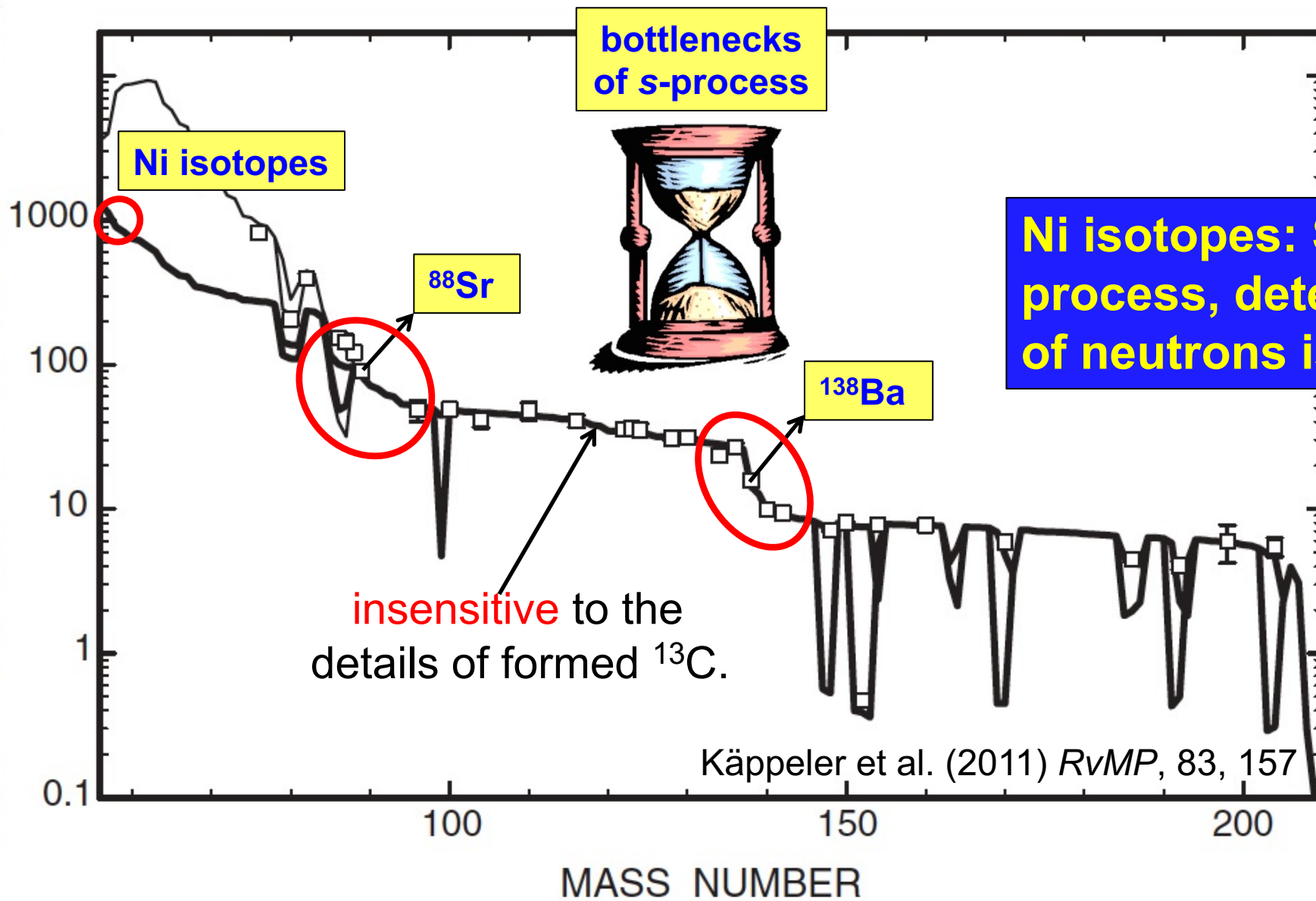


MS SiC Isotopic Data of Sr, Ba and Ni

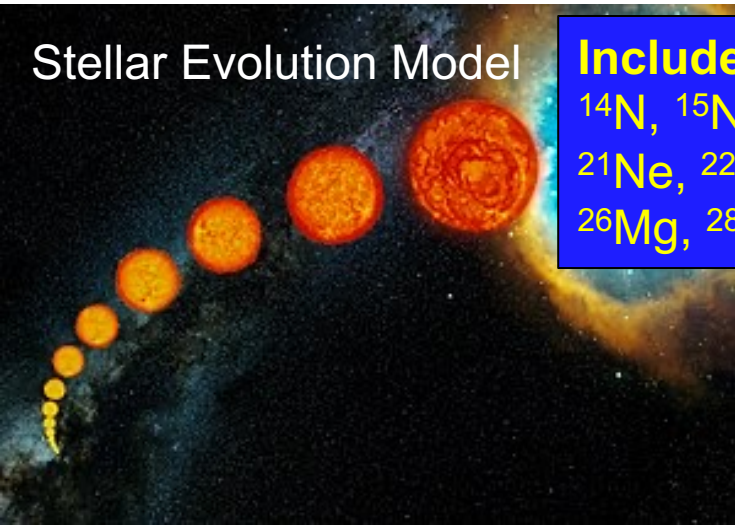


Smoking Guns for Constraining ^{13}C Formation

CROSS SECTION x ABUNDANCE ($\text{Si} = 10^6$)



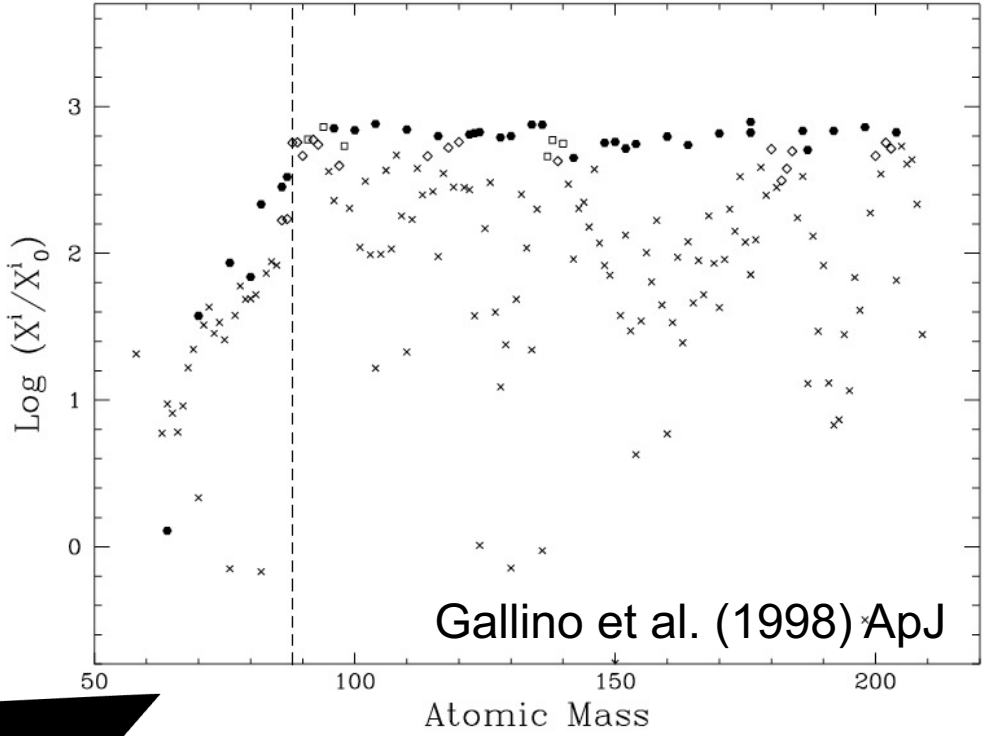
Post-process Nucleosynthesis Calculations



Included : ^1H , ^3He , ^4He , ^{12}C , ^{13}C , ^{14}N , ^{15}N , ^{16}O , ^{17}O , ^{18}O , ^{19}F , ^{20}Ne , ^{21}Ne , ^{22}Ne , ^{23}Na , ^{24}Mg , ^{25}Mg , ^{26}Mg , ^{28}Si , **energy-providers!**

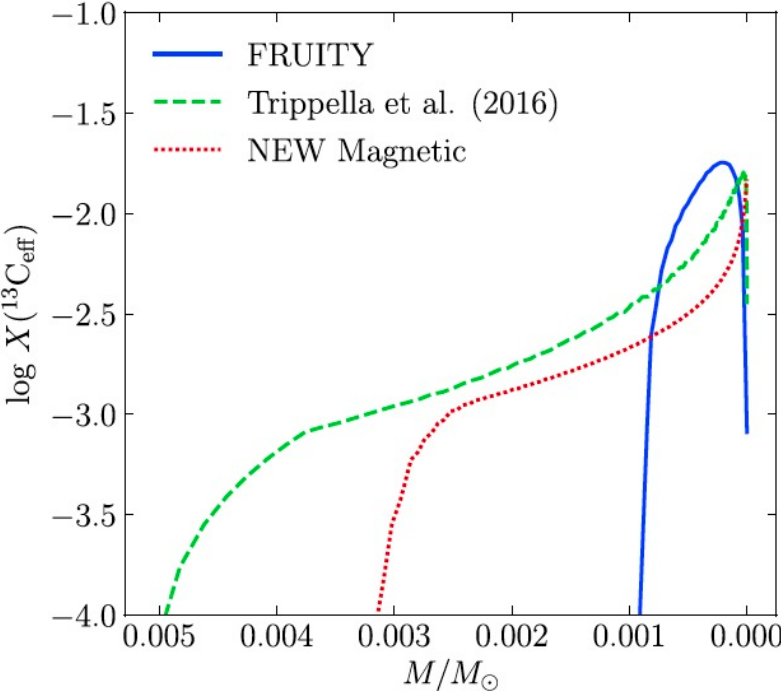
Post-process nucleosynthesis model: the whole nucleosynthesis network is included!

(P, T) conditions with time

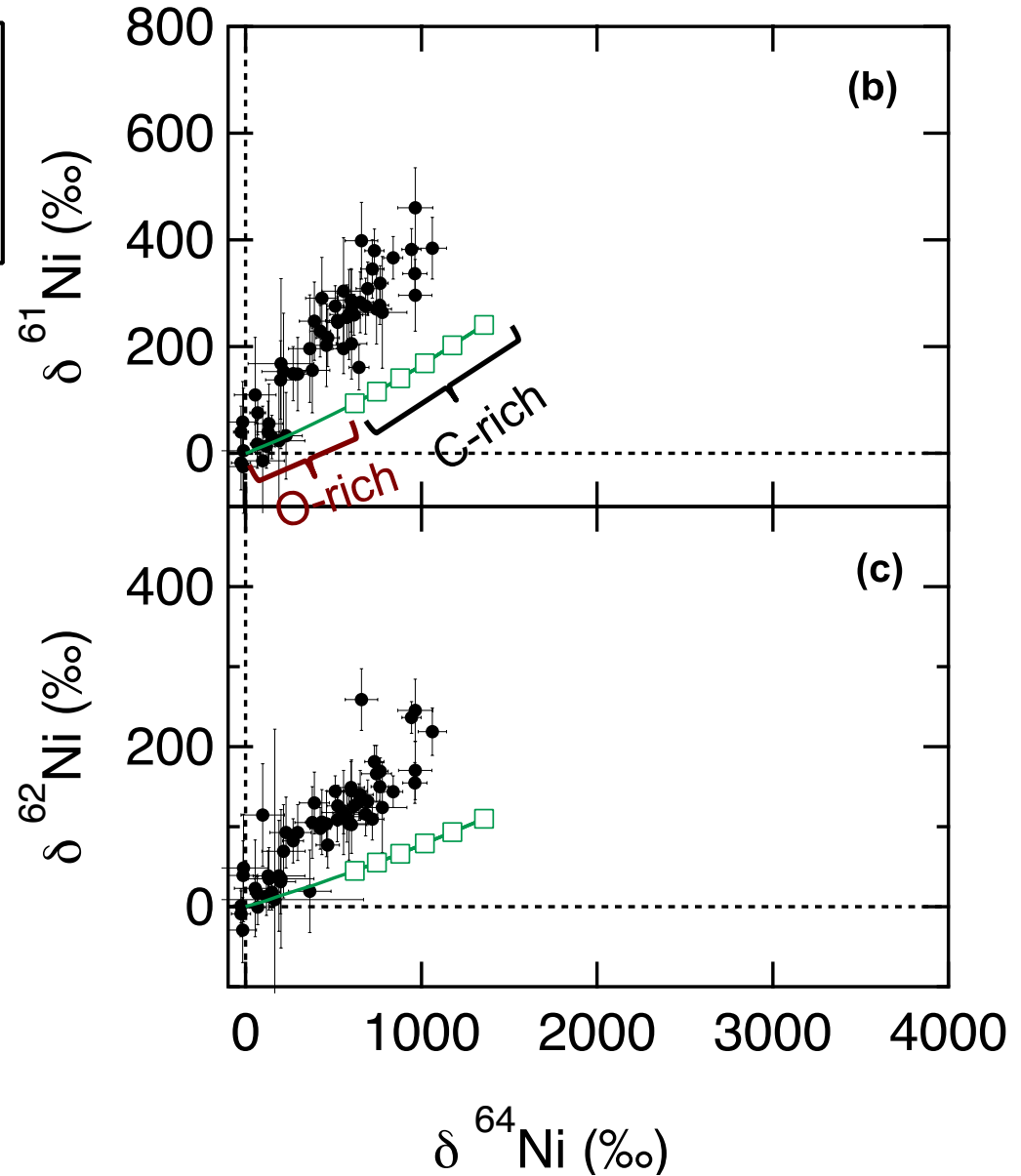
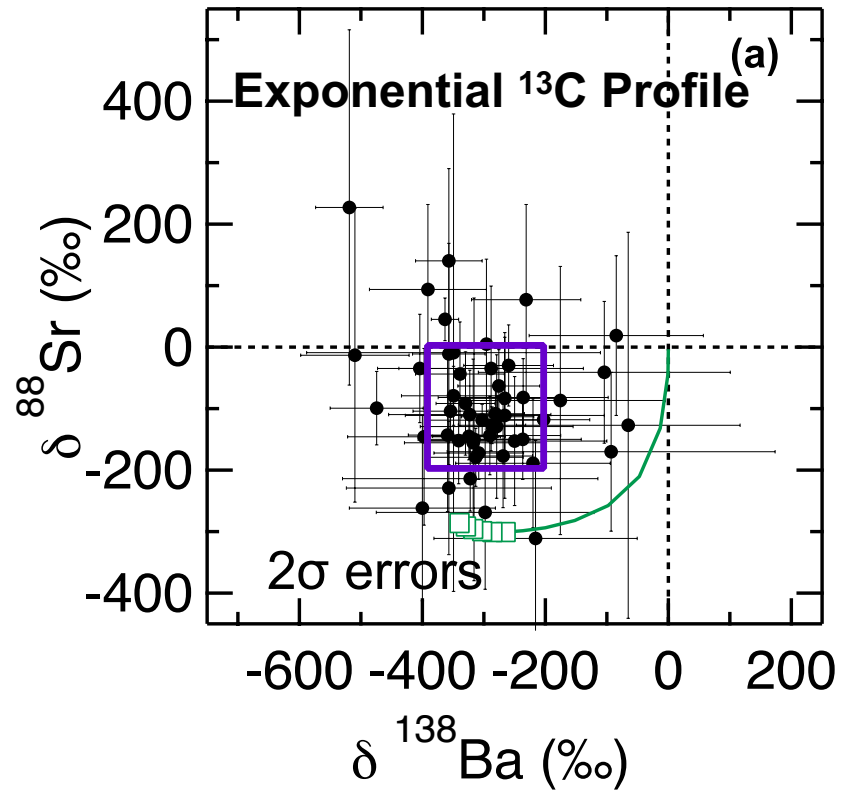
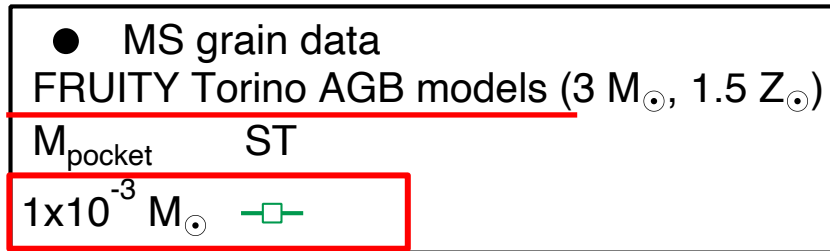


H mixing profile

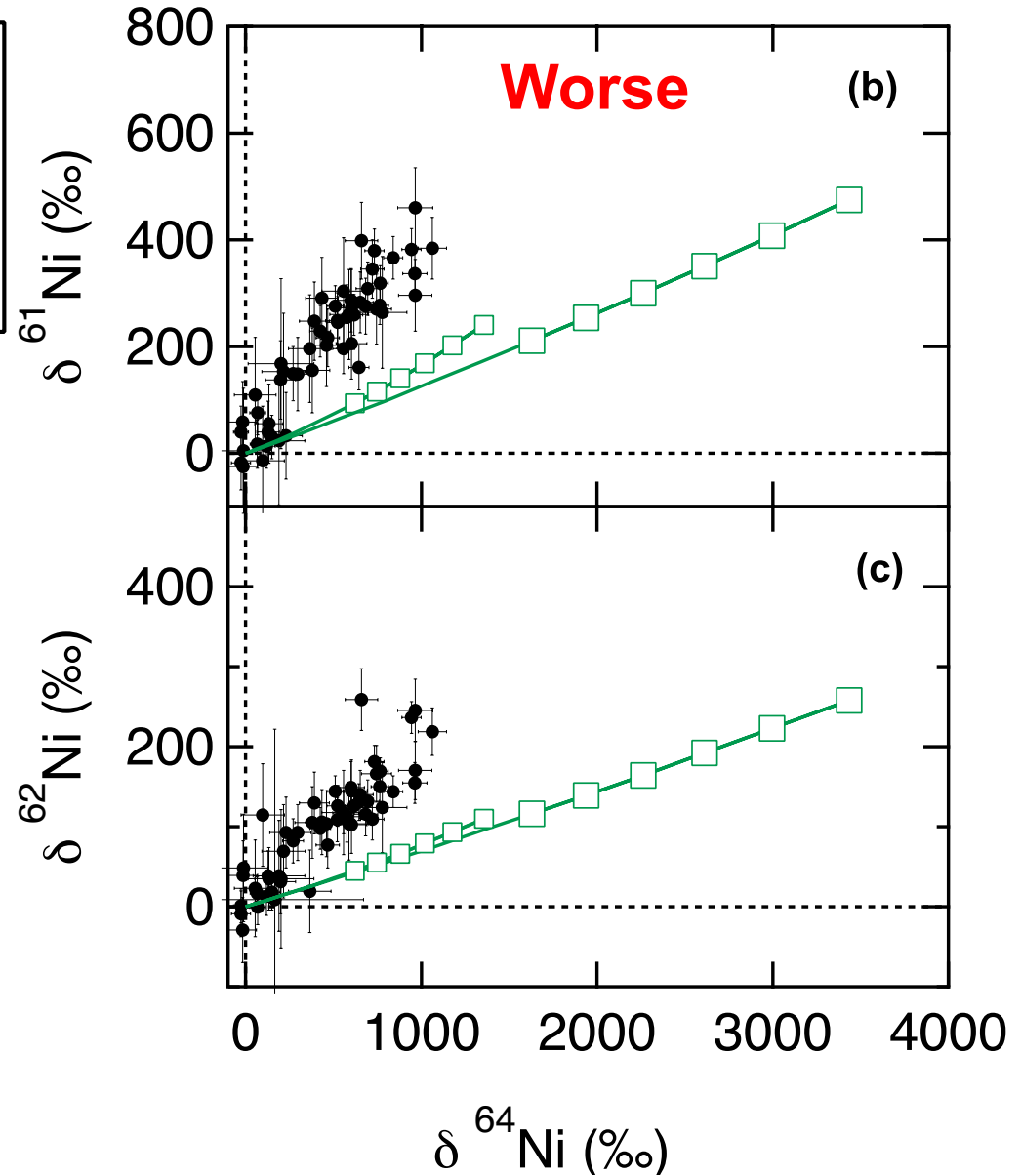
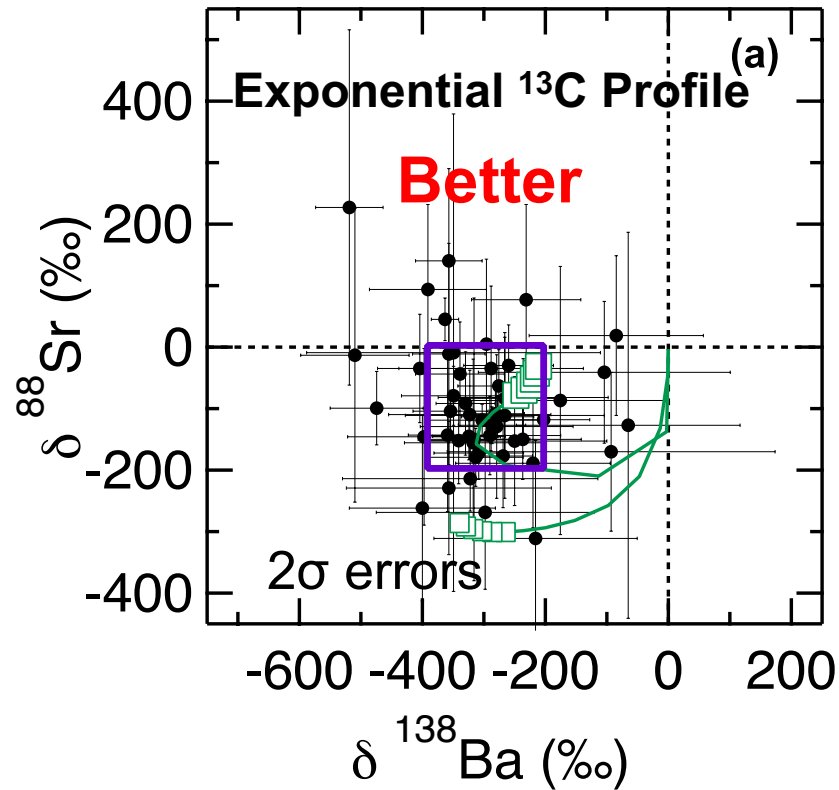
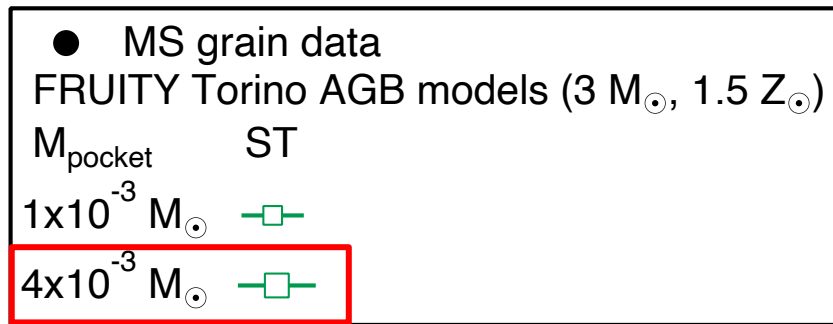
Advantage: easy test of various stellar parameters.



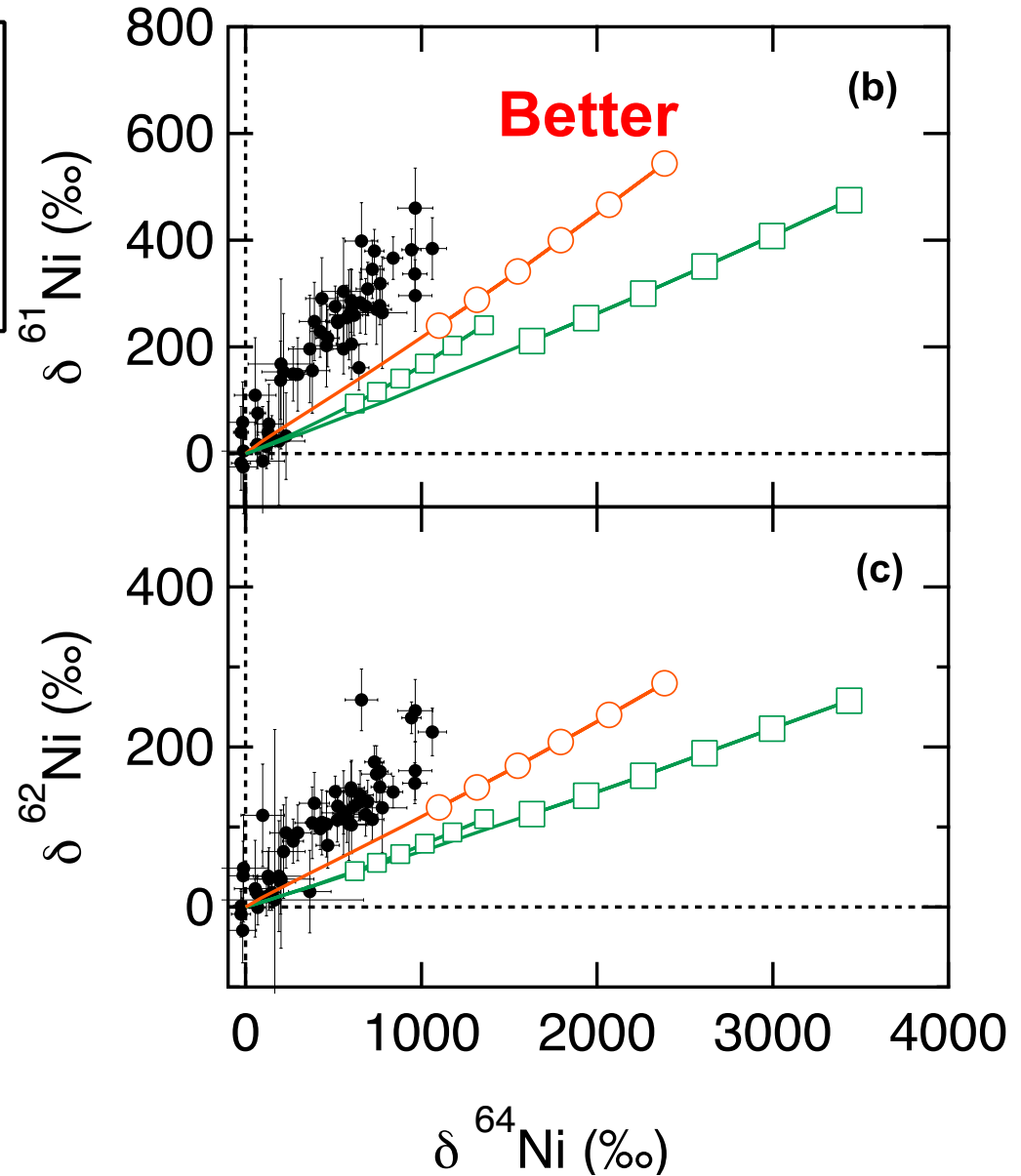
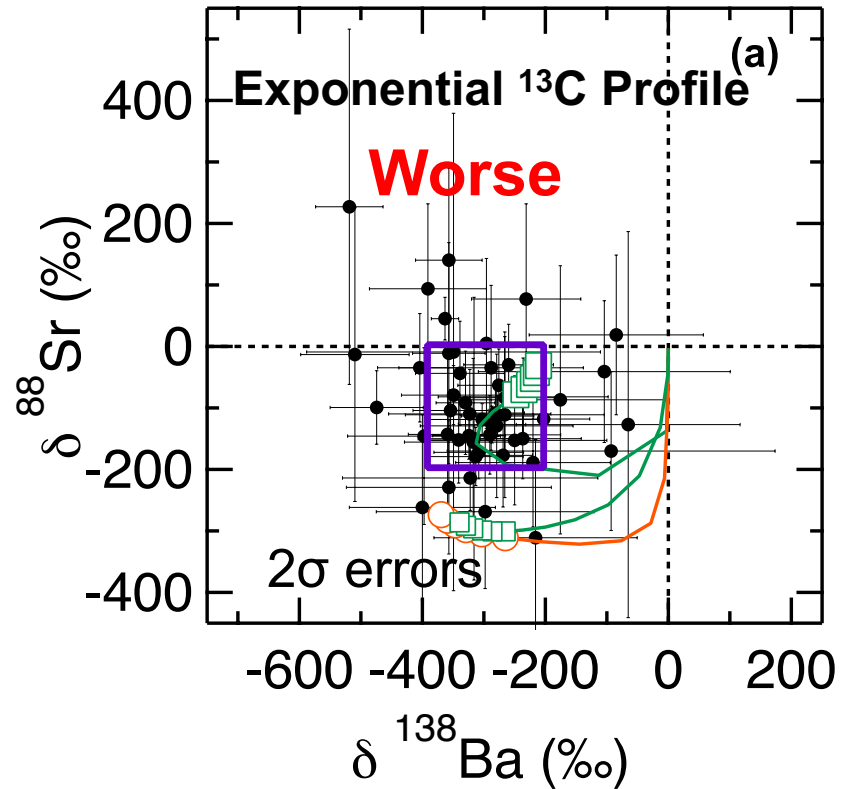
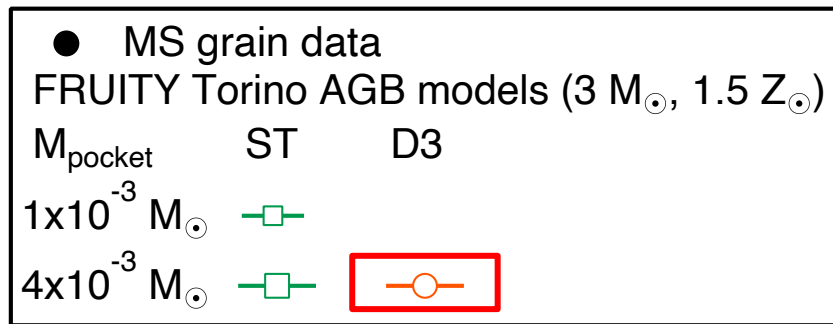
Standard Exponential ^{13}C -Pocket



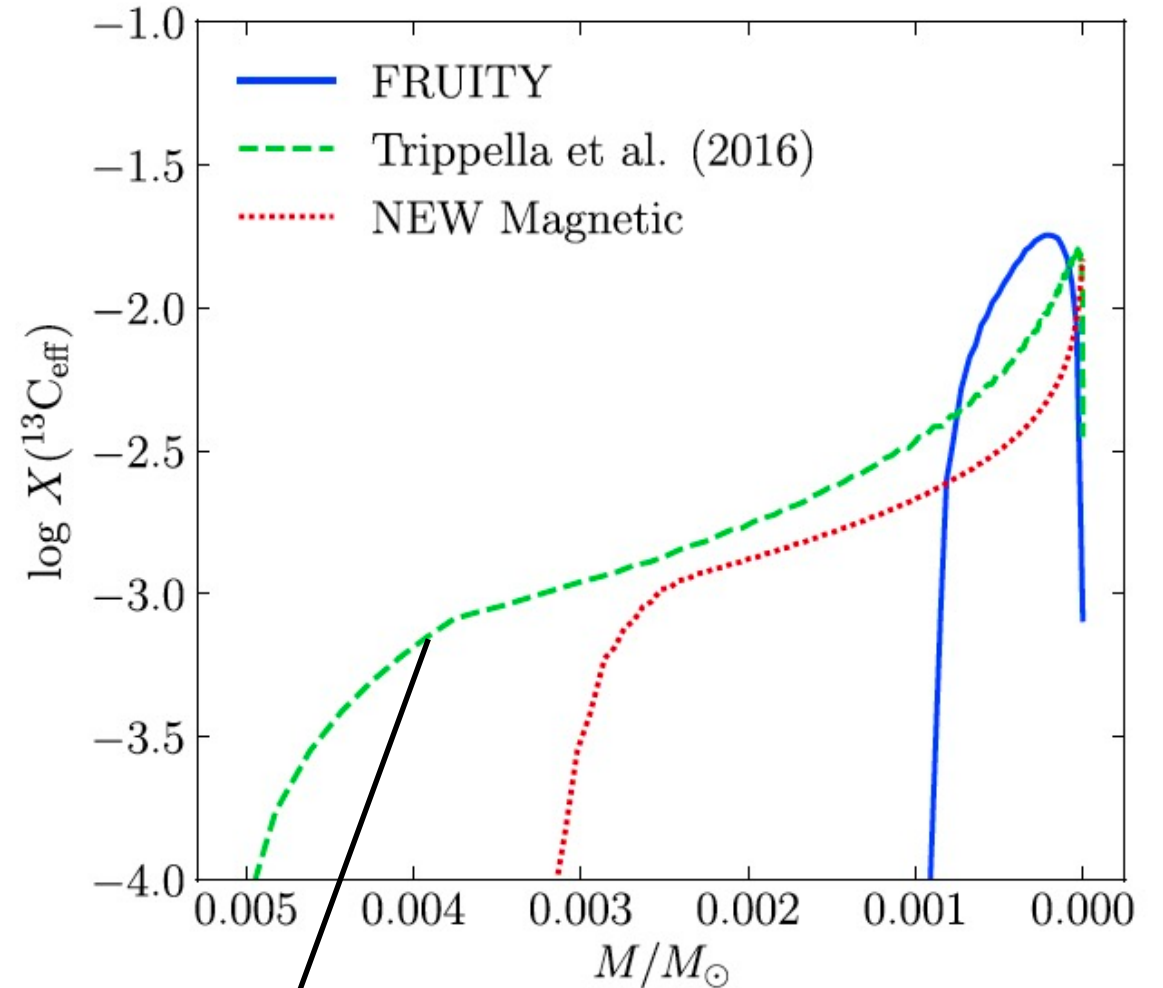
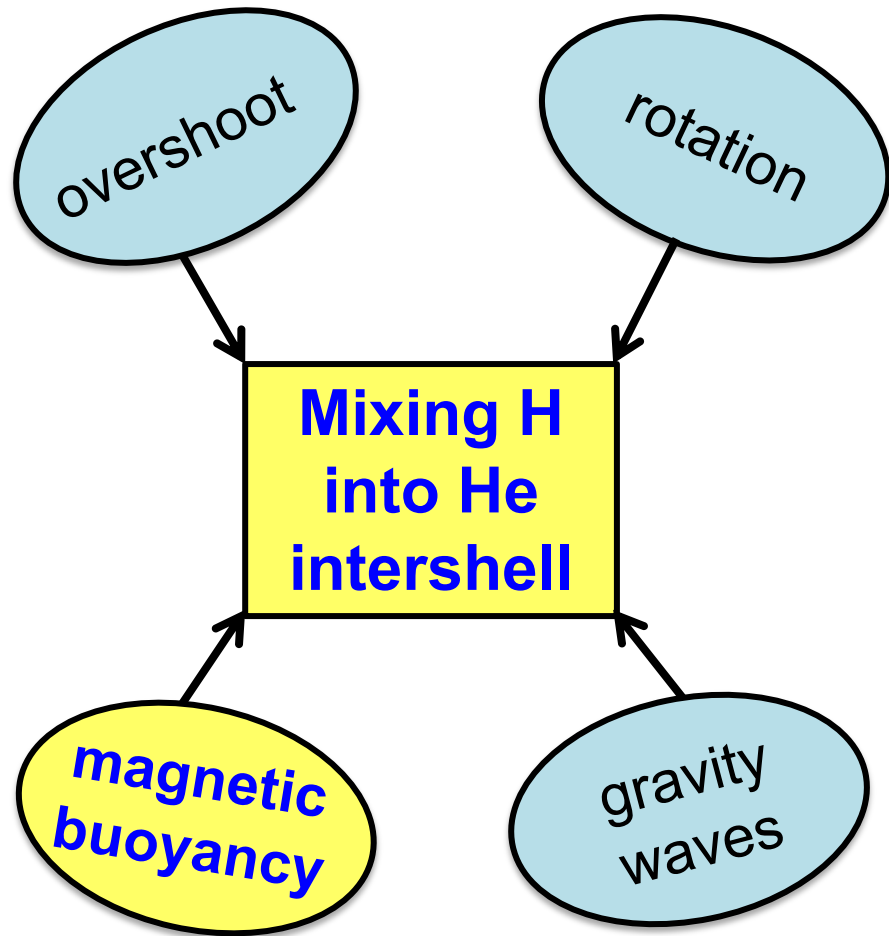
Standard Exponential ^{13}C -Pocket



Standard Exponential ^{13}C -Pocket

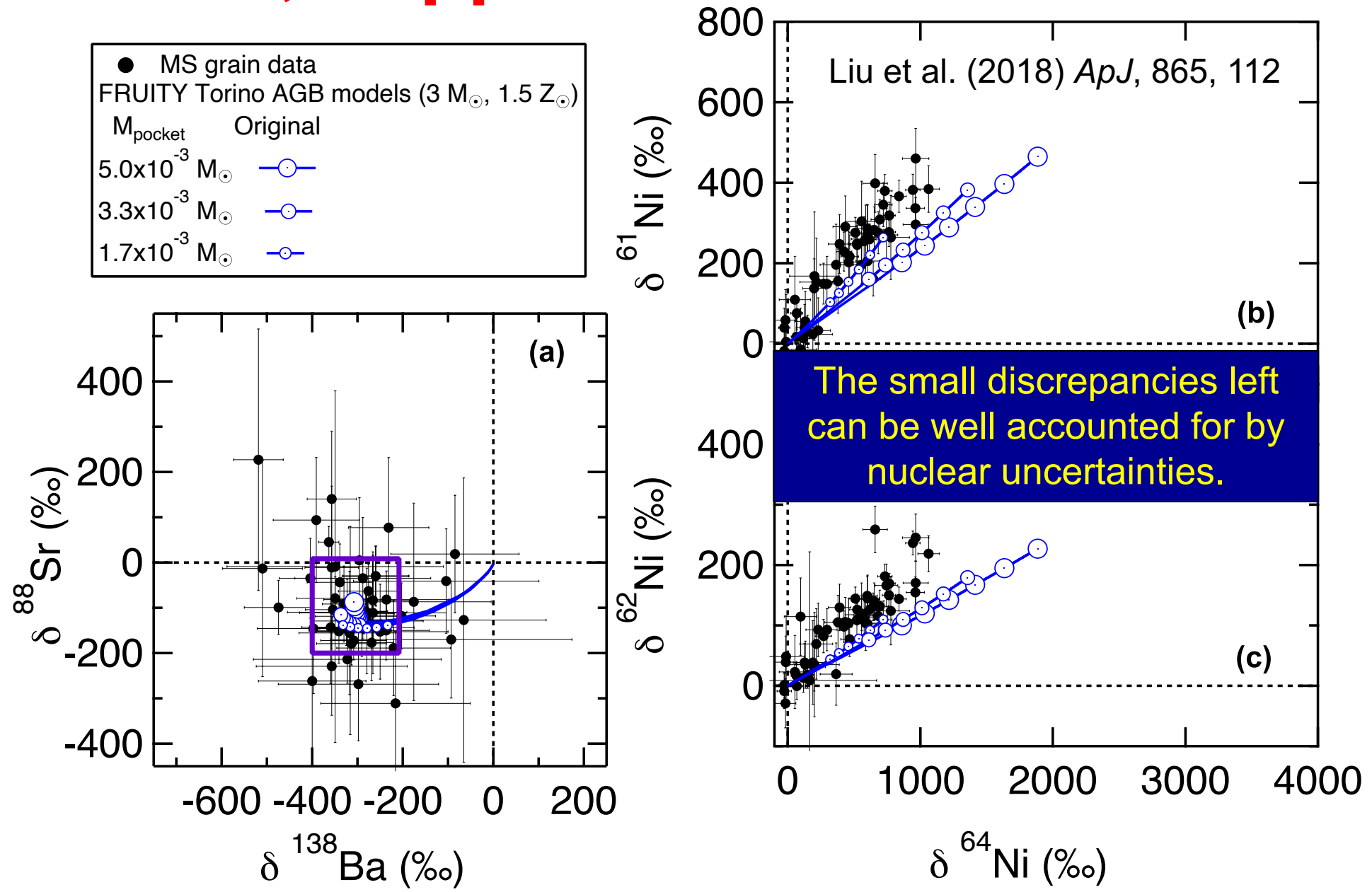


Mixing of H by Magnetic Buoyancy

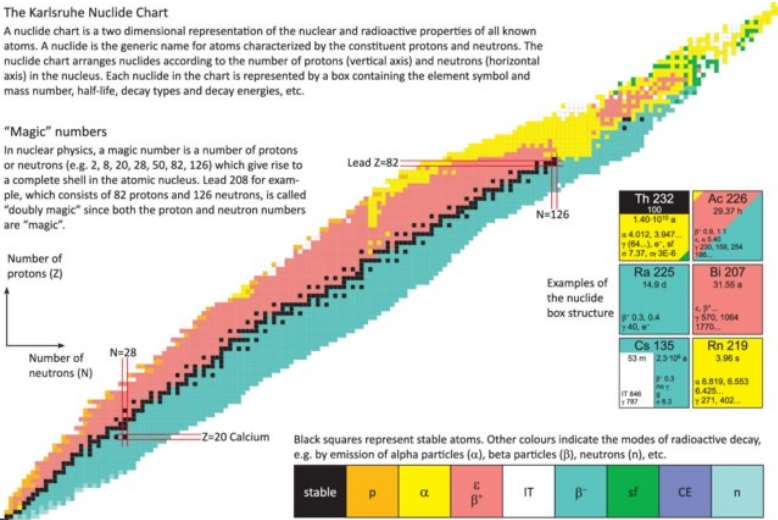


1. deeper mixing
2. lower ^{13}C density on average
3. relatively more flattened

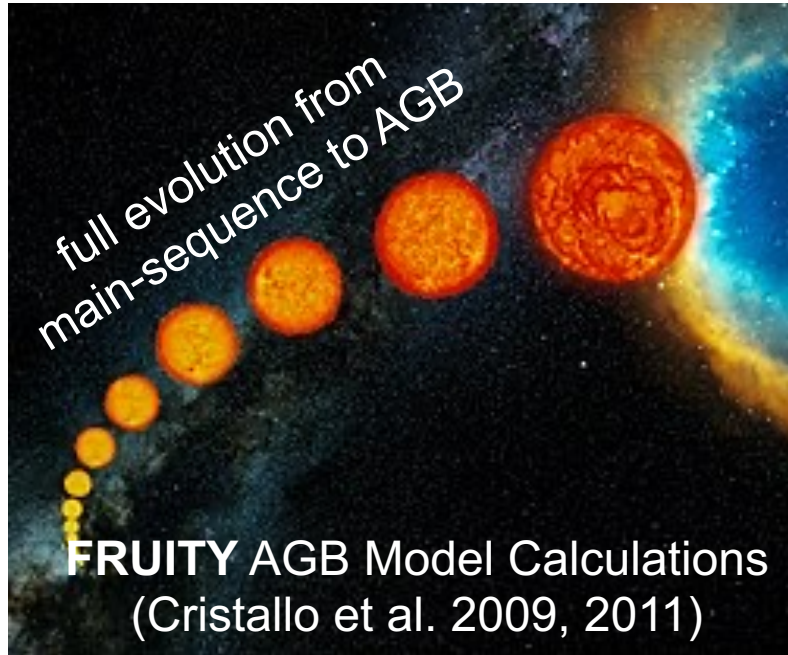
Yes, Trippella Pocket works!



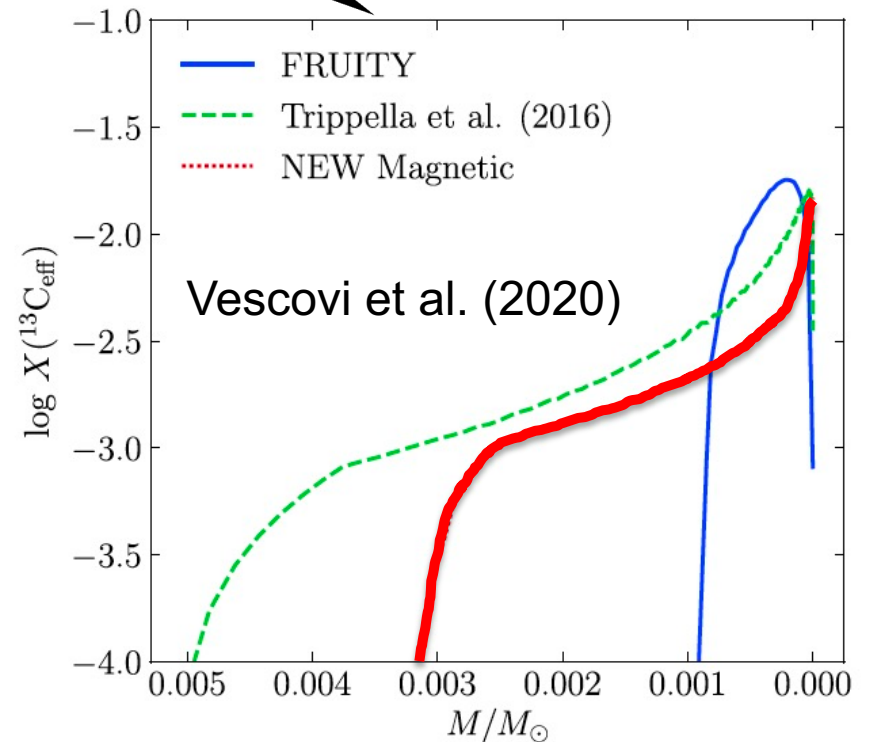
Fully Coupled Stellar and Nucleosynthesis Calculations



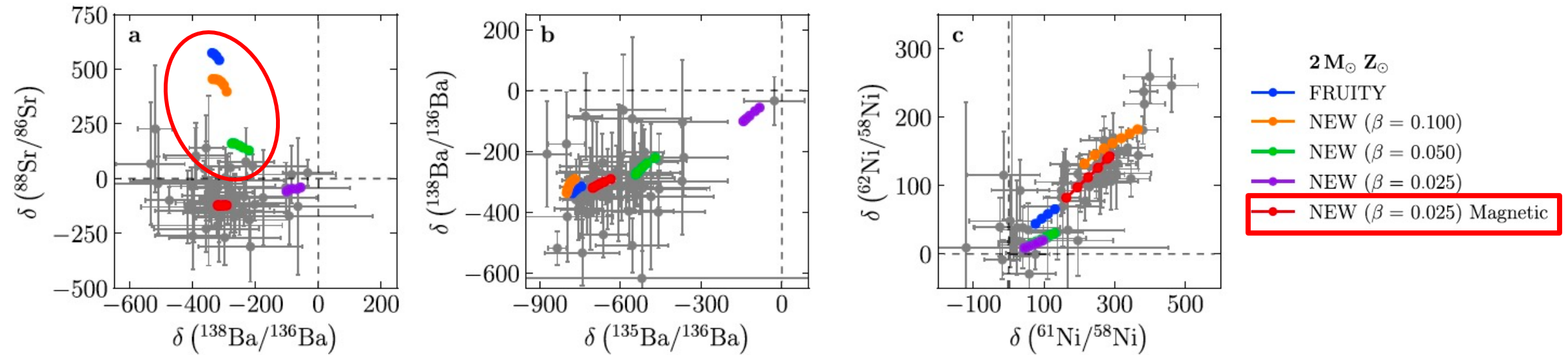
full nucleosynthesis network



Follow ¹³C formation by magnetic buoyancy

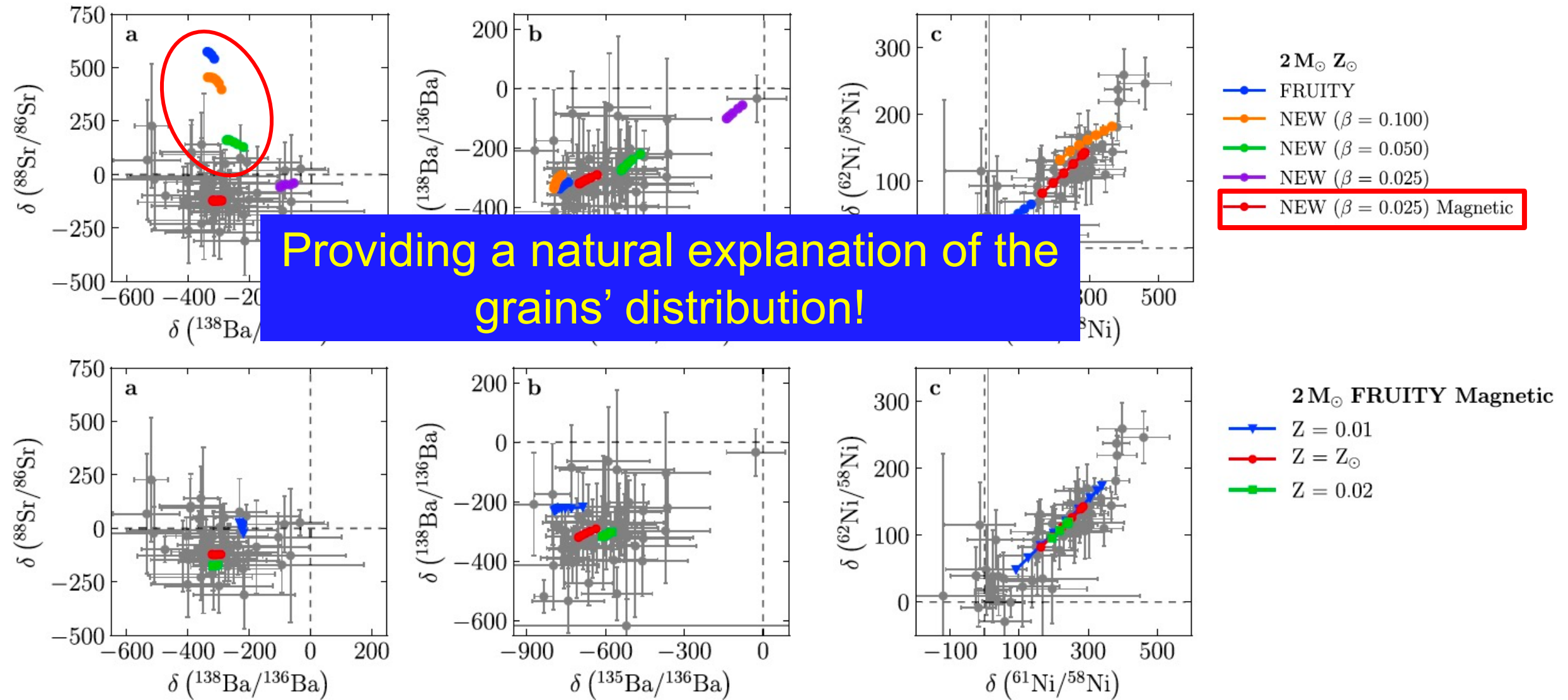


The Crucial Role of **Magnetic Buoyancy** is **Further Supported!**



Overshoot: no consistent match
Magnetic: consistent match

The Crucial Role of **Magnetic Buoyancy** is **Further Supported!**



Outline

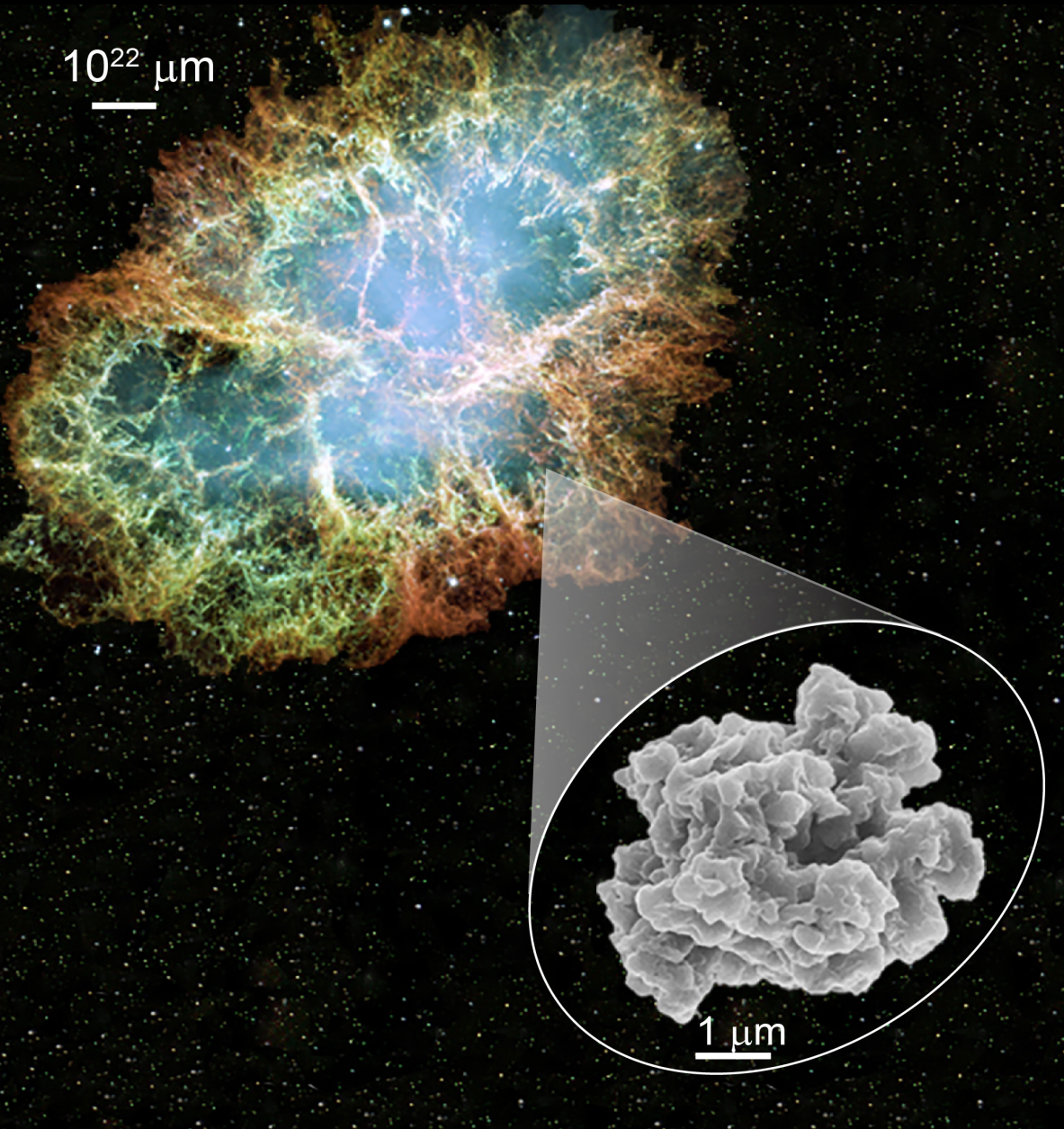
1. Analytical Techniques

2. Different Types of Grains and Their Stellar Origins

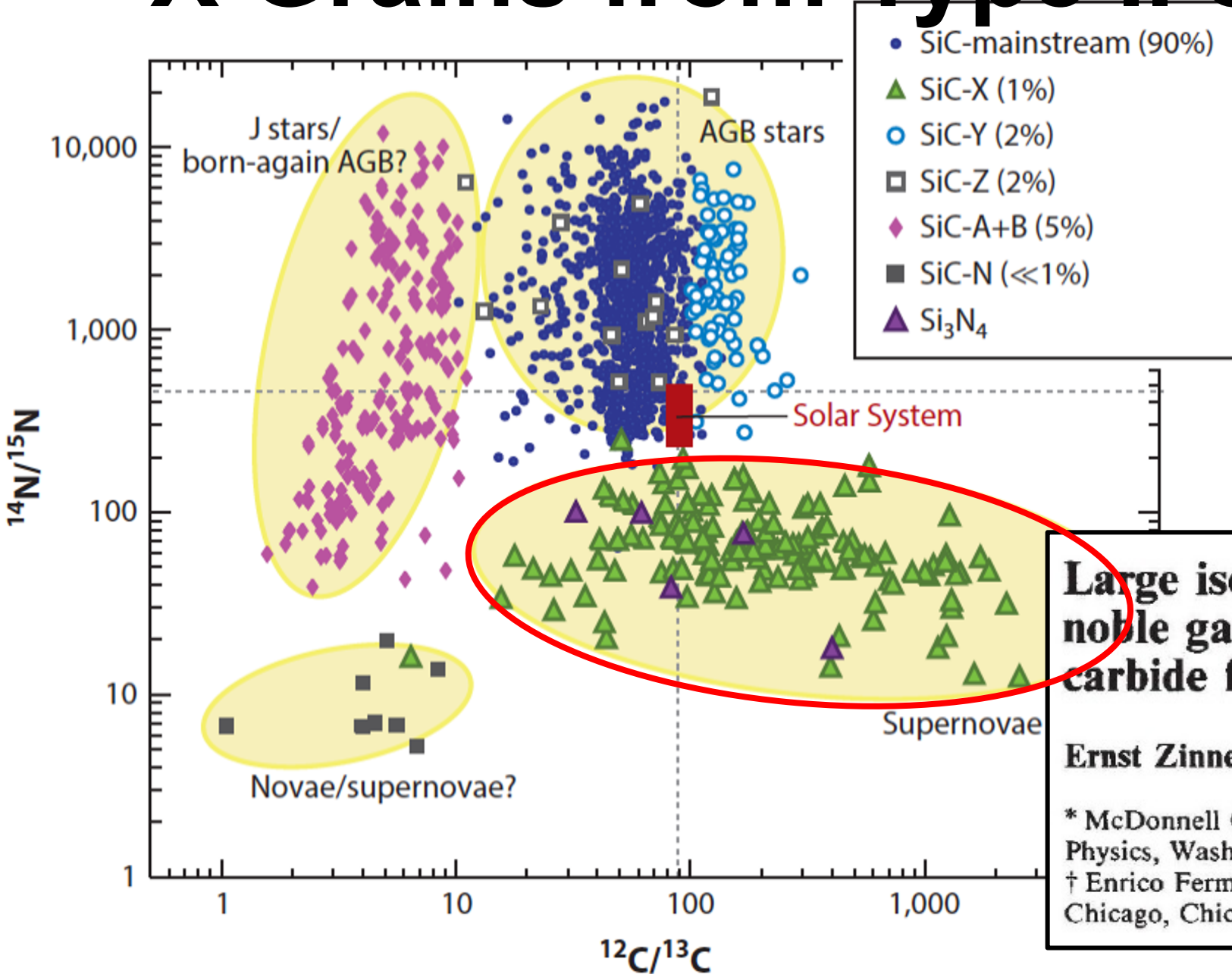
2.1 AGB Dust

2.2 Type II Supernova Dust

2.3 Mysterious ^{13}C -rich SiC Dust



X Grains from Type II Supernovae



Fun Facts

1969: Murchison fall v.s. Lunar sample return

1987: SN 1987A explosion v.s. discovery of presolar SiC

Large isotopic anomalies of Si, C, N and noble gases in interstellar silicon carbide from the Murray meteorite
Nature (1987)

Ernst Zinner*, Tang Ming† & Edward Anders†‡

* McDonnell Center for the Space Sciences and Department of Physics, Washington University, St Louis, Missouri 63130, USA

† Enrico Fermi Institute and Department of Chemistry, University of Chicago, Chicago, Illinois 60637, USA

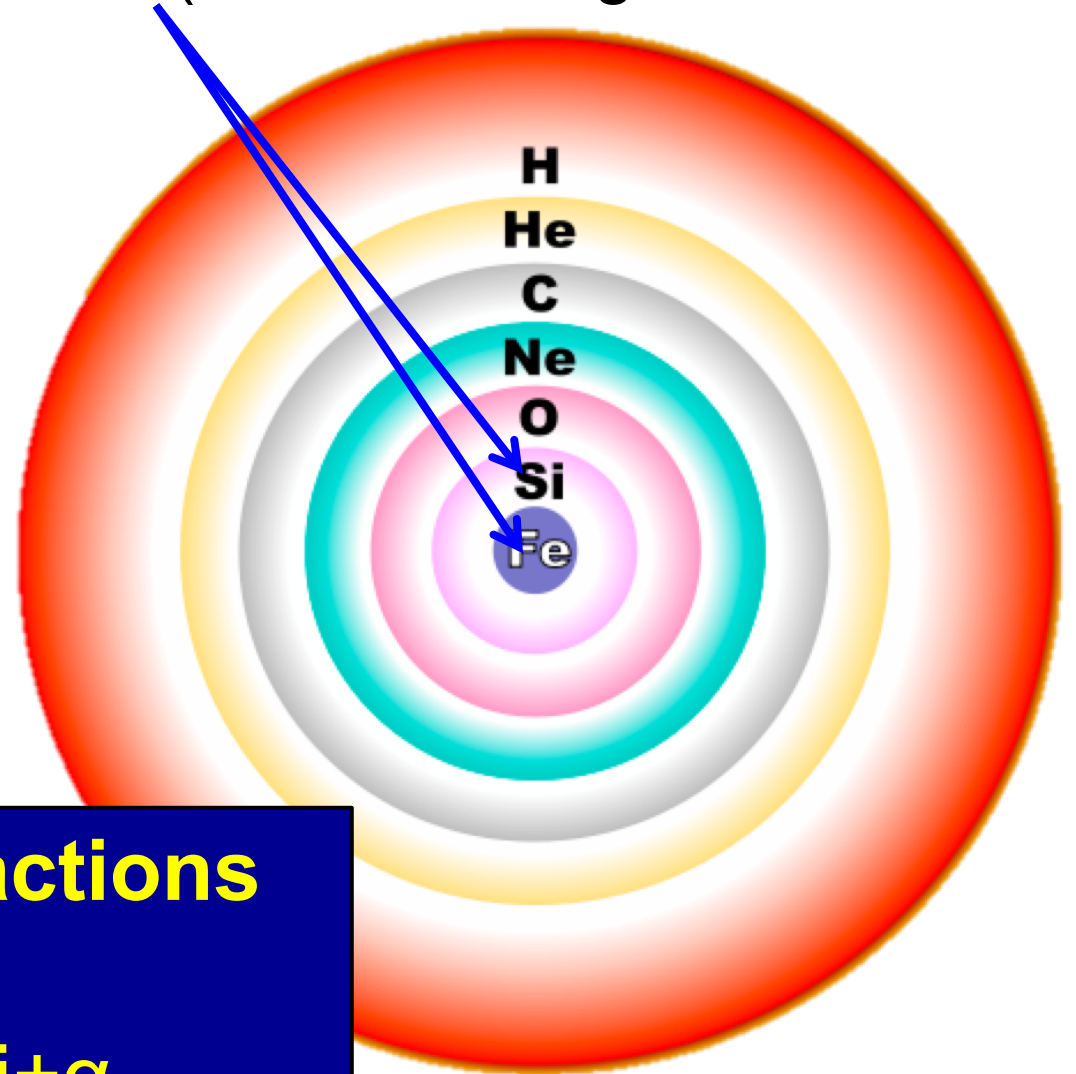
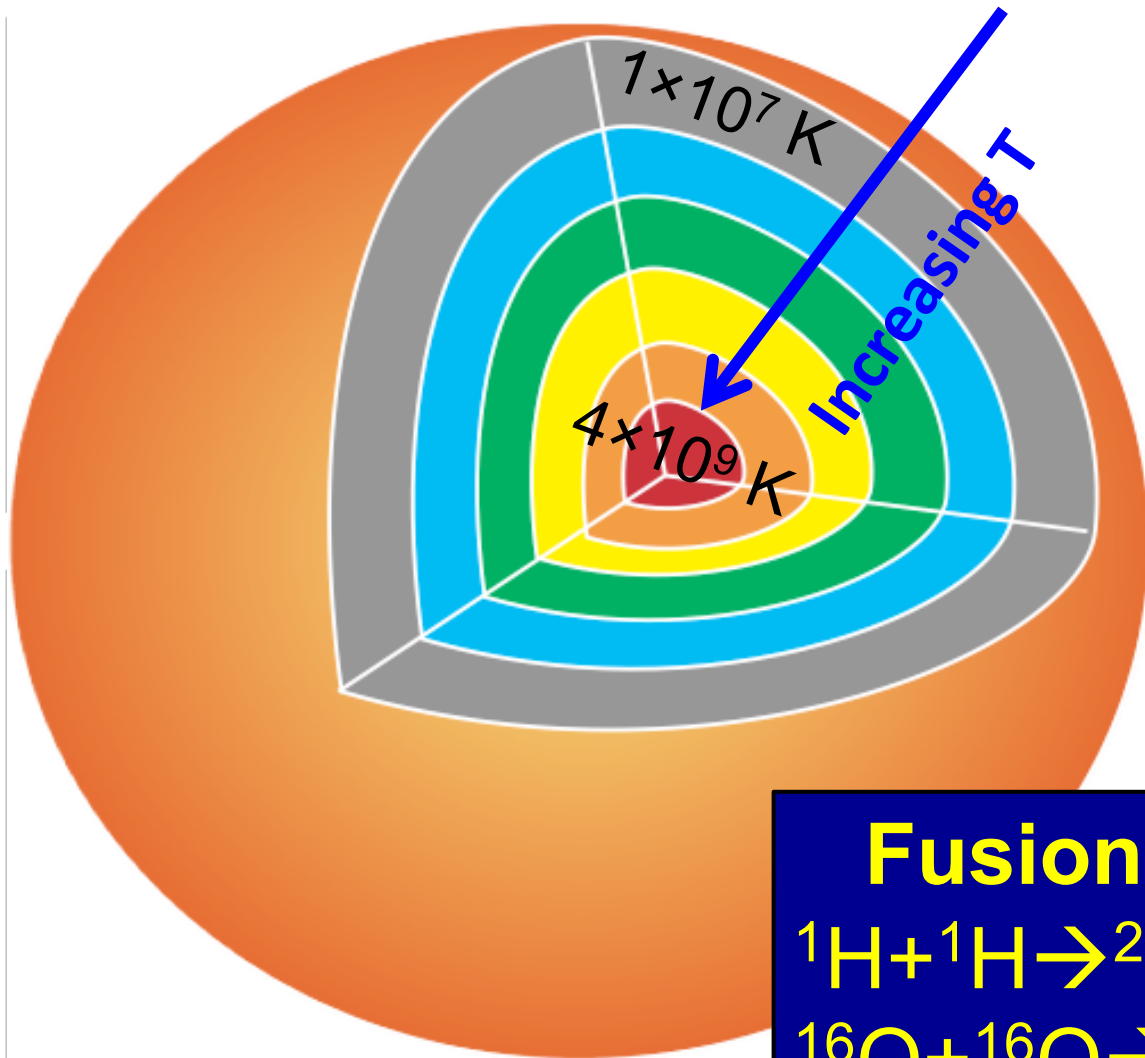
Supernova Explosion & Dust Formation



Scientific visualization of supernova evolution (A. Angelich)

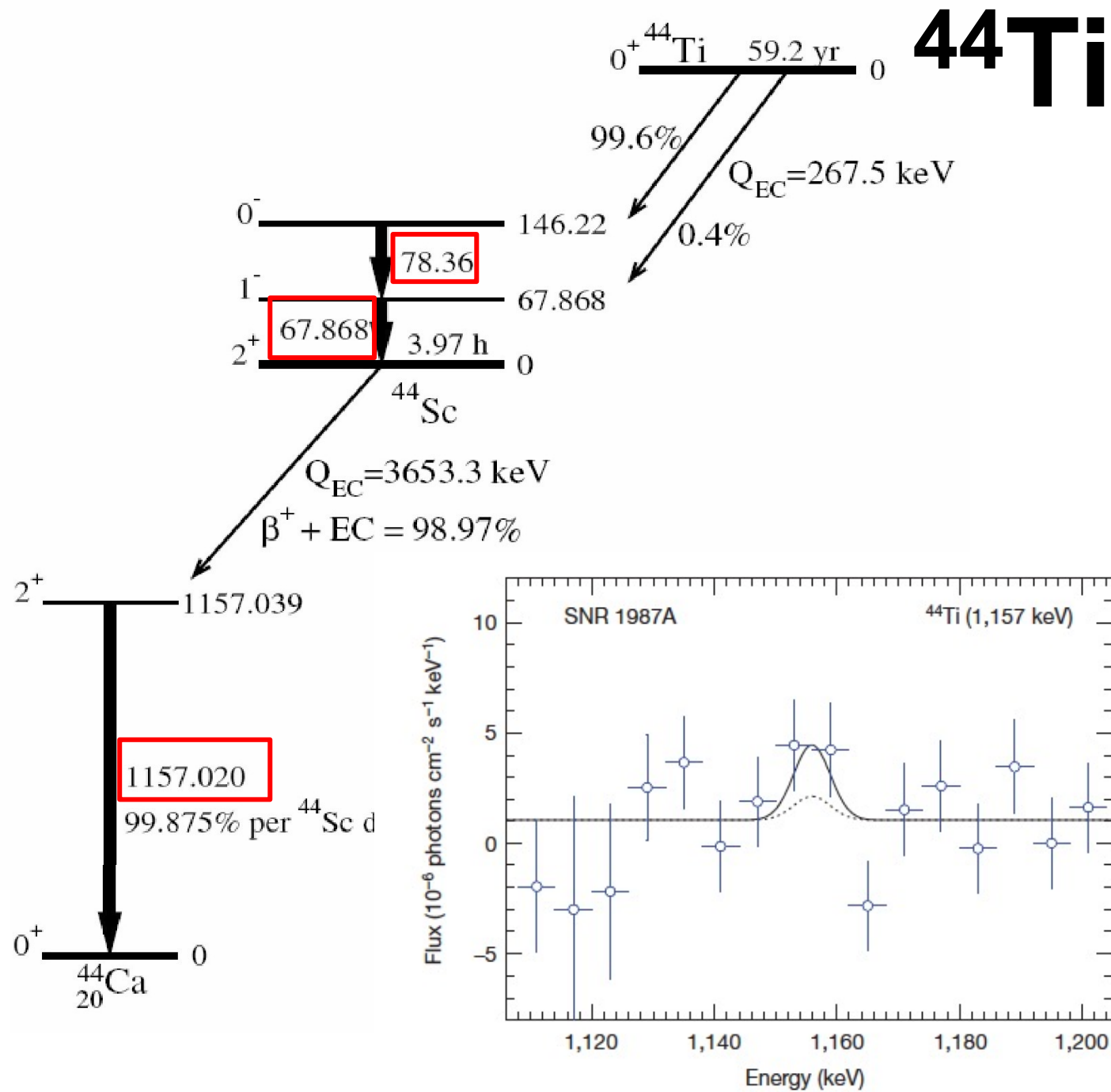
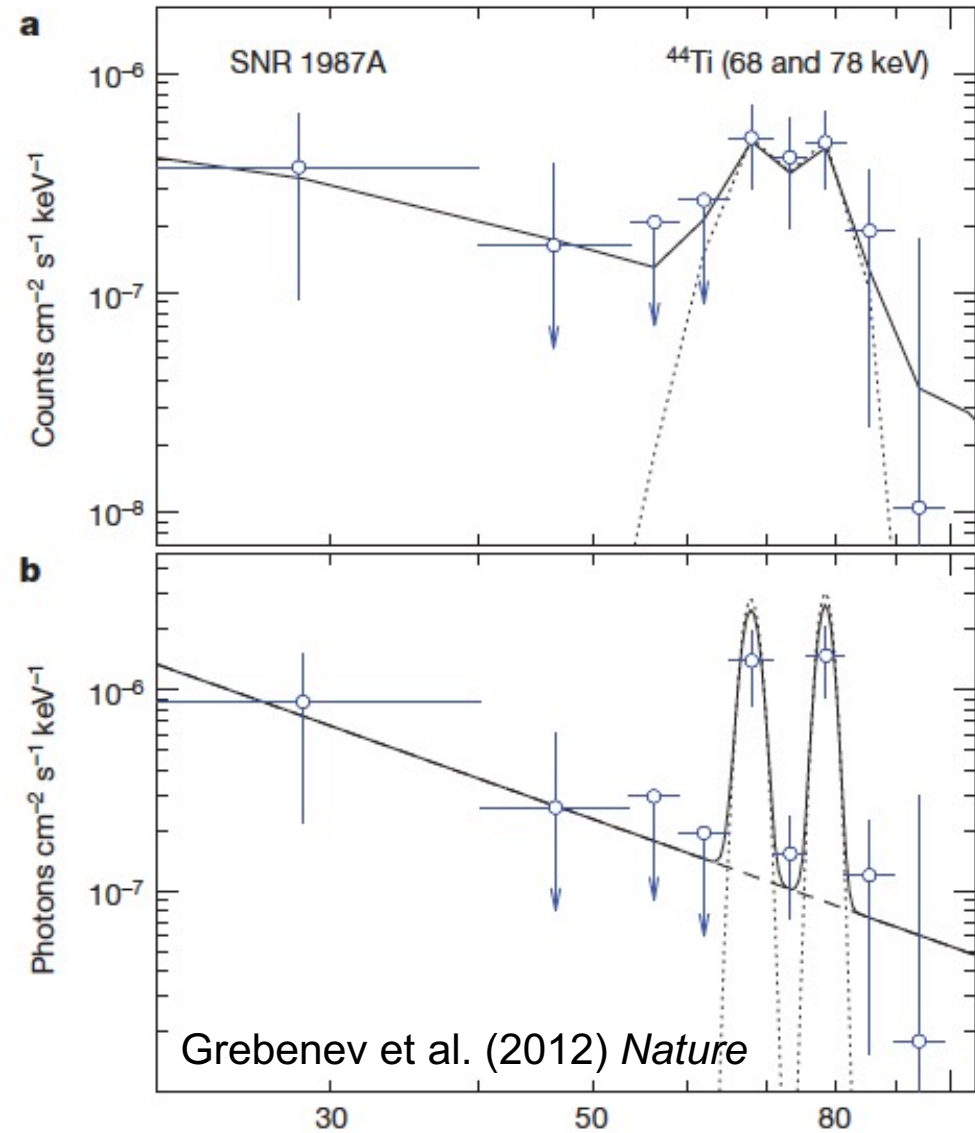
Supernova Nucleosynthesis

^{44}Ti (formed during α -rich freeze-out)



Fusion Reactions

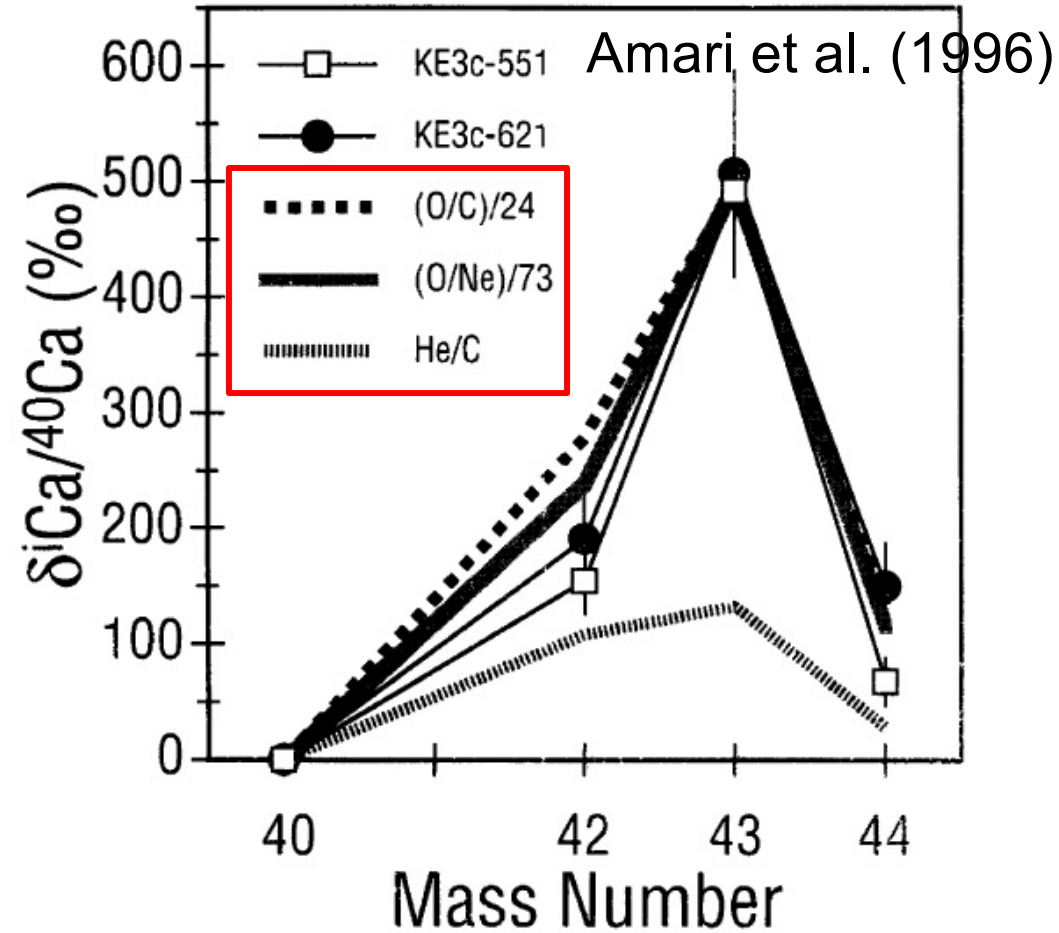
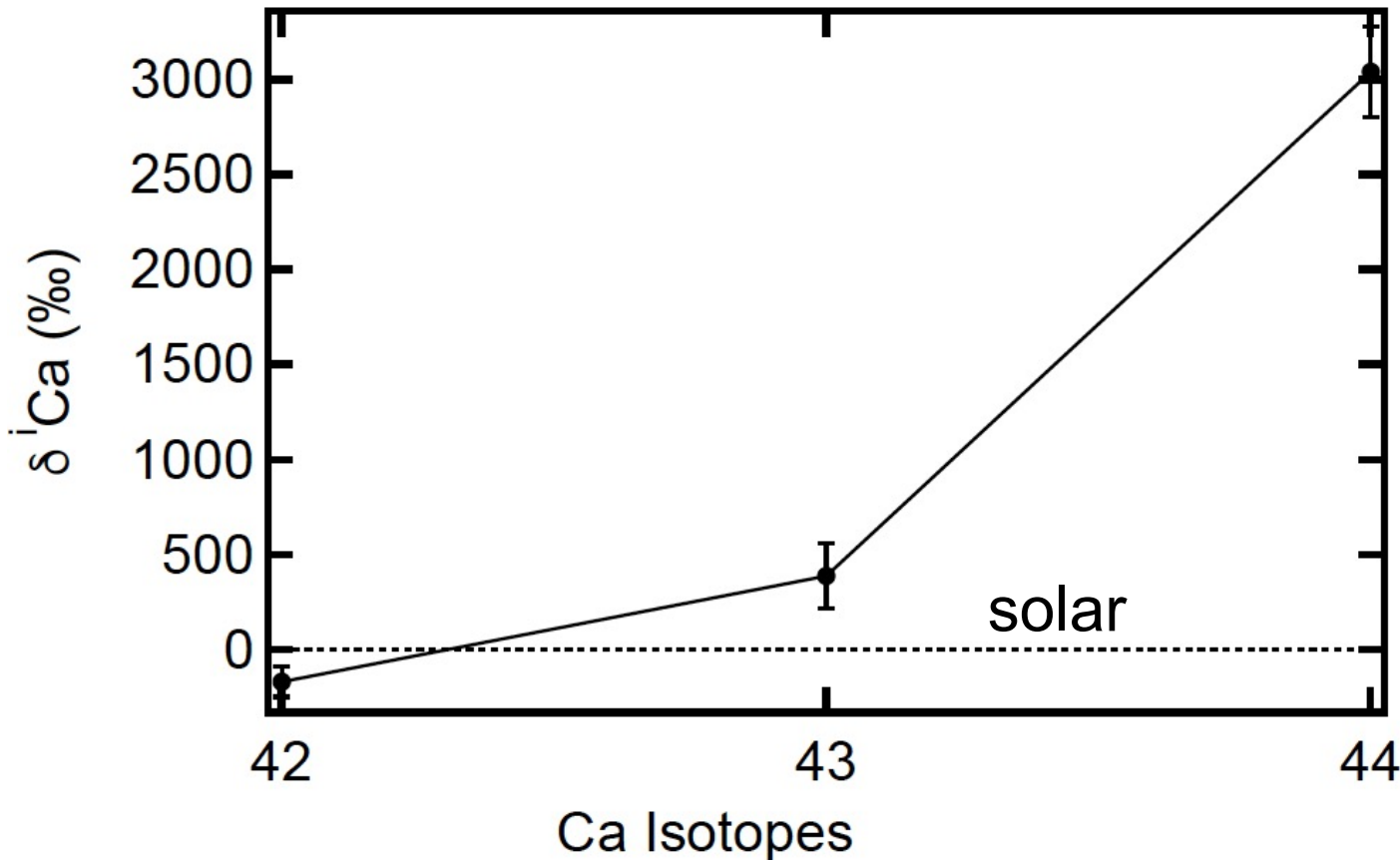




Also observed for Cas A
(Grefenstette et al. 2014)

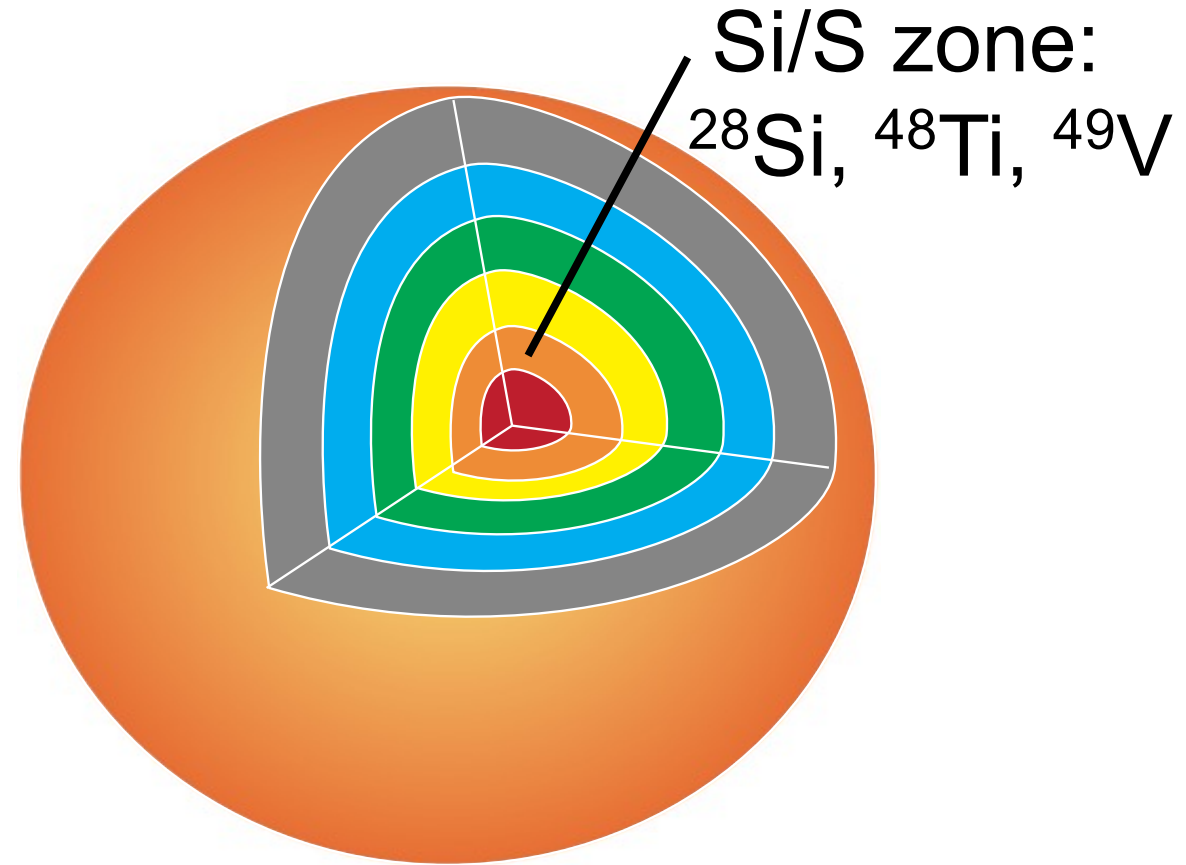
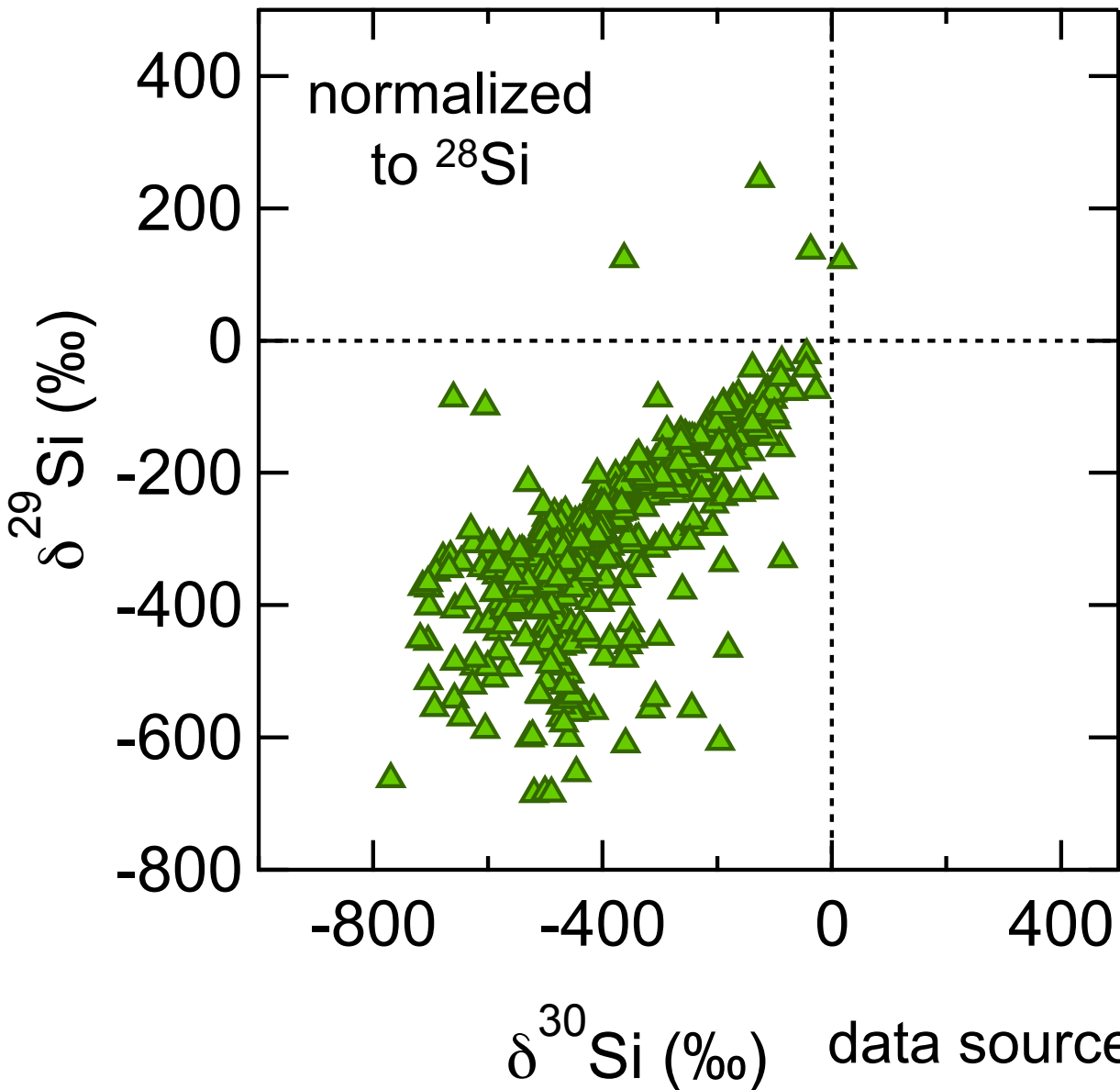
Extinct ^{44}Ti in X Grains

$$\delta^i\text{Ca} = \left[\left(\frac{i\text{Ca}}{^{40}\text{Ca}} \right)_{\text{grain}} / \left(\frac{i\text{Ca}}{^{40}\text{Ca}} \right)_{\text{std}} - 1 \right] \times 1000$$

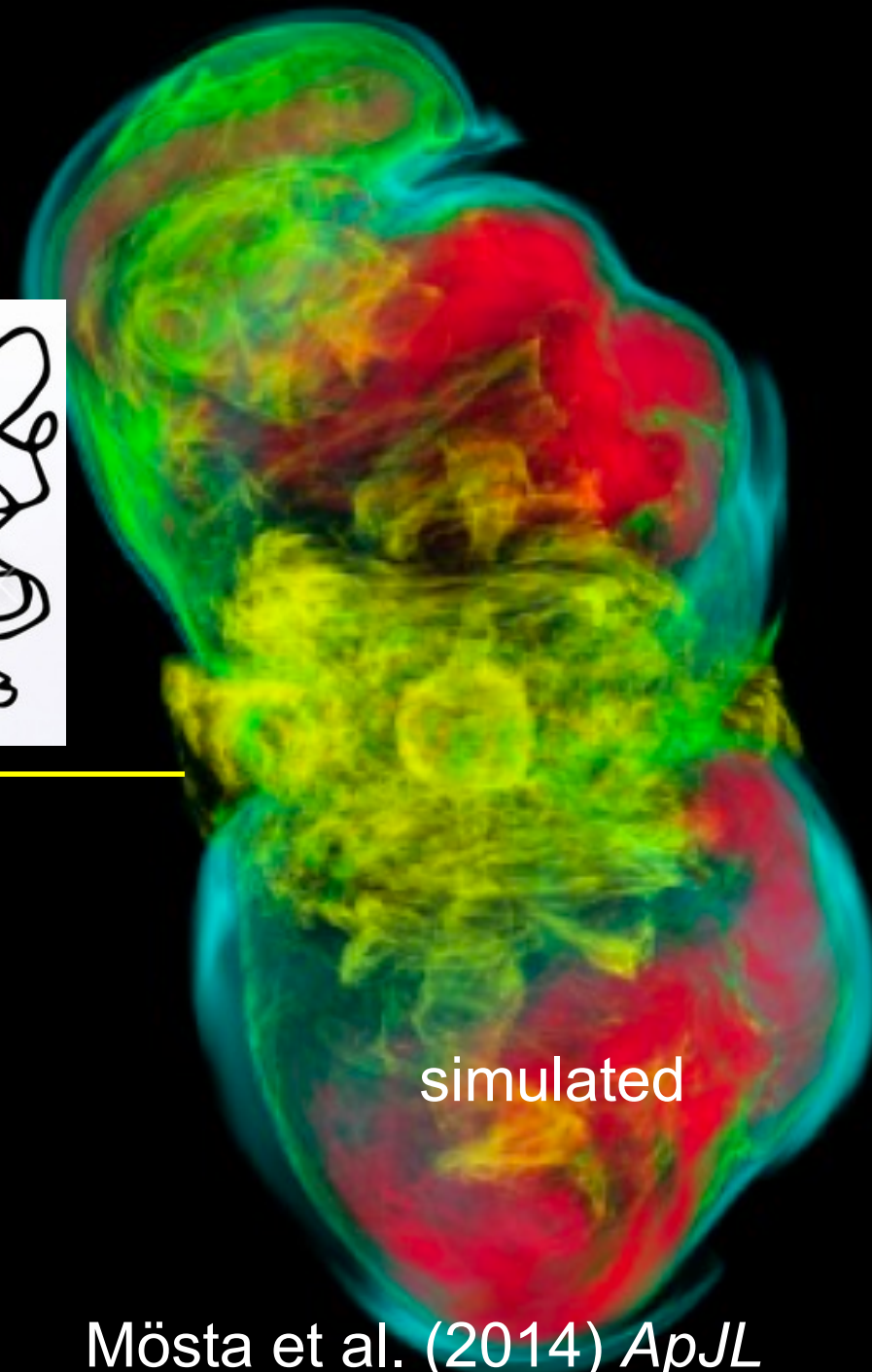
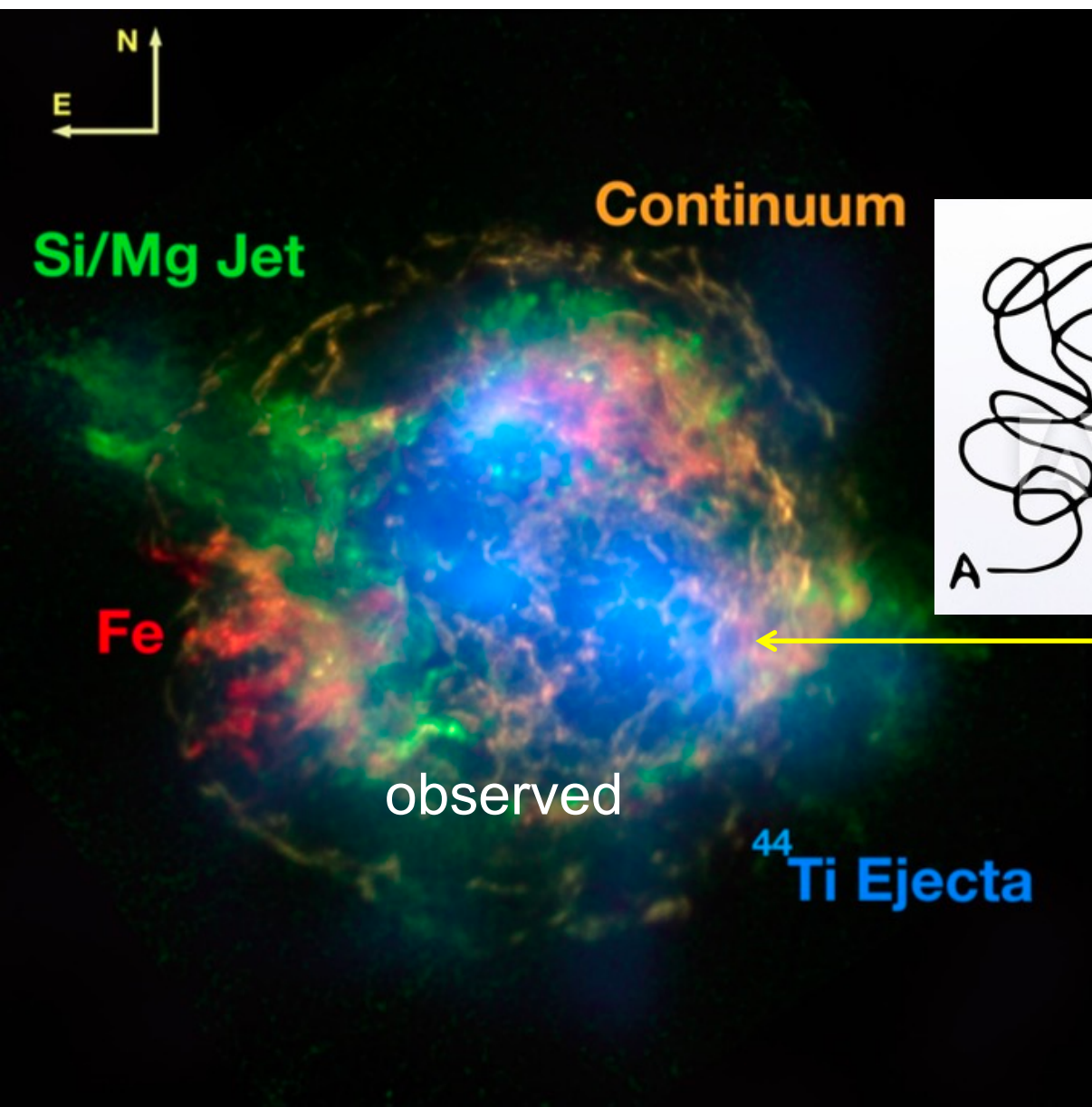


SN models predict large excesses in ^{43}Ca compared to ^{44}Ca . The observed ^{44}Ca excesses therefore point to the decay of ^{44}Ti .

^{28}Si Excesses in Si/S Zone

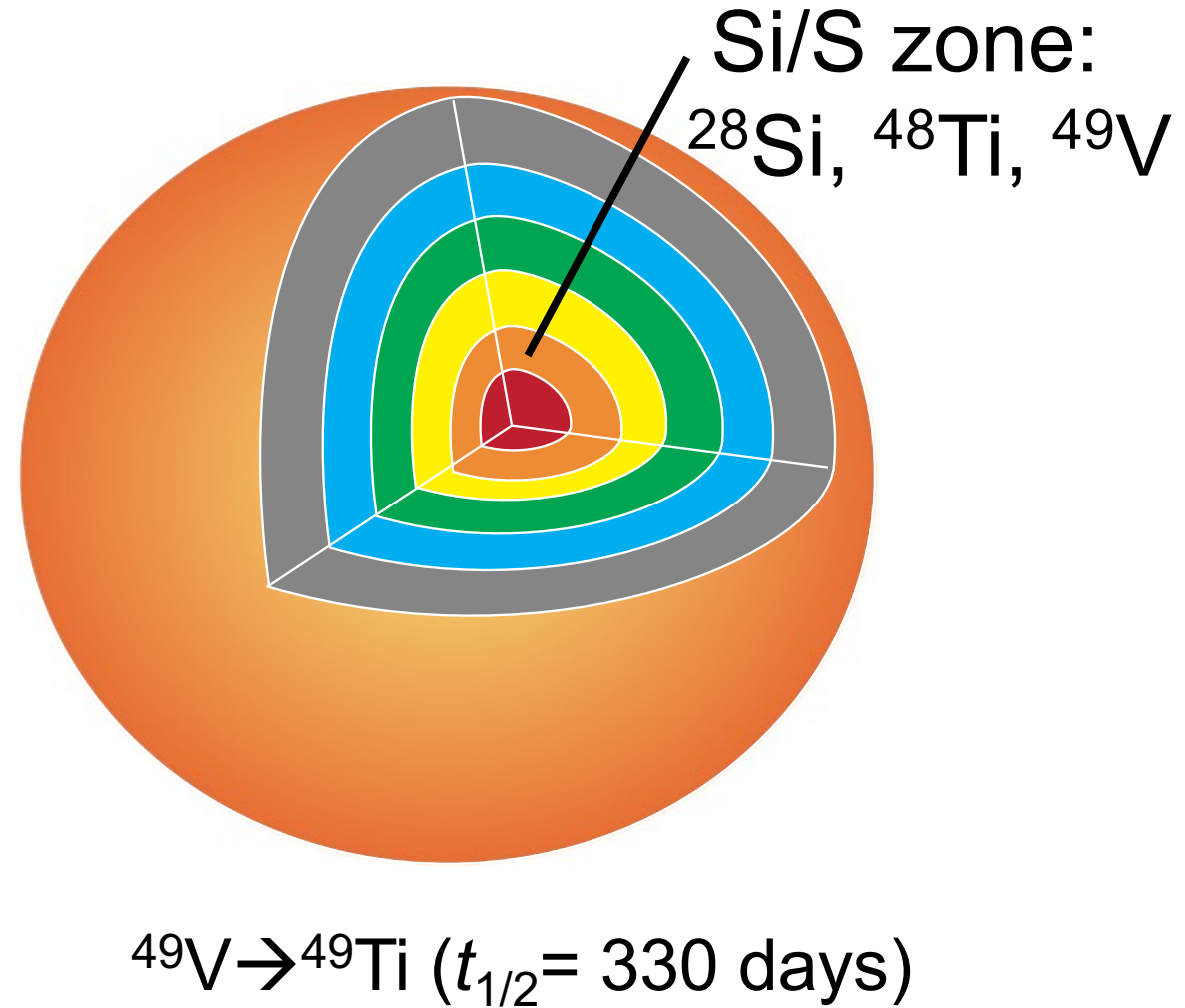
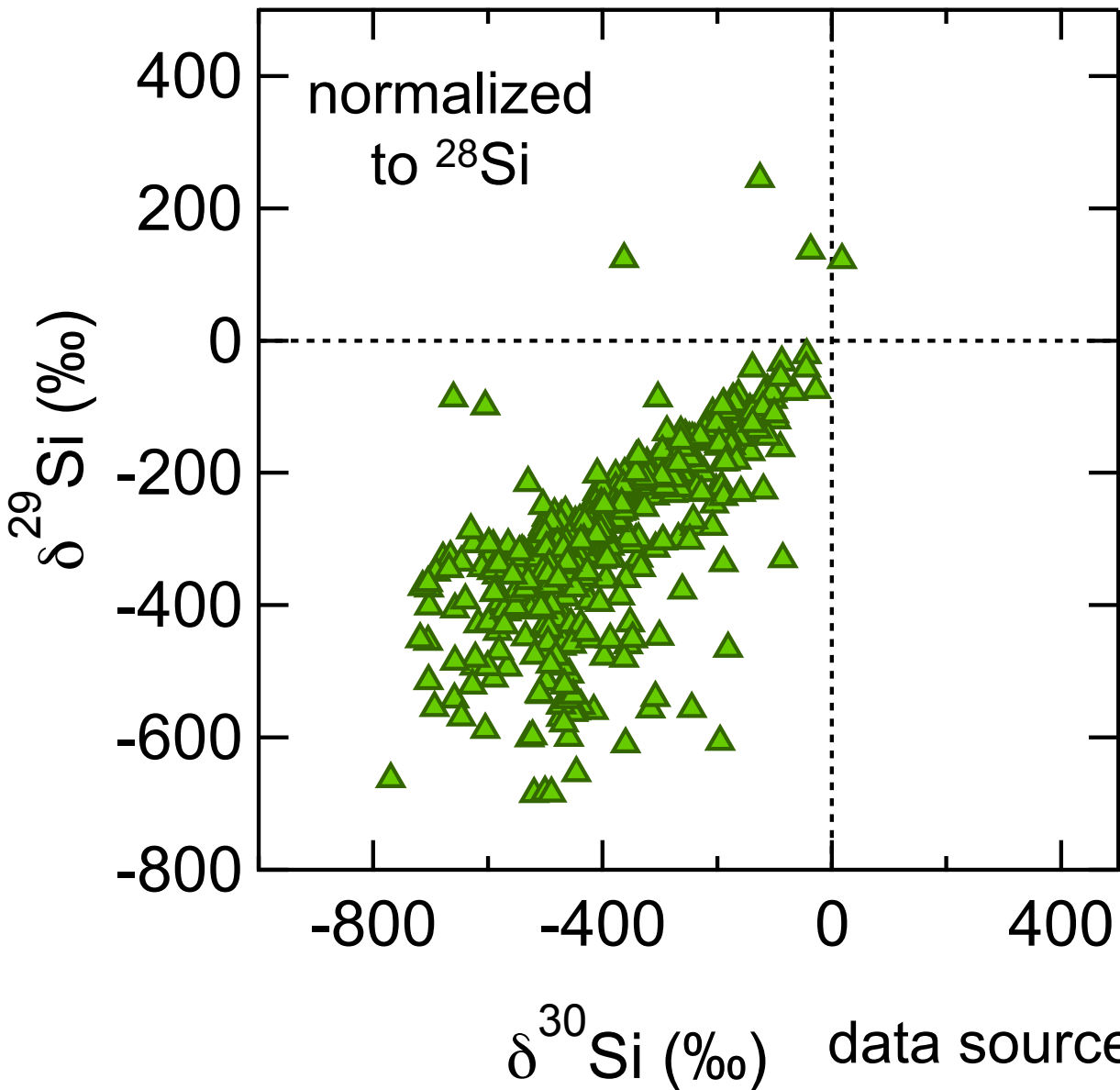


data source: Presolar grain database



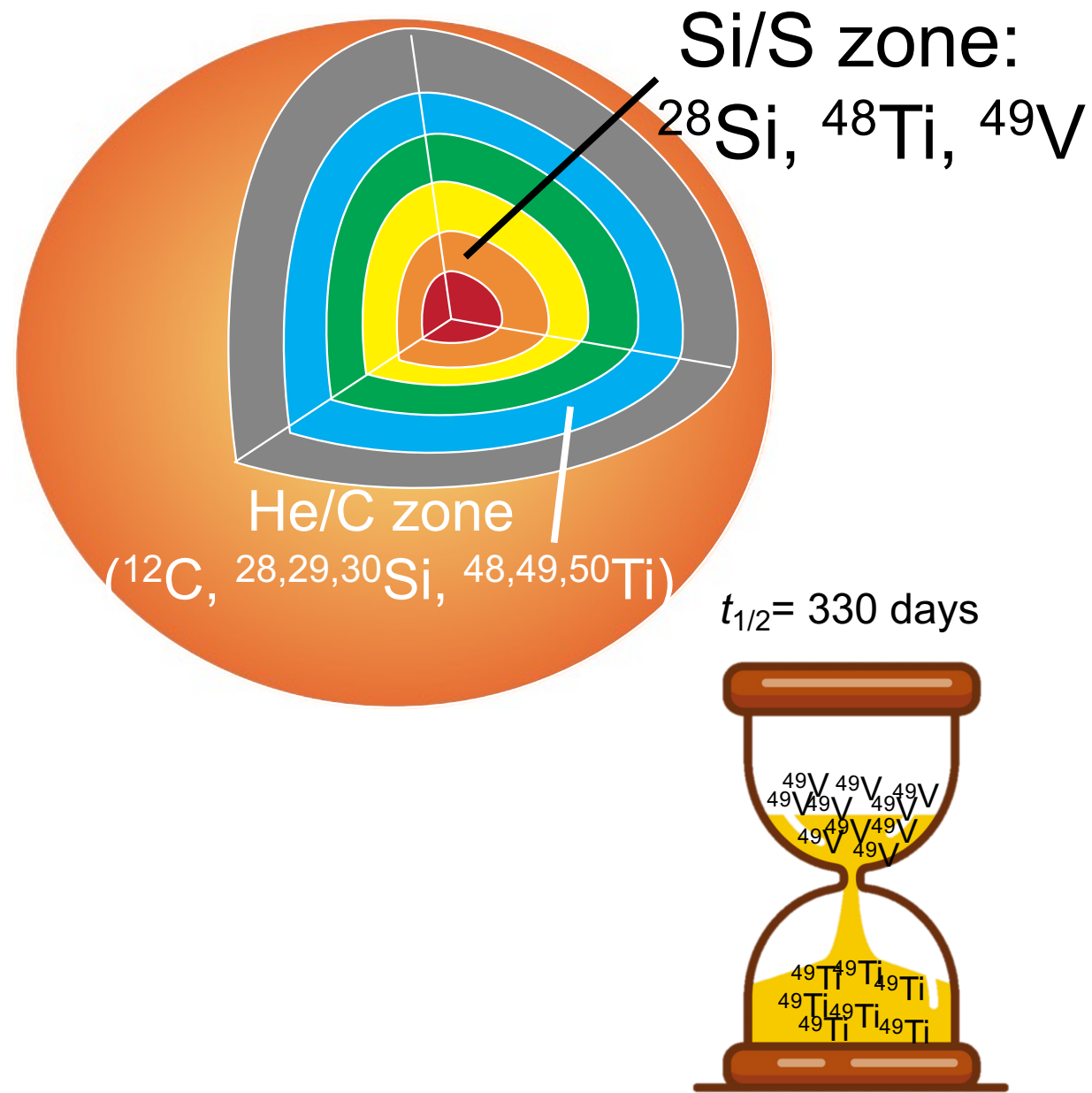
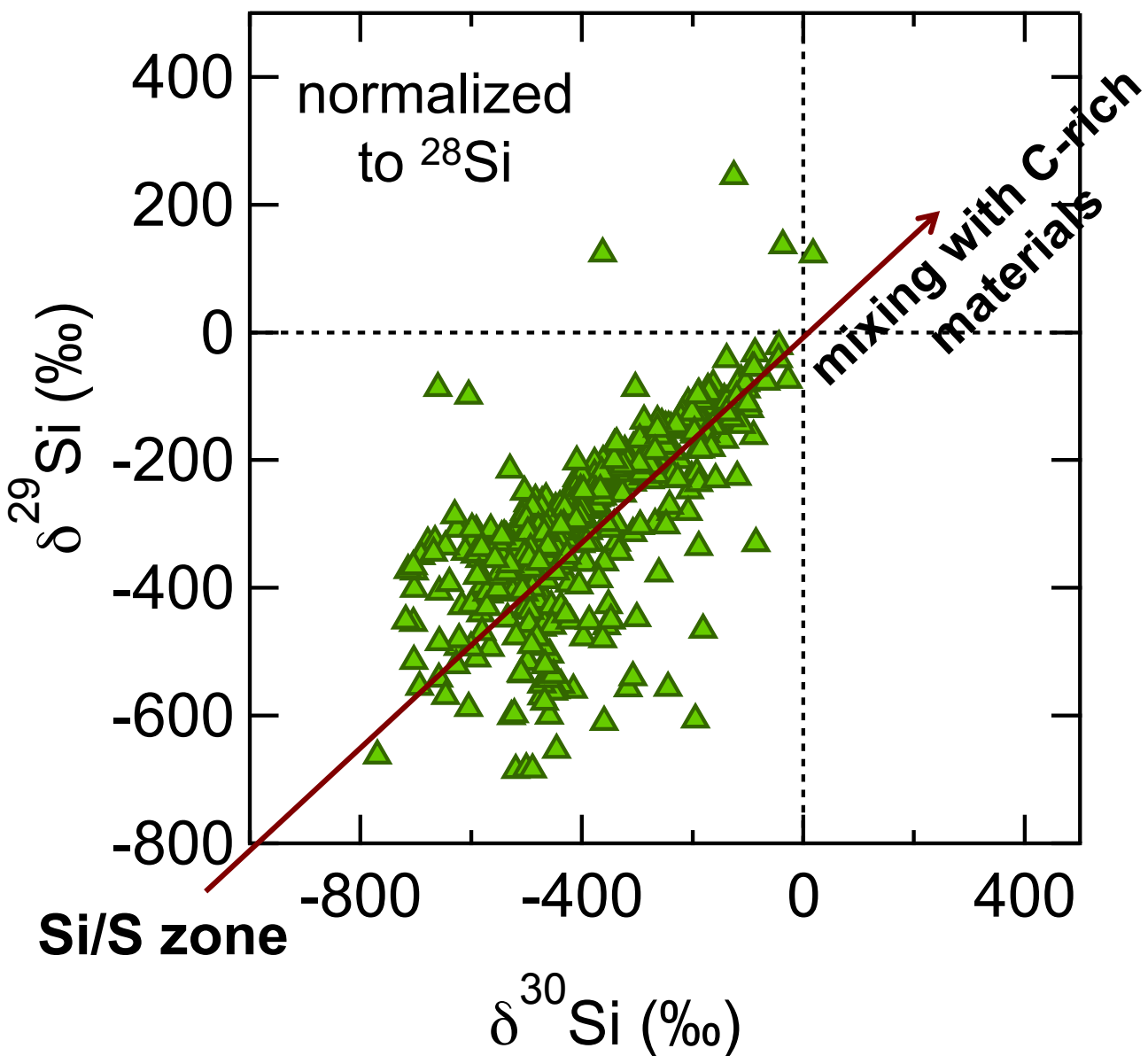
Mösta et al. (2014) *ApJL*

^{28}Si Excesses in Si/S Zone

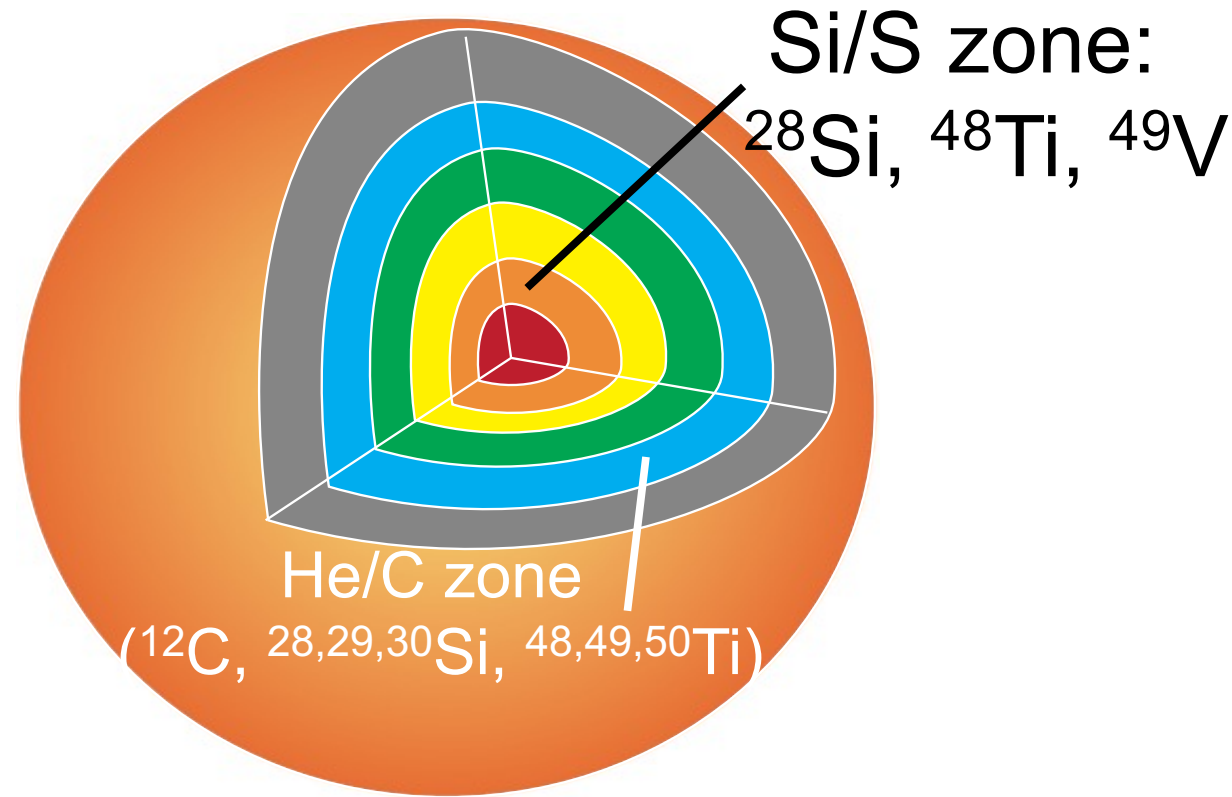
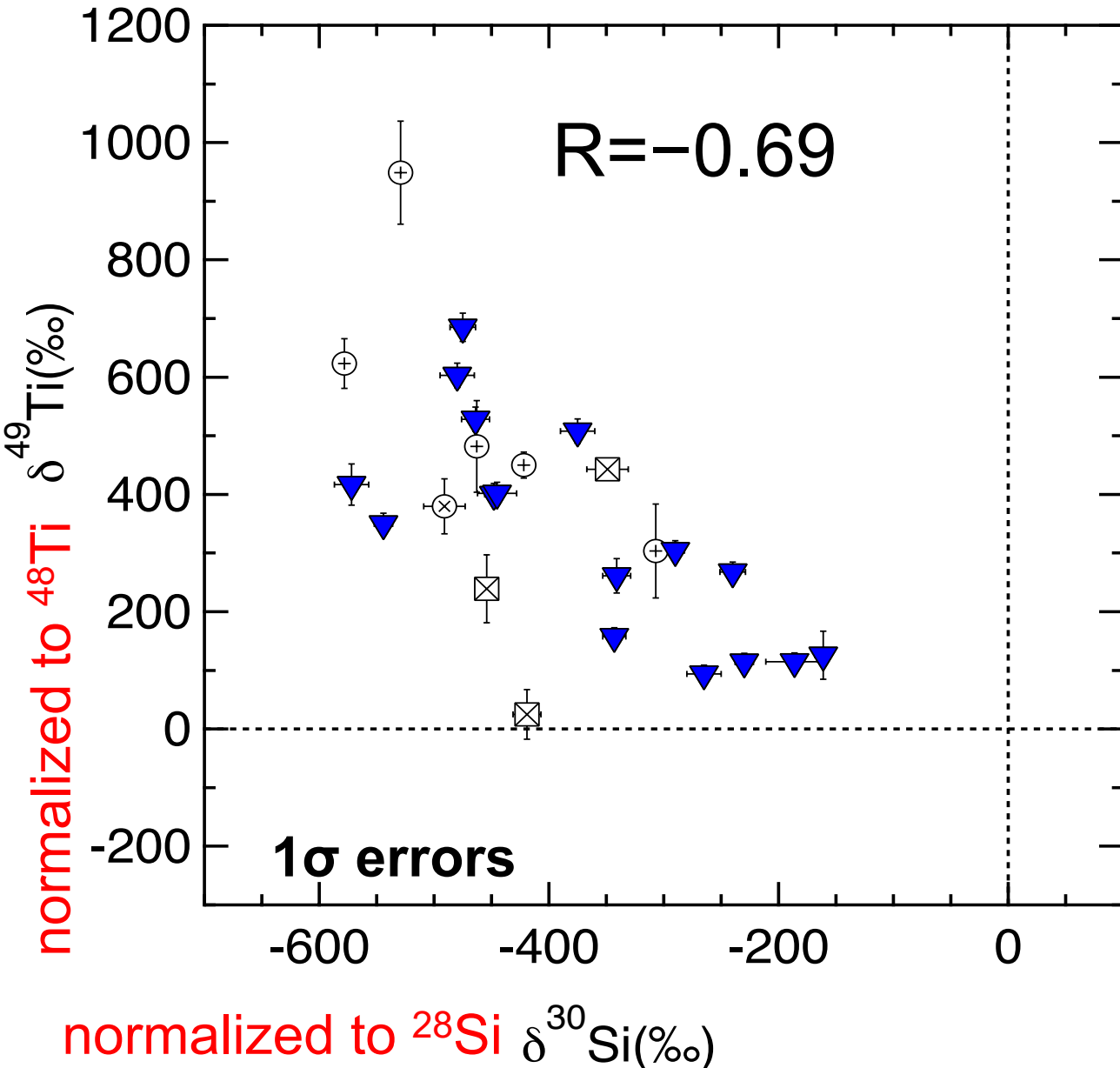


data source: Presolar grain database

Origin of ^{49}Ti in X Grains

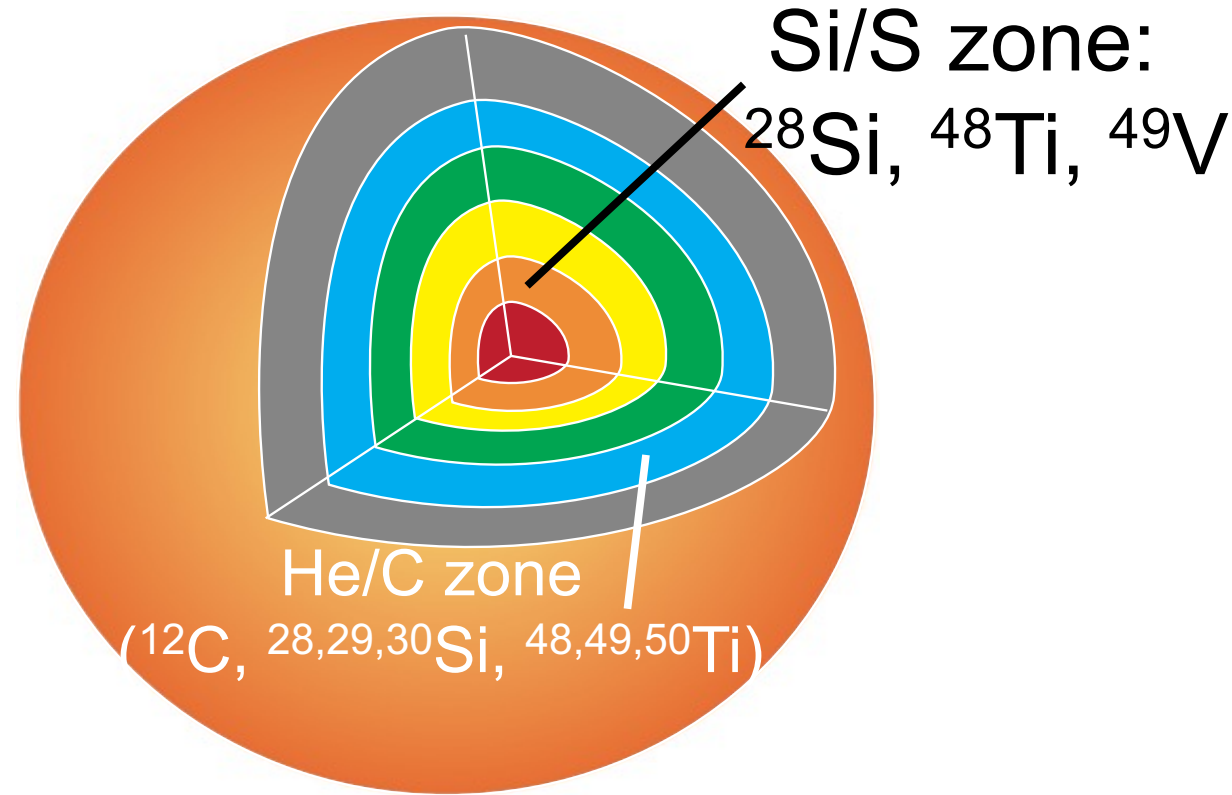
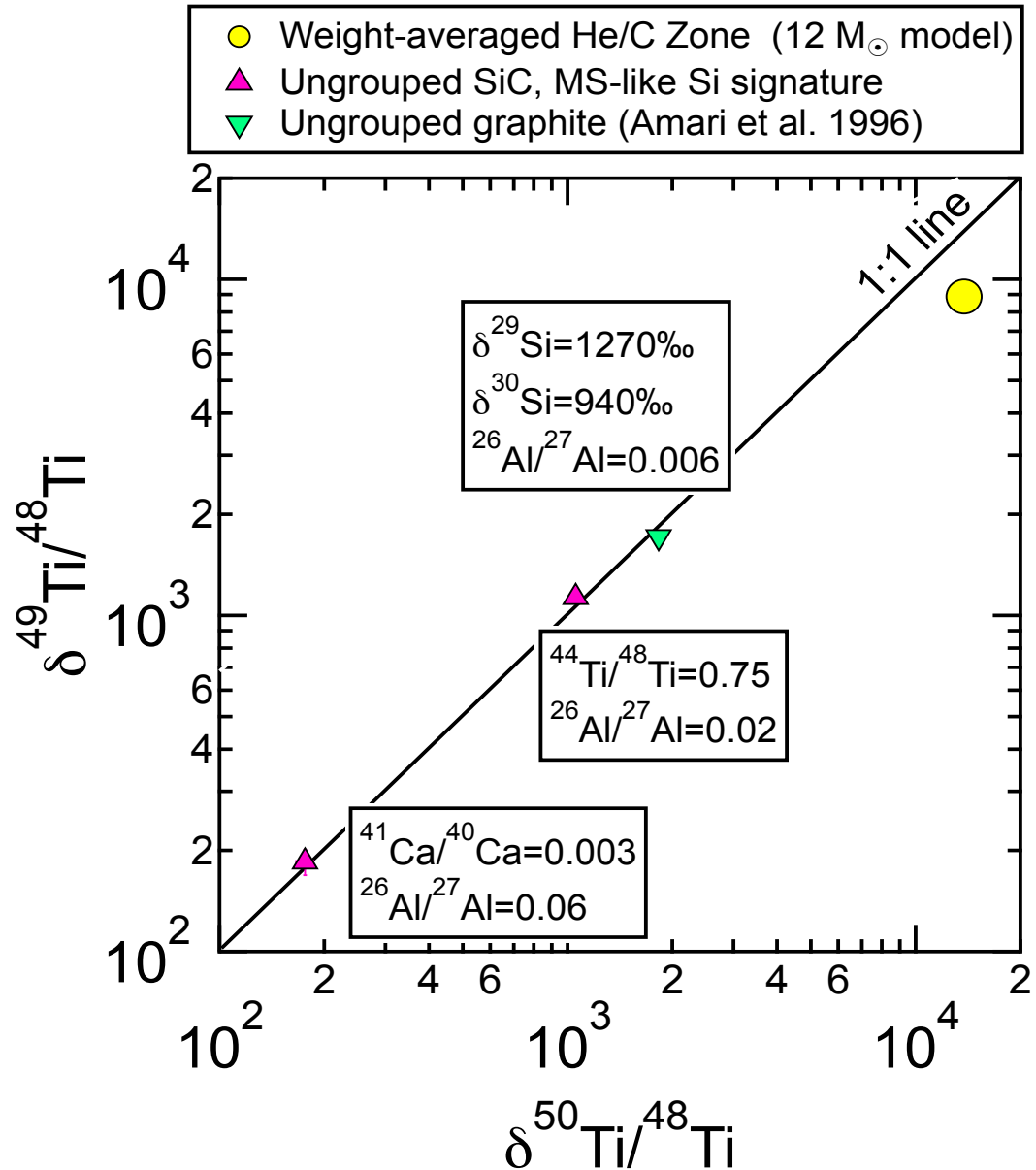


^{49}Ti Correlates with ^{28}Si Excesses



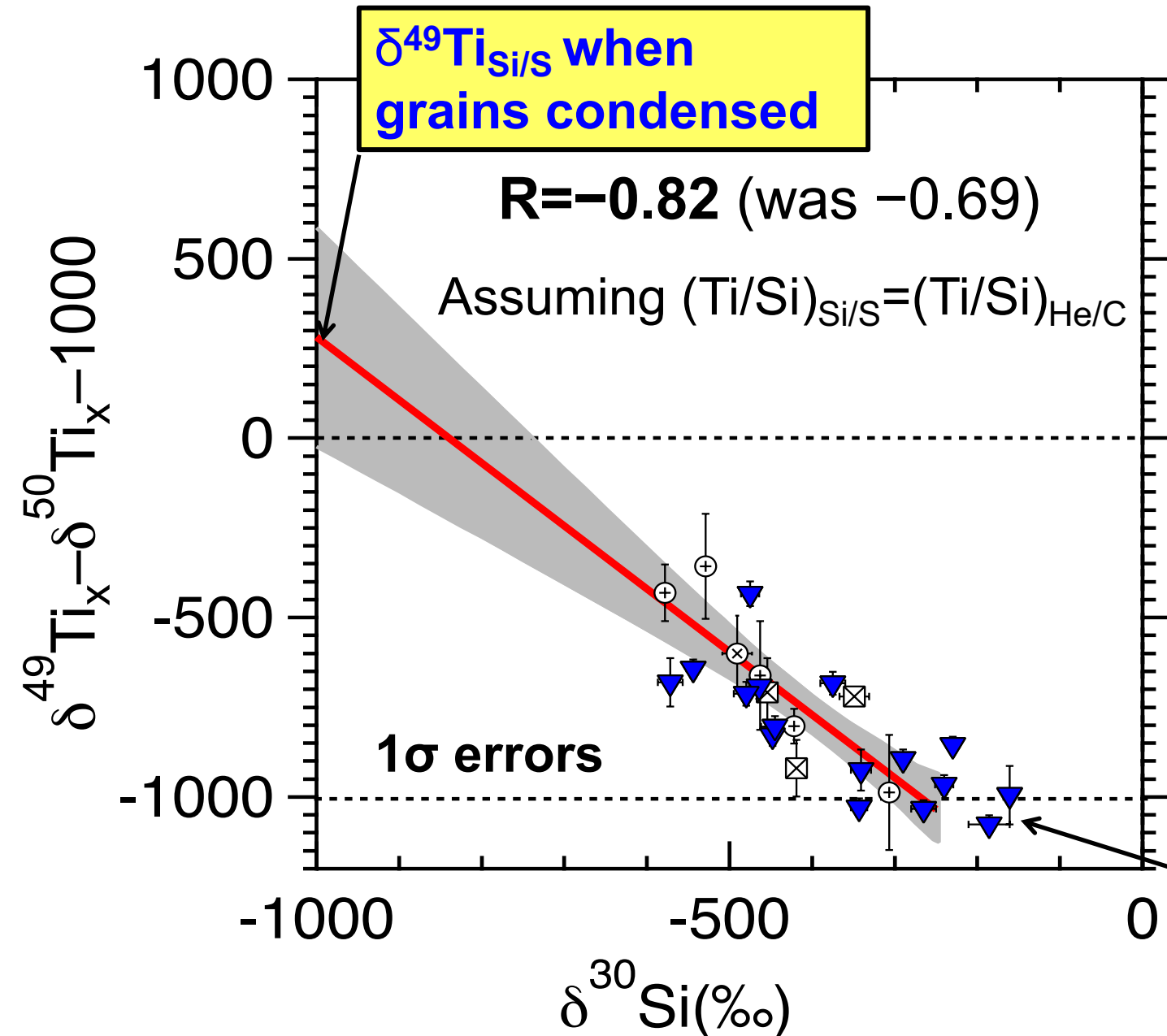
Constraints: small contribution from He/C zone.

^{49}Ti Correlates with ^{28}Si Excesses



Supernova grain data indicate that in He/C zone, $^{49}\text{Ti} \approx ^{50}\text{Ti}$.

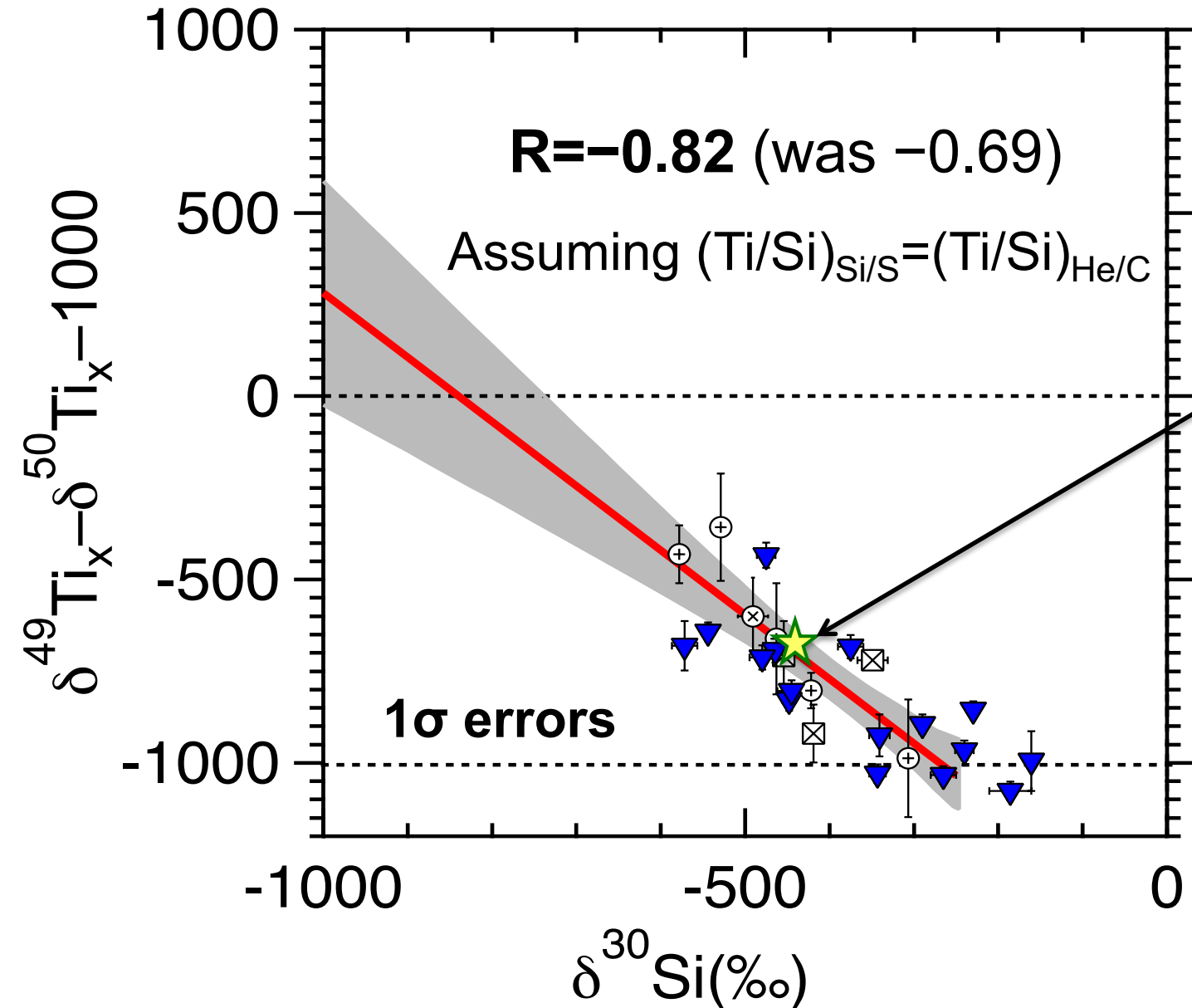
Calculation of $\delta^{49}\text{Ti}$ in the Si/S Zone



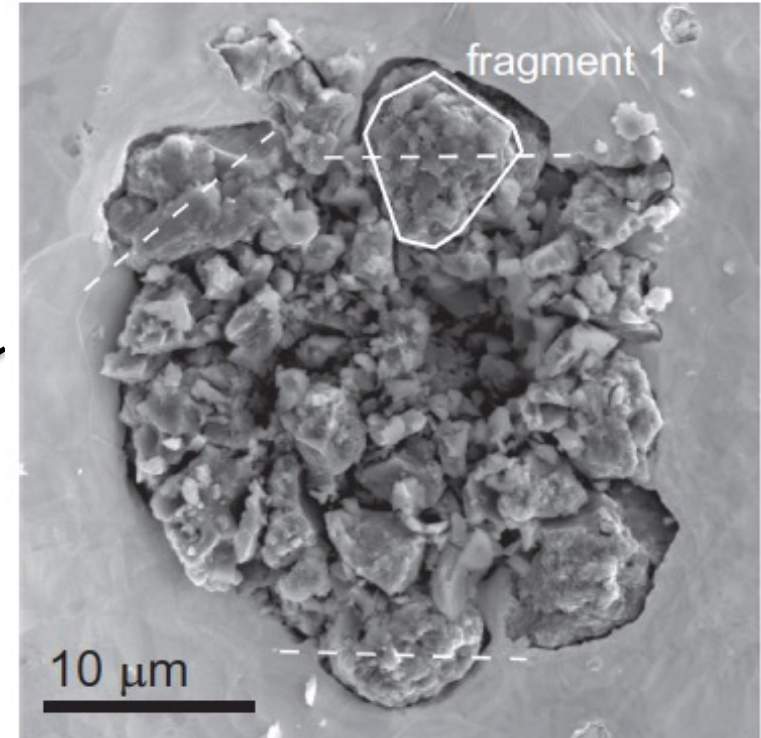
- Subtract He/C Ti to infer Ti isotopic composition of Si/S zone when grains condensed.
- Depends on Ti/Si ratio, linear fit gives **lower limit.**

C-rich ejecta mixed with more outer zone materials

Calculation of $\delta^{49}\text{Ti}$ in the Si/S Zone

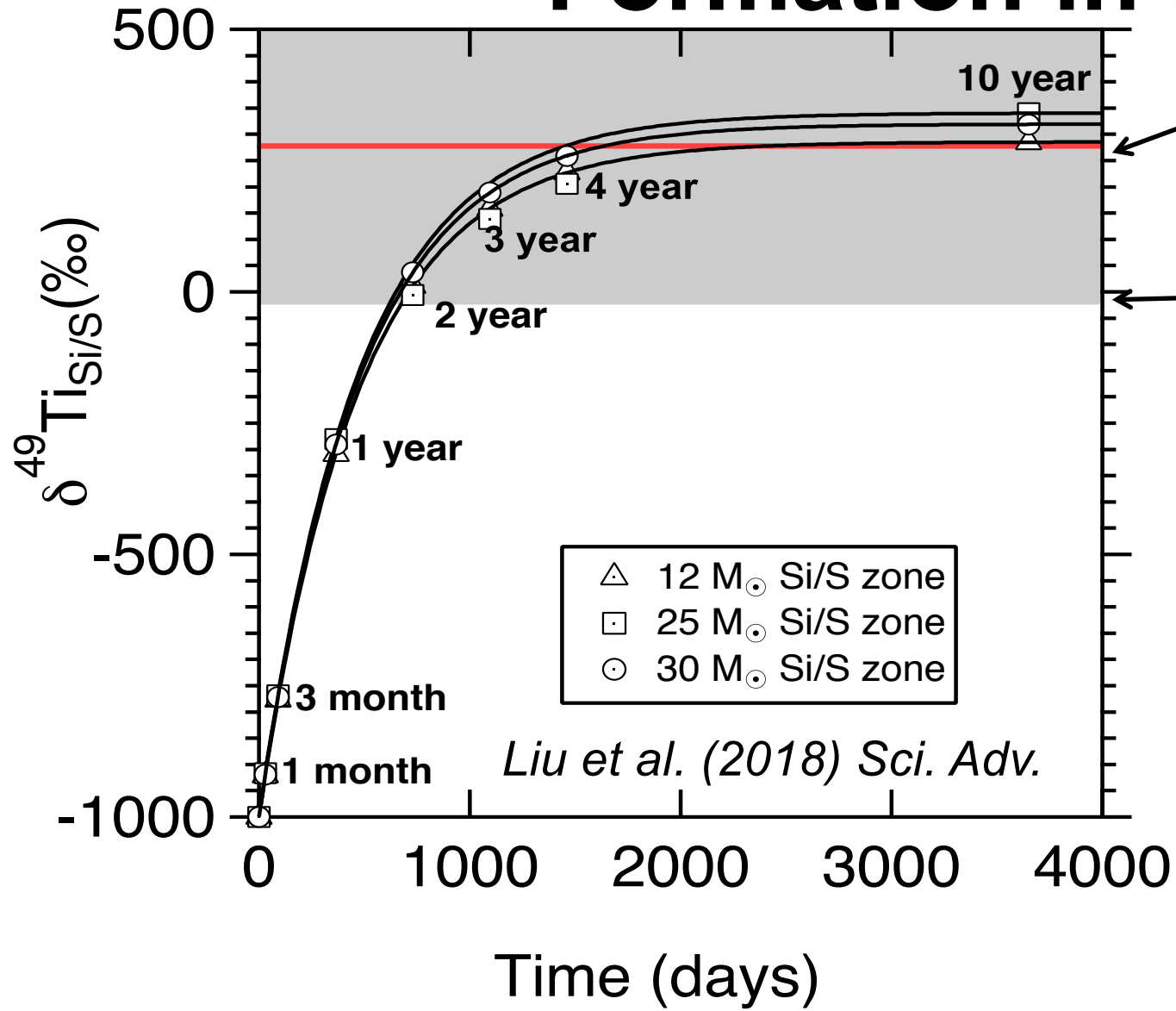


a) Bonanza (LU-13)



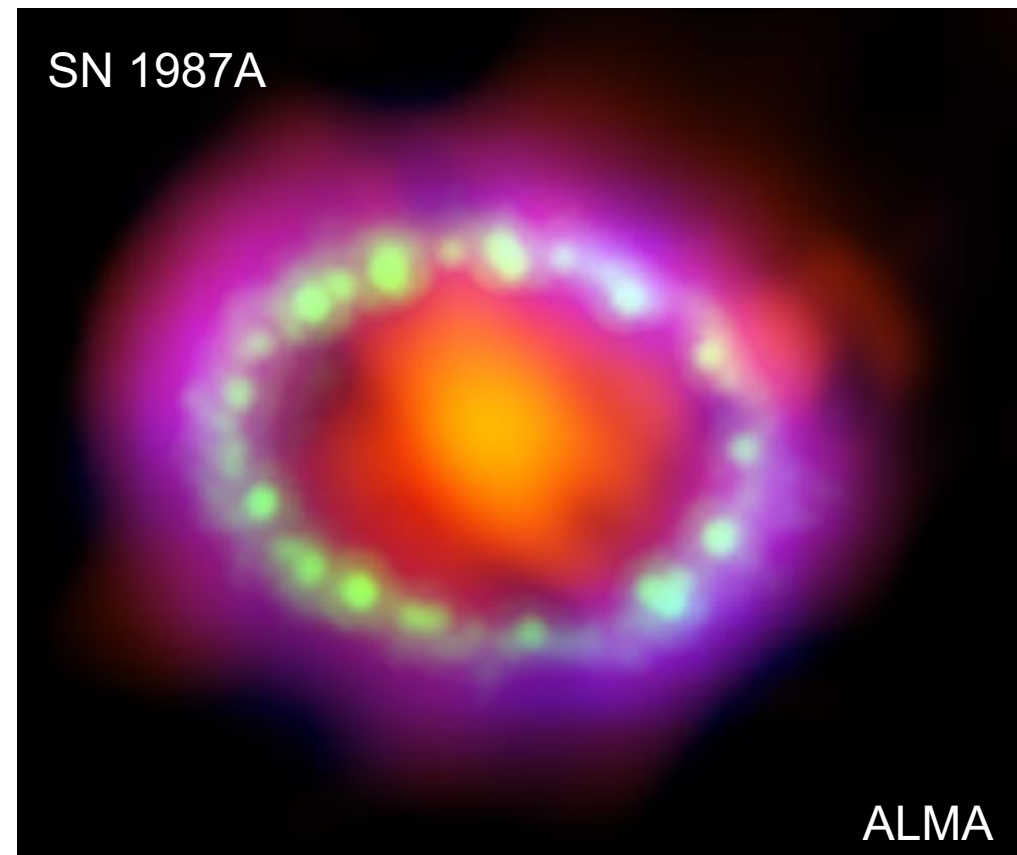
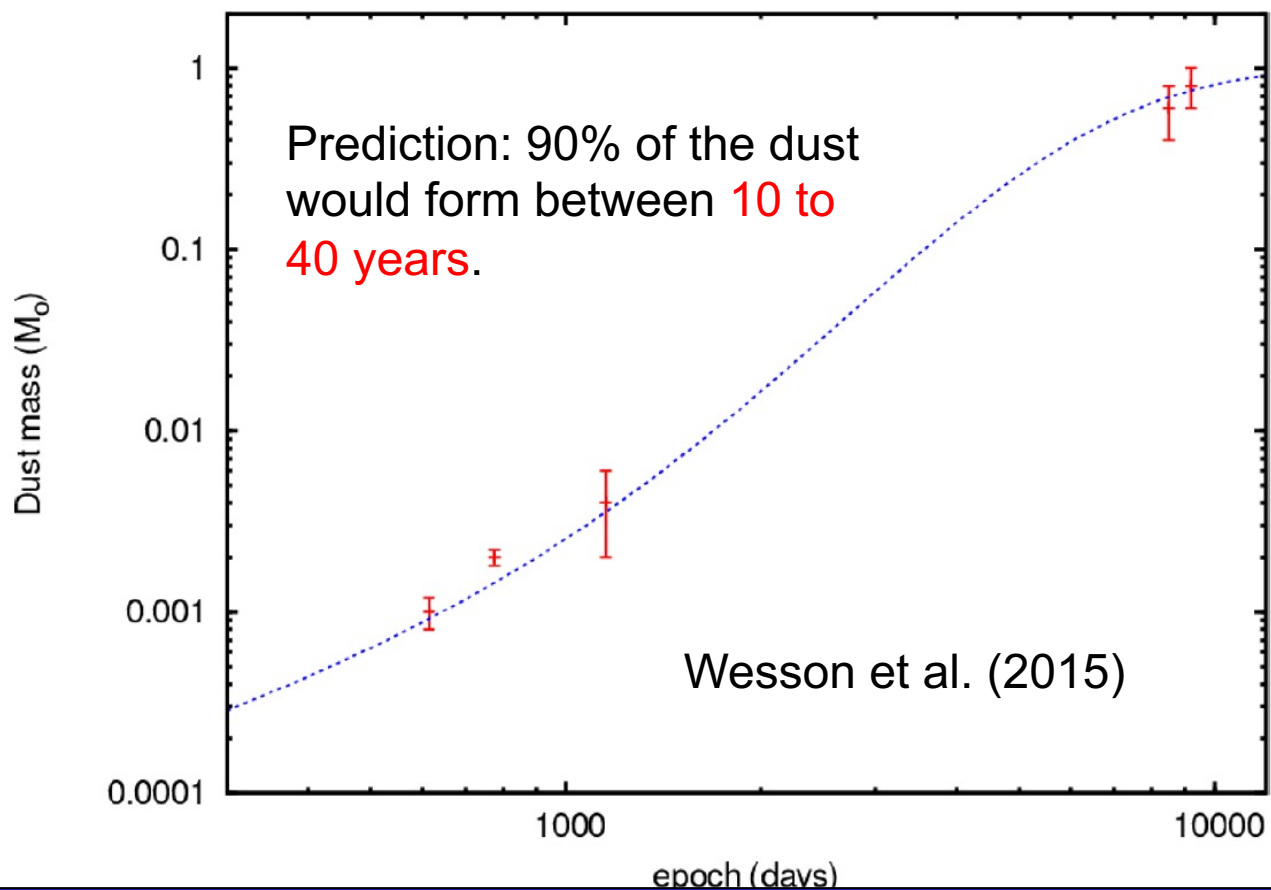
Gyngard et al. (2018) *GCA*

$\delta^{49}\text{Ti}_{\text{Si/S}}$ Constrains Timing of SiC Formation in Supernovae



The **95% lower limit** of $\delta^{49}\text{Ti}_{\text{Si/S}}$ derived by the linear fit constrains condensation to occur at least 2 yrs after SN explosions, consistent with astronomical observations.

Dust Production in SN 1987A Over 30 Years



- ❑ Dust formation can occur as early as a few months after SN explosions (e.g., Andrews et al. 2016).
- ❑ But VERY FEW SNe have been observed to quantify dust production later than 1000 days.
- ❑ The inferred timescale for grain formation in SN 1987A is CONSISTENT with the grain data, >2 yrs.

Outline

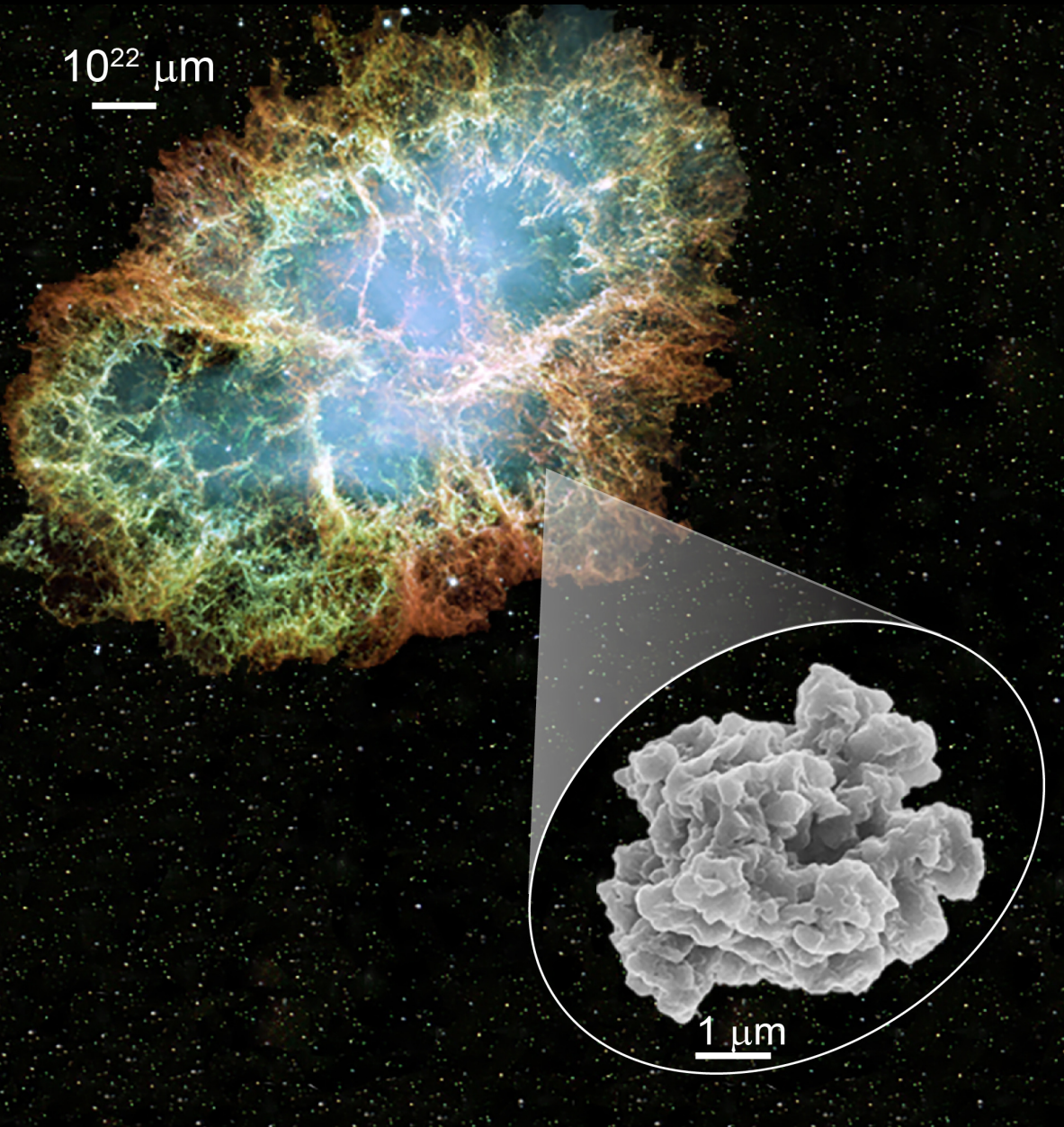
1. Analytical Techniques

2. Different Types of Grains and Their Stellar Origins

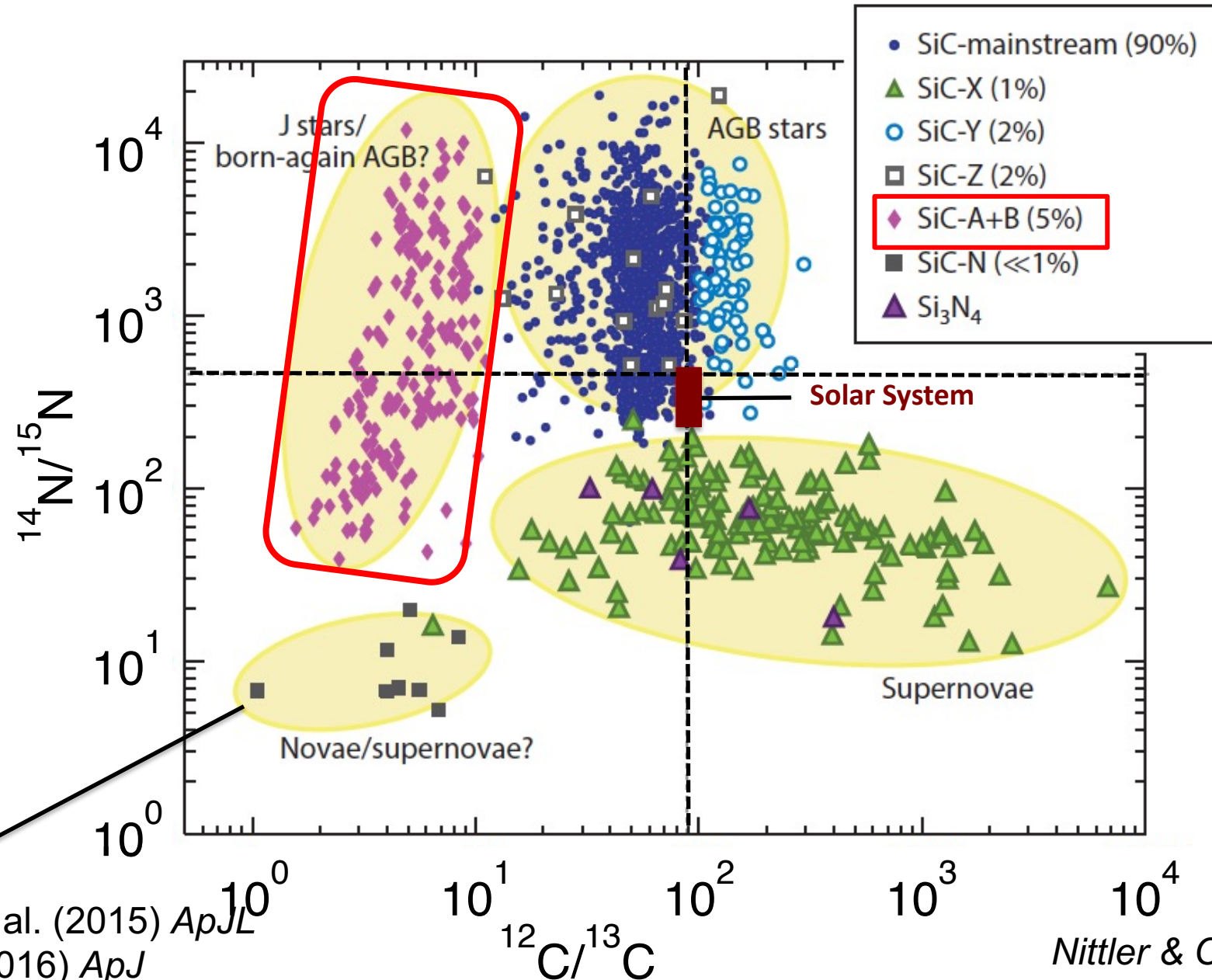
2.1 AGB Dust

2.2 Type II Supernova Dust

2.3 Mysterious ^{13}C -rich SiC Dust



^{13}C -rich Grains: What are Their Stellar Sources?



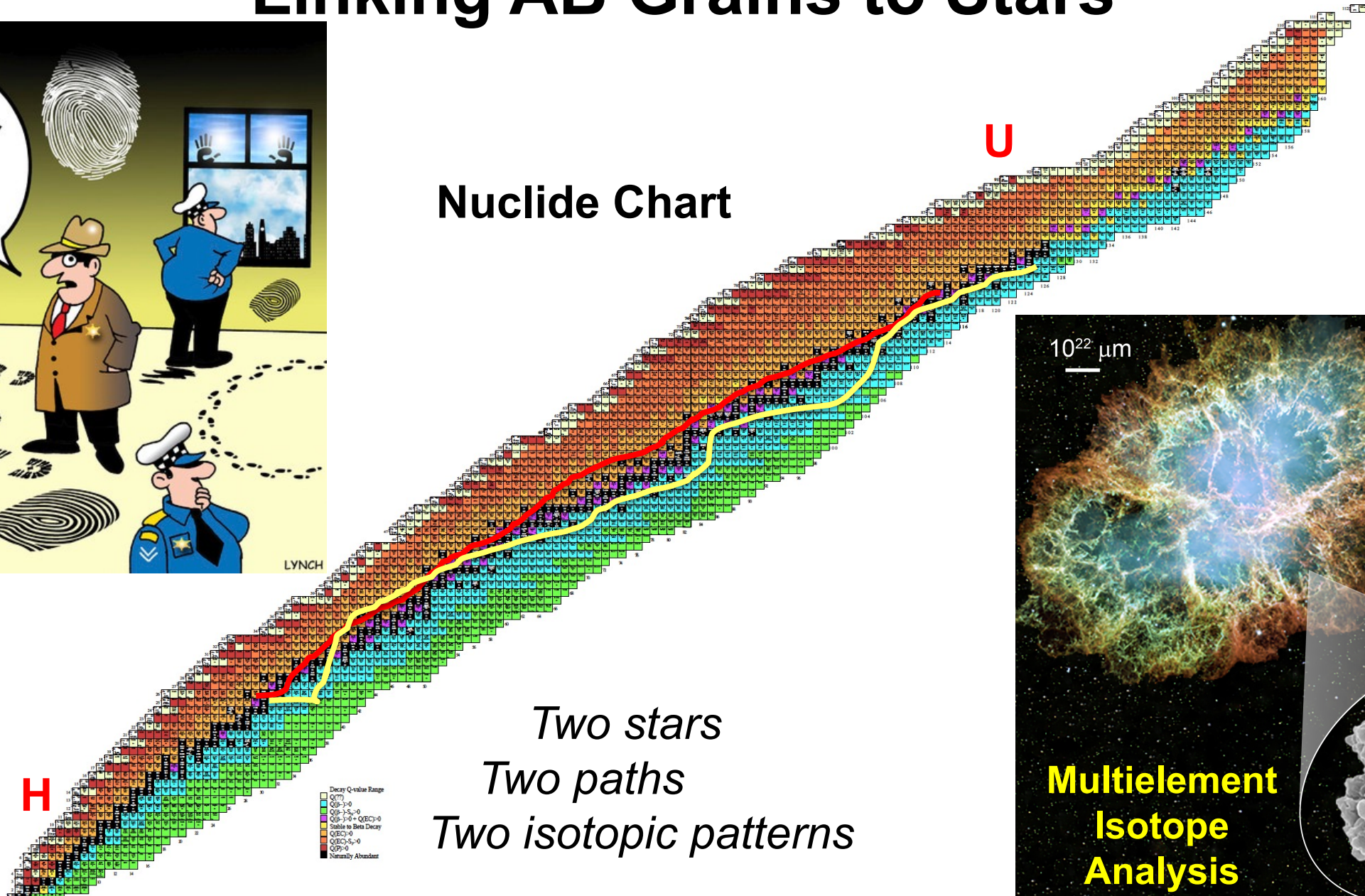
See Pignatari et al. (2015) *ApJL*
Liu et al. (2016) *ApJ*

Nittler & Ciesla (2016) *ARA&A*, 54,53

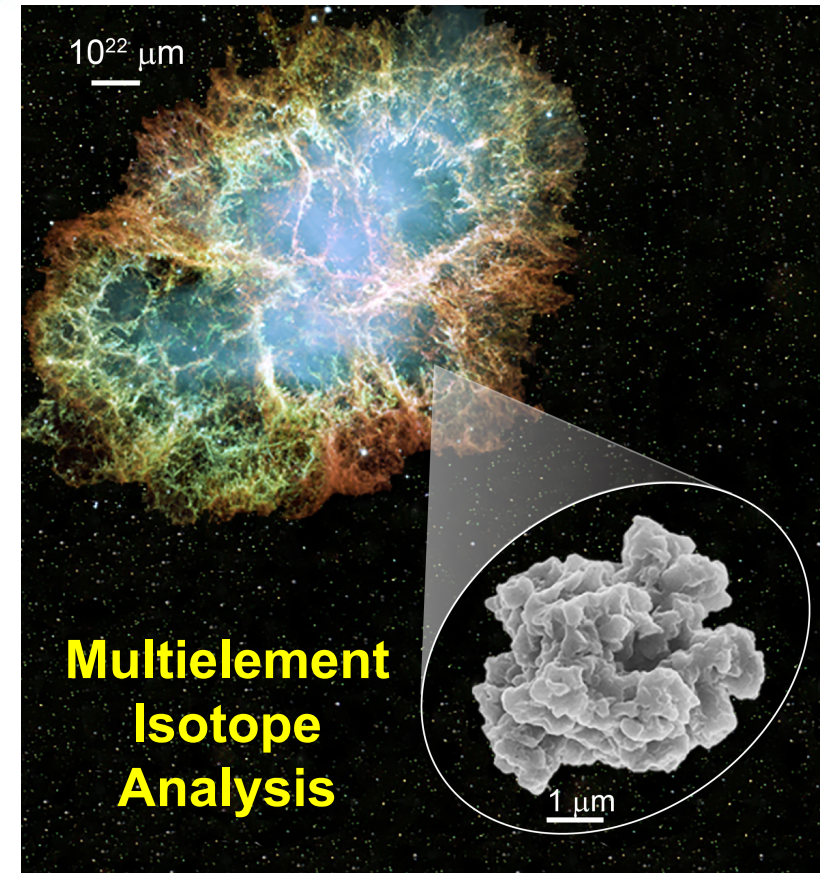
Linking AB Grains to Stars



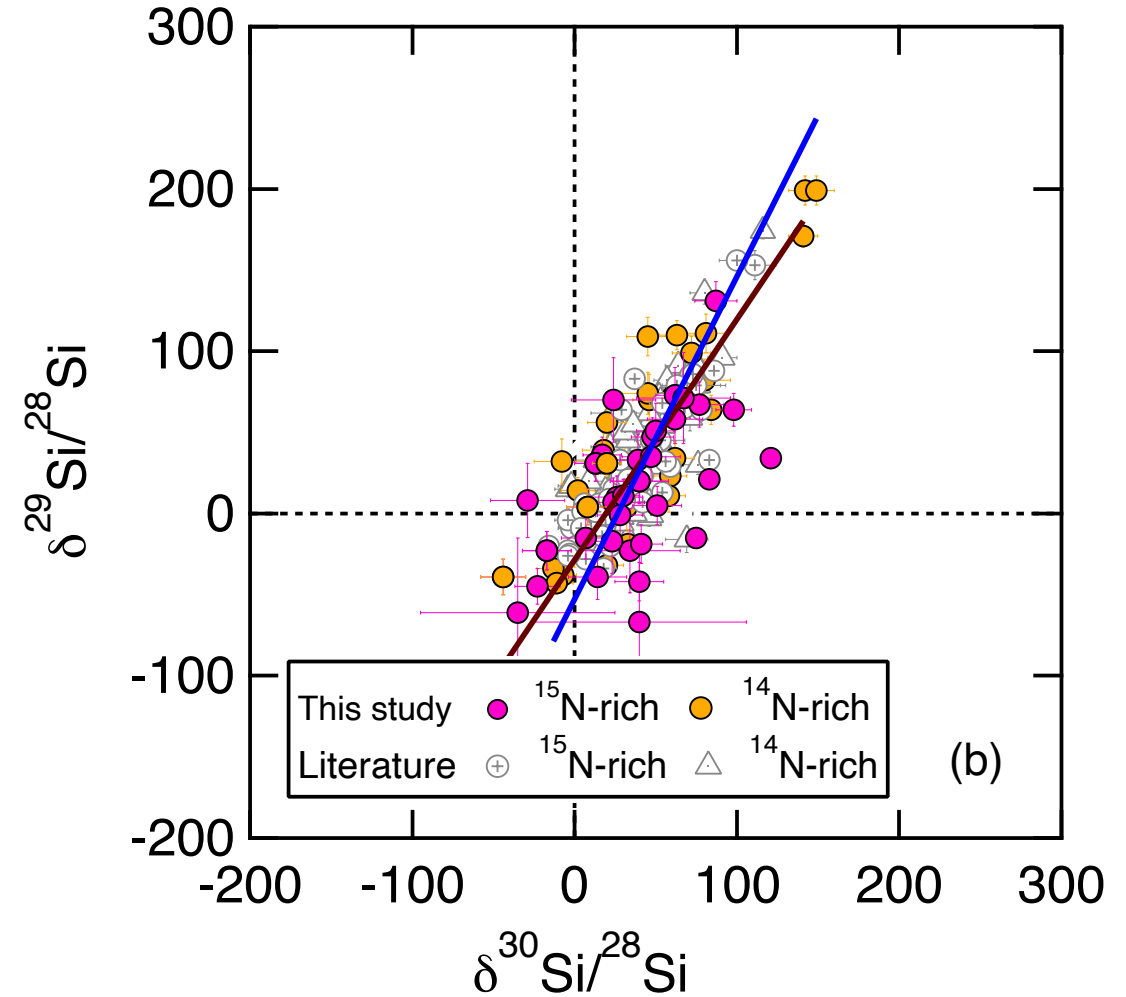
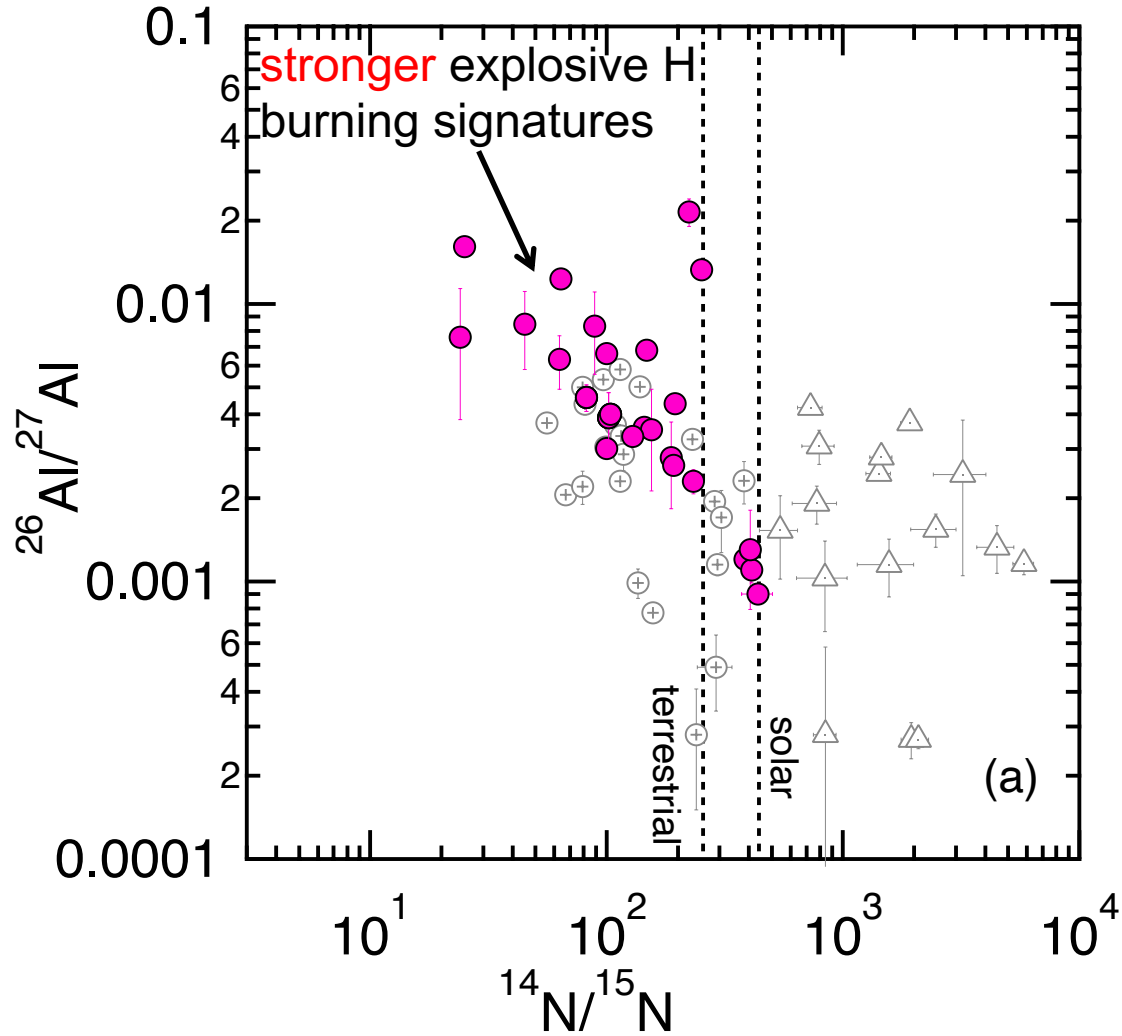
Nuclide Chart



Two stars
Two paths
Two isotopic patterns

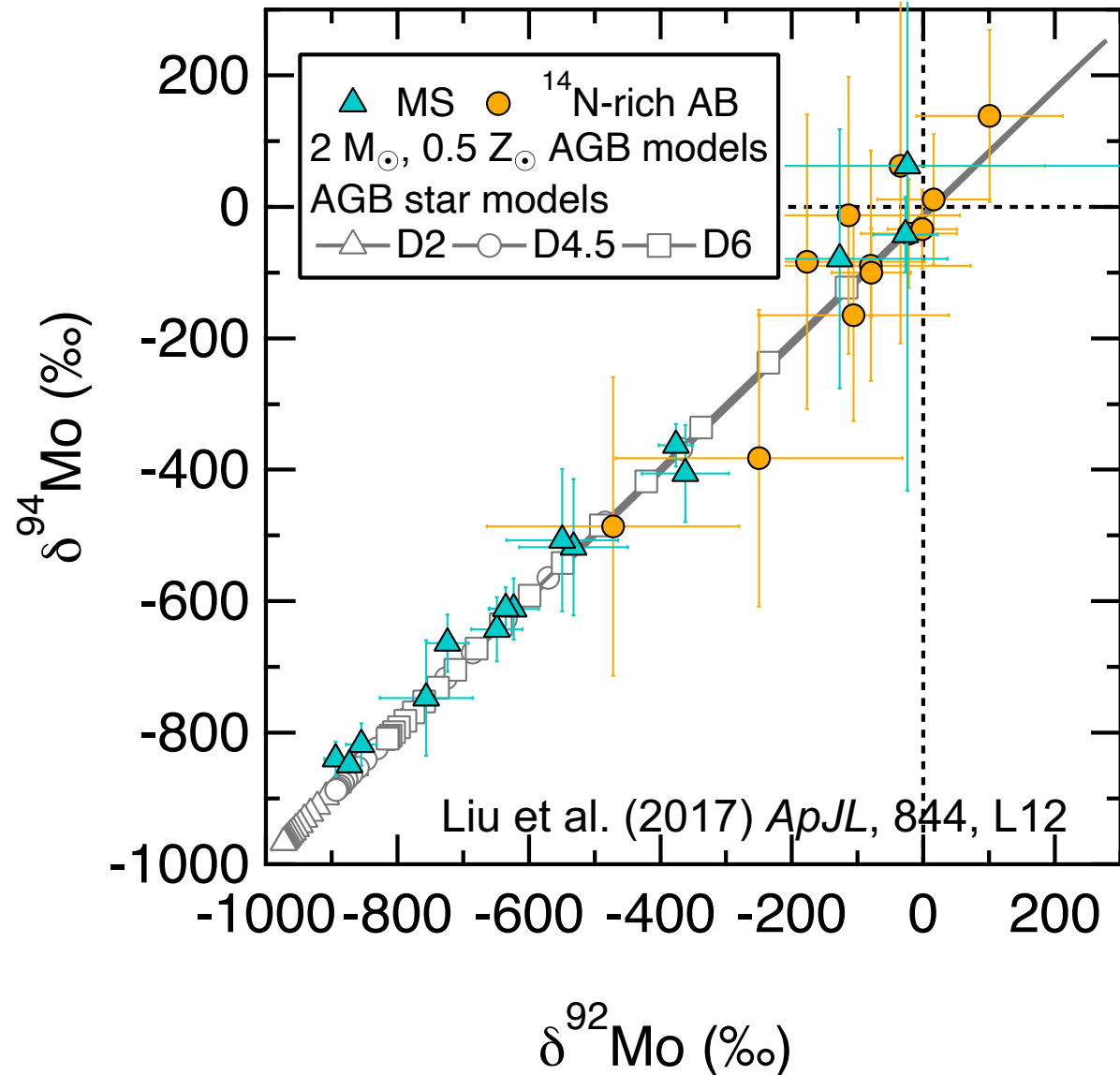


Two Groups of AB Grains



Consistent differences in N, Al, and Si isotope ratios

^{14}N -rich AB : Mainly J-type Stars

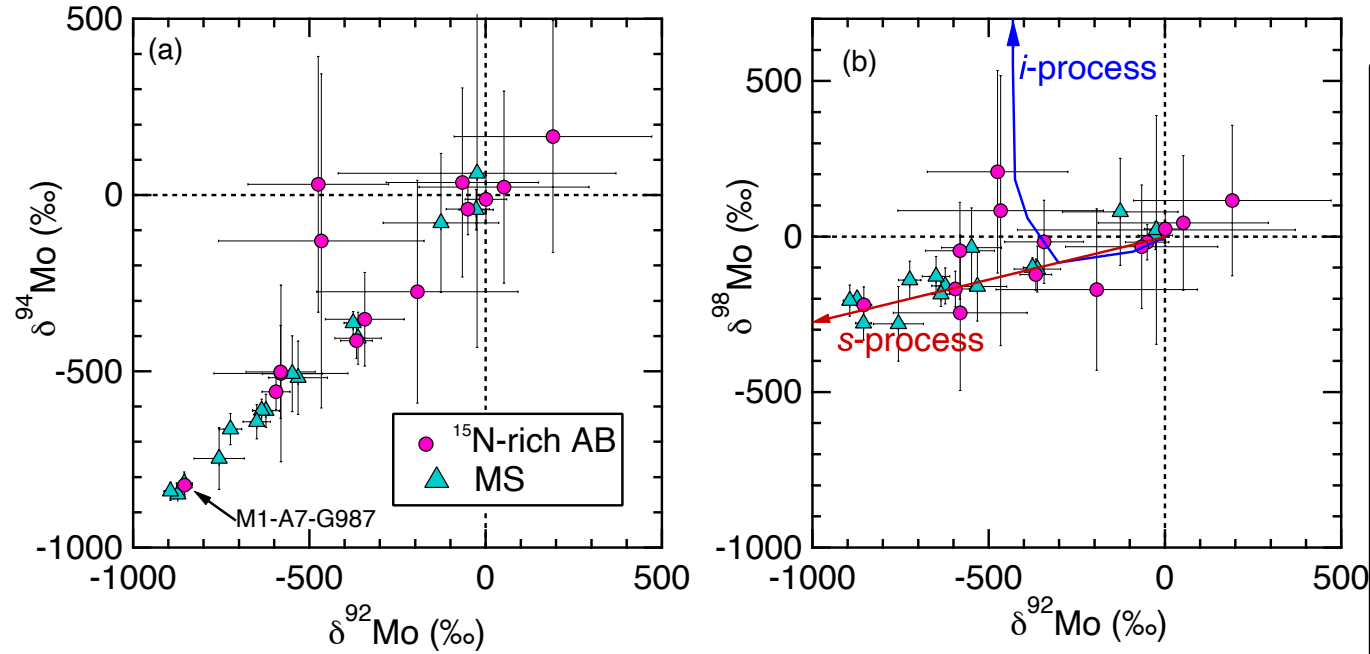


Similarities between ^{14}N -rich AB grains and J-type stars

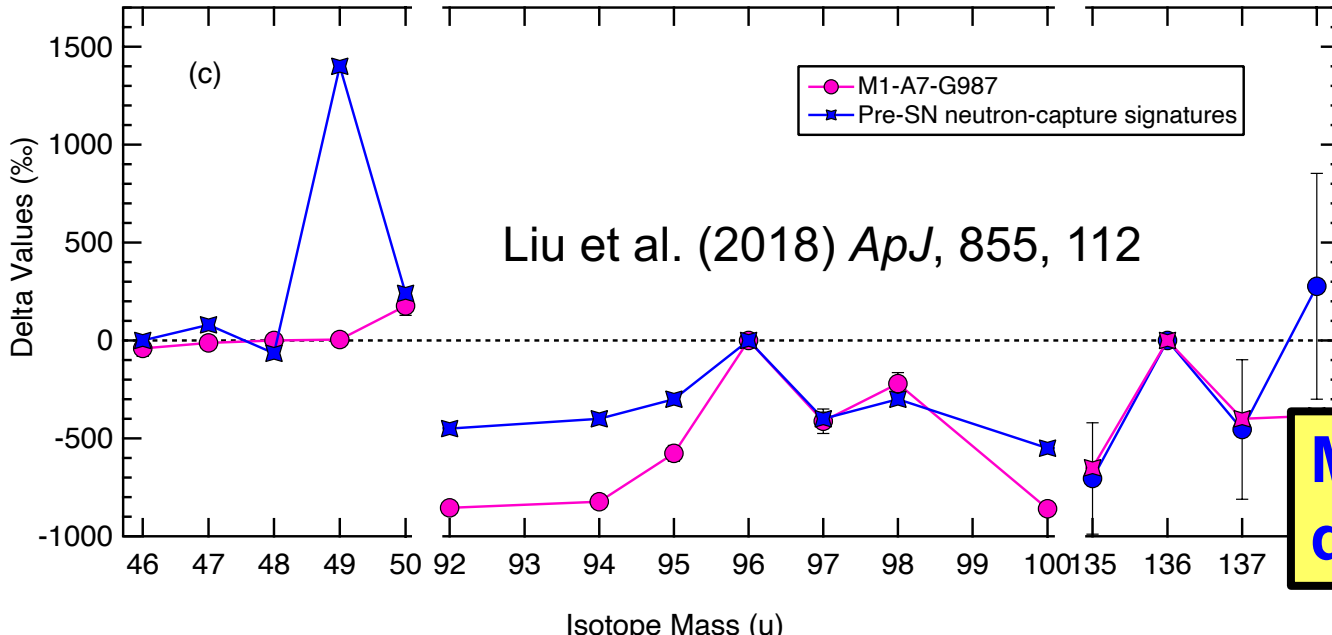
- near-solar metallicities.
- similar C and N isotope ratios.
- close-to-solar heavy-element isotopic compositions.
- Both are relatively abundant.

J-type star observations: Abia & Isern (2000) *ApJ*, 536, 438

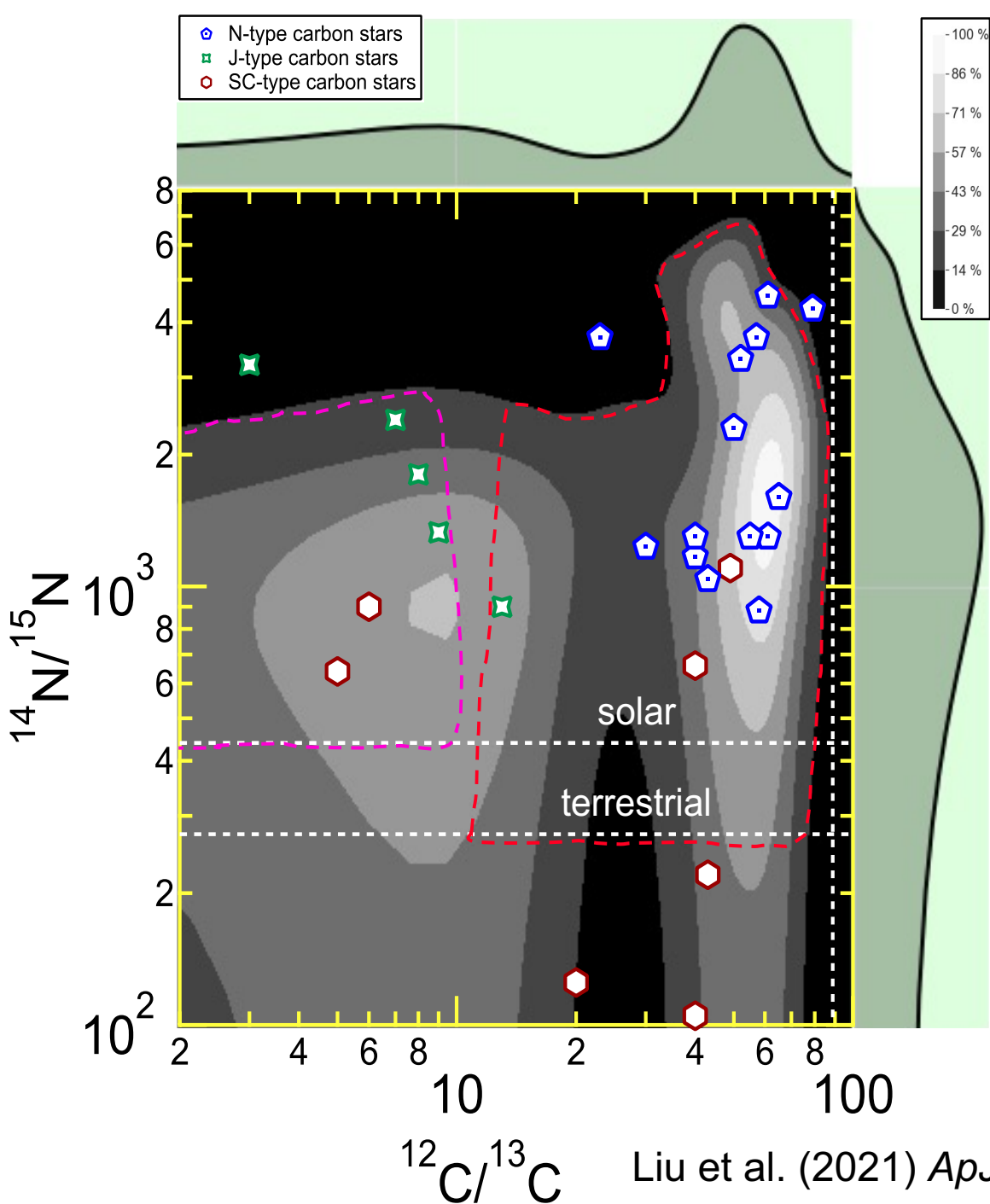
^{15}N -rich AB Grains : *Supernovae?*



The coexistence of ^{13}C , ^{15}N , ^{26}Al , and s-process enrichments together point to **supernovae** as their progenitor stars.



More observational data are NEEDED!



Liu et al. (2021) *ApJL*, submitted

- **^{14}N -rich AB grains** overlap with **J-type carbon stars** and a few **^{13}C -rich SC-type carbon stars** in their C and N isotopic composition.
- No carbon stars lie in the region where **^{15}N -rich AB grains** are located, pointing out that these grains were likely sourced from **the ejecta of explosive events**, e.g., supernovae.

Conclusions

